Università Degli studi di NAPOLI "FEDERICO II"

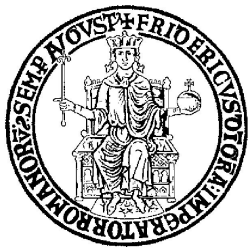

Department of Biology

PhD School in Biology

XXIX cycle

"Effects of heavy metals on plastidial glucose-6-phosphate dehydrogenase: kinetic changes analysis, abundance of isoforms and determination of subcellular localization"

Candidate: Alessia De Lillo

Supervisor	PhD School	Co-Supervisor
Prof.	Coordinator	Prof.
Adriana Basile	Prof. Salvatore Cozzolino	Sergio Esposito

Summary

1 Introduction

Glucose-6-phosphate dehydrogenase (G6PDH - EC 1.1.1.49) is the key enzyme of the oxidative pentose phosphate pathway (OPPP). The OPPP is ubiquitous in living organisms (except the majority of Archea) and plays fundamental roles for the cells.

The main functions of this cycle are the synthesis of precursors for nucleic acids and fatty acids; and the furnishing of NADPH, which is essential for the biosynthesis (Senturk et al. 2009), and to counteract oxidative stress (Kruger and von Schaewen 2003).

The G6PDH catalyses the first reaction of the cycle by conversion of glucose-6-phosphate to 6-phosphogluconate in the presence of $NADP^+$ and $MgCl_2$. The magnesium is indeed essential for G6PDH activity cause G6PDH requires ions Mg^{2+} for the stabilization of the structure (Esposito et al. 2001).

In plants, different isoforms of G6PDH have been described: cytosolic-G6PDH (cy), plastidial G6PDH (P2), chloroplastic- G6PDH (P1) (Kruger and von Schaewen 2003; Wakao and Benning 2005); a further isoform, enzymatically inactive, named P0-G6PDH has been identified (Wakao and Benning 2005), and its possible function discussed later. These isoforms can be easily distinguished, and undergo to distinct regulation mechanisms. Various studies reveal that G6PDH activity is generally increased during plant exposition to different biotic (Scharte et al. 2009) and abiotic stress (Valderrama et al. 2006; Wang et al. 2008; Cardi et al. 2011, 2015; Landi et al., 2015).

Among pollutants, heavy metals give great concern due to their persistence in the environment, and the possibility to be absorbed and accumulated in living organisms (Pinto et al. 2004; Cho et al, 2003) and particularly in plants (Basile et al., 2015). HMs toxicity causes different effects as: changes in cell structure and functionality (Taulavuori et al., 2005), alterations of key metabolic processes (Prasad, 2004; Schützendübel et al., 2001), generation of free radicals (Schützendübel and Polle, 2002; Hall, 2002) and exchanges in enzymatic co-factors (Van Asscheet al, 1986); furthermore enzyme inhibition is always considered an important biomarker of HM response (Timbrell, 1998).

Previous studies suggested a possible correlation between metals and changes in total G6PDH activity in various organisms, e.g. HMs induce a decrease of total G6PDH activity in rainbow trout liber (*Oncorhynchus mykiss*)(Cankaya et al., 2011); Zn^{++} caused variation of G6PDH activity in *Bufo arenarum* toad ovary (Fonovich de Schroeder , 2005).

Namely in plants, iron excess on *Nicotiana plumbagnifolia* caused an increase of the

cytosolic G6PDH isoform (Kampfenkel et al., 1995), in wheat roots *(Triticum aestivum*) aluminium caused changes in G6PDH activities (Slaski et al., 1996).

Interestingly, no data are available about the effect(s) of specific effects of HM on the G6PDH plastidial isoforms, which are greatly involved in the abiotic stress response (Cardi et al., 2011).

In order to establish the possible direct effect of specific HM on enzymatic activity and regulatory properties, the recombinant, his-tagged plastidial G6PDH isoform from *Populus trichocarpa* was incubated in the presence of HM to establish the role(s) of specific elements.

Moreover, mutagenized enzymes, lacking of cysteine residues were similarly produced and tested for the possible interactions of HM with disulphide bridges present in the active enzyme.

HM are also well known to induce oxidative stress that in its turn results in the increase of activities of enzymes involved in ROS-scavenging. The effects of these heavy metals were so tested directly in plant and as model organism was utilized *Hordeum* vulgare (barley).

Furthermore, subcellular localization analyses of *Hordeum vulgare* P2-G6PDH and P0-G6PDH isoforms by transient expression of reporter fusion proteins in *Arabidopsis/*Tobacco protoplast, and by Agro-infiltration in tobacco leaves were prepared in order to verify if the P2-G6PDH is directed in the non-photosynthetic plastids solely, or in the chloroplasts as well.

1.1 Heavy metals

Heavy metals (HMs) are metals with specific characteristics:

- Density up to 5,0 gr/cm^3
- Cationic property
- Low solubility
- Affinity towards the sulphides
- Tendency to form organic compounds

They could be divided in two group: essential and non essential. Between the essential metals there are copper and zinc, while between the non-essentials there are Nickel, lead and cadmium which are toxic at low levels. Only a few of the many metals present in the environment are essential to all plants (Fig. 1).

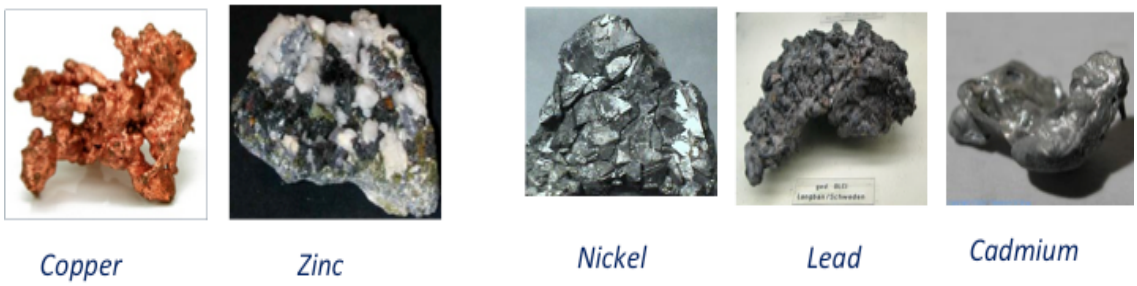

Fig. 1: Heavy metals

Heavy metals (HM) indeed represent one of the most dangerous sources of pollution in Ecosystems.

In many areas, free radicals have been demonstrated as directly involved in molecular damages associated with exposure to a wide range of heavy metals. Plants need a range of HMs which must be acquired from the soil, transported along the plant, distributed, and compartmentalized in different tissues and cells.

It should be underlined that, if on one hand these heavy metals are essential micronutrients (Salt et al., 1995), on the other hand the same elements can cause different toxic effects on the plant like induction of oxidative stress, variation of the water status of the plant and alteration to the structure and of the activity of several enzyme when exceeding given limit levels.

Heavy metal ions are able to bind to sulfhydryl groups of proteins (Viarengo, 1985), thus inducing changes in the structure of proteins and enzymatic activities, resulting in the toxic effects observed (Hodson, 1988).

Heavy metal ions like Cd, Cu, Zn, and Pb could induce oxidative stress, causing

changes in the activities of several enzymes. The oxidative damage caused by metals such as Cu and Fe can be explained by the changes in redox state (Fenton reaction) (Halliwell and Gutteridge, 1988), but the molecular mechanisms are still poorly understood.

Toxic levels of metals in soils could be found in the environment, and may be caused by both natural soil properties or by anthropic pressure, generally produced by agriculture, mining, manufacturing, and industrial waste (Garrido et al., 2002 e Rascio et al., 2011).

These HM are required as basal cofactors for various enzymatic reactions, and for stabilization of macromolecules, but when their concentration exceeds a physiological level, these could became toxic to the cell.

The plant cell has different homeostatic defence mechanisms regulating the concentrations of HMs in the cell in order to minimize the possible damage (Benavides et al., 2005); in addition, the affinity of the specific transport mechanism(s) affecting the accumulation of metals is essential (Clemens et al., 2002). Transport of inorganic ions occurs in plant through both apoplastic and symplastic pathway (White et al. 2002): e.g. Zn could be transported chelated to small molecules, including organic acids, histidine and nicotianamine (NA) (Broadley et al., 2007 and Trampczynska et al., 2010).

The first protection of the plants is in the roots: HM could be immobilized by extracellular carbohydrates (mucillogine, callose) in the cell wall; and on the external surface of the cell membrane (Verkleij e Schat, 1990; Nishizono et al., 1989; Wagner 1993).

Moreover, the metals toxicity could be limited by the inhibition of membrane carriers, or changes in the composition in lipids and fluidity of membrane (Meharg, 1993). HMs uptake may also occur by ionic channels for different elements like K^{+}, Ca^{++}, Mg^{++}, Fe^{++}, Mn^{++}, Cu^{++}, Zn^{++} (Clarkson e Lüttge, 1989; Rivetta et al., 1997). Generally, all the metals are able to induce a stress response in the plant by different mechanisms; a survey of the effects of the HMs is described in the table 1.

Metals	Type	Redox species	Toxic mechanism	Effects
Copper Cu^{++}	Essential	Redox active	Oxidative injury, ROS, oxygen free radicals (Chen et al., 2000).	Damage to the permeability of root cell, DNA strand breakage, defragmentation of proteins, or thylakoid of cell membrane and damage to photosynthetic pigments (Doncheva and Stoyanova, 2007; Mishra and Dubey, 2005; Lombardi and Sebastiani, 2005; Alaoui et al., 2004)
Zinc Zn^{++}	Essential	non-redox active	It can substitute other metals, especially those with similar ionic radii in the active sites of enzymes or transporters (Fukao et al., 2011)	Can produce ROS and adversely influence integration and permeability of membrane (Mishra et al., 2010; Hosseini et al., 2013)
Nickel Ni^{++}	Non Essential	non-redox active	It can readily move through phloem and xylem vessels. it can pass through the endodermal barrier (Ishtiaq and Mahmood, 2011; Seregin and Kozhevnikova, 2006)	Indirectly inflict oxidative stress via multiple mechanisms interfering with other enzyme and pathway (Yan et al., 2008; Siddiqui et al.,
Cadmium Cd^{++}	Non Essential	non-redox active	Interfere with the uptake, transport and use of several elements (Ca,Mg,P and K) and water by plants (di Toppi and Gabrielli, 1999)	Different cell damage as decreased in biomass (Mediouni et al., 2006)
Lead Pb^{++}	Non Essential	non-redox active	It can react with active groups of different enzymes and with the phosphate groups of ADP or ATP, and by replacing essential ions. Ahmed and Tajmir-Riahi, 1993)	Change cell membrane permeability, inhibition of ATP production, lipid peroxidation, DNA damage by increase of ROS, inhibition of seed germination, root elongation, transpiration, chlorophyll production. (Verma and Dubey, 2003; Seregin and Ivanov, 2001;

Table 1: Effects of heavy metals in plants

1.2 Nickel Stress

Among the HMs, Nickel represents an essential nutrient for higher plants.
Ni has various oxidative states but its divalent state (Ni^{2+}) is the most stable type in nature (Poonkonthai and Vijayavathi, 2012). It is an important micronutrient required by plant cells. Ni, especially at high levels, is able to move through phloem and xylem vessels, and thus rapidly translocated from roots to leaves (*Ishtiaq and Mahmood, 2011).* This transport is caused by the Ni distribution in root tissues, differently from other HMs; Ni can pass through the endodermal barrier and accumulate in pericycle cells (Seregin and Kozhevnikova, 2006) as described in maize (Seregin et al., 2003), and cowpea (Kopittke et al., 2006).
Moreover, the rate of Ni transport in the xylem was directly related to citrate and malate contents which are able to interact with the metal ion to transport it from roots to leaves and to store it into the vacuole, and this could help the plant to gain higher tolerance to the metal (Amari et al., 2016).
When present in small amounts, Nickel could be have positive effects on plants (Lin and Kao, 2005). It has been demonstrated that Nickel is essential for the activation of urease, involved in nitrogen metabolism (Bai et al., 2013; moreover, Ni is important for seed germination, and iron uptake (Nishida at al. 2011).
As expected, high Ni levels are phytotoxic, as recently described for wheat (*Triticum aestivum* L.) var. Bhakar-02 (Shafeeq et al., 2012).
Plant growth parameters and attributes could be actually negatively affected by Ni toxicity. In bean (*Phaseolus vulgaris*) it was demonstrated that Ni severely reduced plant height and leaf area at 150 $\mu g \cdot g^{-1}$ of soil (Al-Qurainy et al. 2009), or affects germination and seedling growth traits by reducing enzymes activities and breaking up the hydroxylation of nutrients in the endosperm of germinating seeds (Aydinalp and Marinova, 2009; Sethy and Ghosh, 2013).
Toxic levels of Ni could compete with several cations, as Fe^{2+} and Zn^{2+}, preventing their uptake by plants, and inducing deficiency and consequent plants chlorosis (Khan and Khan, 2010).
The induction of ROS caused by Ni toxicity was also observed. In wheat this results in physiological and biological disorders as enzymatic imbalance (Siddiqui et al., 2013).
Ni levels in soil and in plant tissues are variable: the average concentration in soils ranges between 2 - 200 mg/kg dry weight (Lepp 1981), while the average levels in plant tissues the interval 0,4 - 4 mg/kg dry weight (Markert 1996).
Different plants are able to hyper-accumulate Nickel.
This metal is a key factor affecting the production of secondary plant metabolites and so Ni accumulation could influence plant resistance to diseases (Wood and Reilly, 2007).
Threshold for Nickel hyperaccumulators is 1000=0,1% mg/kg dry weight (Adriano 2001)
Hyperaccumulation of Ni has been found in 390 taxa and 42 families: *Alyssum bertolonii* Desv. was the first hyperaccumulator of Ni found in 1948 (Minguzzi and Vergnano, 1948); *Thlaspi caerulescens* is able to hyperacumulate Ni, Pb , Zn, and Cd (Banásová, 2008).
In the last decades, several studies revealed that Ni hyperaccumulators could store this metal in non-protein amino acids, and nicotianamine (NA). NA is a small molecular weight chelator, enzymatically synthesised in a pathway involving four NA synthase genes (NAS1–4). In *T. caerulescens* ecotypes able to hyperaccumulate Ni, was identified the gene *Tc*NAS1 gene; once cloned in yeast, *Tc*NAS1 conferred high

levels of Ni tolerance (Mari et al., 2006). In plant, *Tc*NAS1 is expressed in shoots and is induced after 6h from Ni treatment; its expression determined accumulation of high levels of NA. In response to Nickel, NA seems to be translocate to the roots where chelates Ni, thus facilitating its transport to the shoot by xylem. Moreover, transgenic tobacco and *A. thaliana* overexpressing *Tc*NAS1 (Pianelli et al., 2005) showed an increase in Ni tolerance and higher Ni accumulation in the shoot.
Another mechanism consists in the sequestration by histidine (Haydon and Cobbett, 2007). Histidine (His) forms stable complexes also with Zn and Cd, and is present at high concentrations in the roots of hyperaccumulators such in *Alyssum lesbiacum* where the levels of His are increased by Ni treatment, even if the genes involved in the biosynthetic pathway were not induced (Persan et al., 1999; Ingle et al., 2005). Same results were obtained in *T. caerulescens,* showing high His levels in the roots, suggesting that His could be form complexes with Ni in the cytoplasm of root cells, thus decreasing the sequestration of Ni in vacuoles, and promoting the loading of the heavy metal in the xylem (Richau et al. 2009).

1.3 Hordeum vulgare

Hordeum vulgare (barley) is the world's fourth most important cereal crop. It's a member of the grass family and it is an important model for ecological adaptation.

About two-thirds of the global barley crop is used for animal feed, although for humans it is still the major source of Kcal in several parts of the world.

It's very important as model organism for different reasons:

- Barley is the fourth most important cereal plant in the world
- It has a short life cycle and morphological, physiological, and genetic characteristics
- It is simple to grow in both field and in laboratory
- Barley is diploid (2n = 2x = 14) self fertile inbreeding plant with genome size roughly 5.3 billion base pairs divided in 7 chromosomes (Fig. 2)
- Barley genome has been completely sequenced (International Barley Genome Sequencing consortium and also the UK Barley Sequencing Consortium 2012)

Barley genome is one of the largest diploid genomes sequenced to date, and this makes it a natural model for the genetics and genomics analyses for the Triticeae tribe, including wheat and rye. During the last years a great numbers of studies were done on barley in order to disclose many physiological mechanisms occurring in barley, in order to improve crop yield under biotic and abiotic stress.

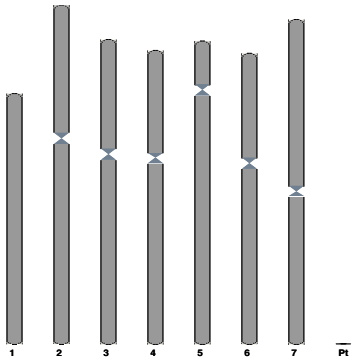

Coding genes	24,287
Non coding genes	1,512
Small non coding genes	1,498
Long non coding genes	14
Pseudogenes	268
Gene transcripts	64,096
Short Variants	18,331,939

Fig. 2: Barley genes.

1.4 Glucose 6P-dehydrogenase

The Oxidative Pentose Phosphate Pathway (OPPP) provides an alternative route to glycolysis for carbohydrate catabolism.

In higher plants, this pathway produces both reducing power (as NADPH) for amino acid and fatty acid anabolic pathways; and precursors of nucleotides and aromatic amino acids (Dennis et al., 1997) (Fig. 3).

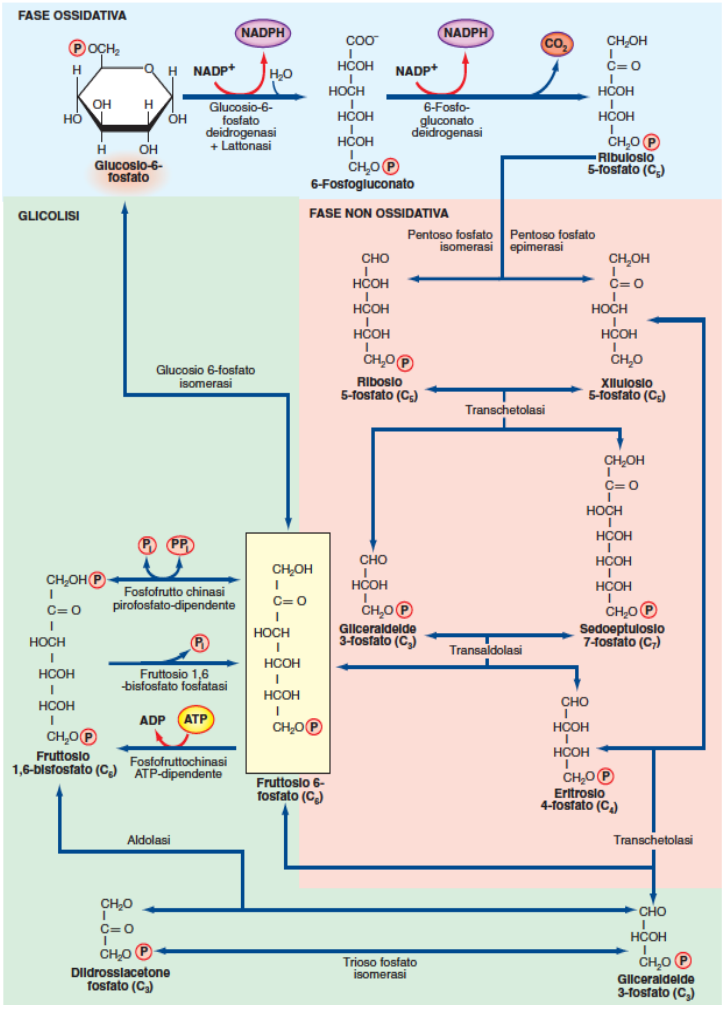

Fig. 3: reactions of OPPP cycle (Pentose Phosphate Pathway).

The presence of an OPPP in the plastids, as occurs in the cytosol, has been hypothesized in both photosynthetic (Schnarrenberger et al. 1973), and non-photosynthetic tissues (Nishimura e Beevers, 1981), and in cells cultures as well (Krook et al. 1998).

In higher plants an incomplete OPPP generally, but not always, occurs in the cytosol; a complete pathway occurs in the plastids (Debnam and Emes 1999).

The main functions of this cycle are the synthesis of:

- Precursors for nucleic acids
- Precursors for fatty acids

- Reduction of NADPH is essential for the biosynthesis (Senturk et al. 2009), and to counteract oxidative stress (Kruger and von Schaewen 2003) induced by abiotic stress (Bredemeijer and Esselink 1995; Nemoto et al., 2000; Cardi et al 2011, 2015); and pathogen attack (Scharte et al 2009).

The G6PDH is a most important enzyme of the cycle, catalysing the first reaction of the OPPP, converting glucose-6-phospate to 6-phosphogluconate-Δ-lactone and reducing $NADP^+$ to NADPH.

NADPH is a fundamental cofactor in many biochemical reactions of plant cells:
• NADPH is an essential cofactor in the reduction of nitrate and ammonium during N organication; in fact, in the roots the nitrite reductase glutamate synthase (GOGAT) require the reducing power produced in the pentose phosphate pathway.
• In plant cells, various stress induce an increase of oxygen radicals (ROS), acting as intracellular signals that activate the defence systems; ROS, however, are toxic to cells, thus scavenging systems are activated, requiring moieties of reductants such as NADPH.

Sequences coding for G6PDH exist in all organisms except for Archaebacteria (Wendt et al., 1999), and G6PDH enzymes from many living organisms have been characterized and the kinetic properties have been described extensively (Rosemeyer 1987; Levy and Cook 1991; Esposito et al. 2001a, 2001b; Ozer et al. 2001; Wang et al 2002; Cardi et al. 2013).

The existence of cytosolic and plastidic OPPPs in plants has been reported in leaves (Schnarrenberger 1973), roots (Emes et al., 1983) and cultured cells (Krook et al., 1998) based on the presence of cytosolic (Cy-G6PDH), chloroplastic (P1-G6PDH), and plastidic (P2-G6PDH) isoforms of G6PDH (Kruger and von Schaewen 2003; Esposito 2016)

G6PDH isoforms were firstly sequenced and described in *Solanum tuberosum,* where a cytosolic isoform (Graeve et al., 1994); and chloroplastic P1 isoform (von Schaewen et al., 1995); and a plastidic P2 isoform (Wendt et al., 2000) are present. All G6PDH are encoded by nuclear genes, and the compartmented enzymes show a plastidic transit peptide at the N-terminus.

When the sequences were grouped in a phylogenetic tree (Fig. 4)

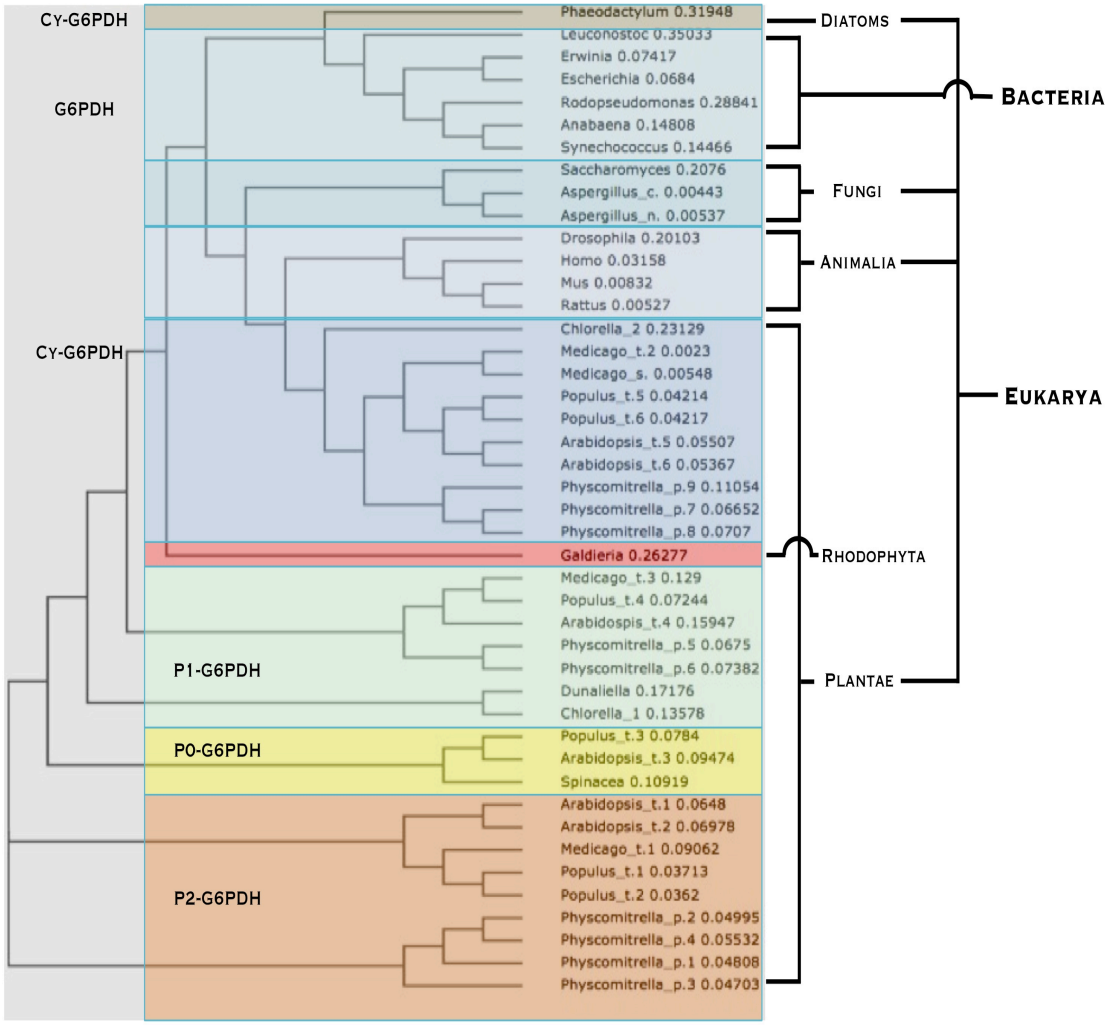

Fig. 4: Phylogenetic tree of the different G6PDH isoforms (Esposito 2016).

The active form of the enzyme is an omo-tetramer of 200–250 kDa - but it could be present also as homodimer of 100–120 kDa - constituted by 50–60 kDa subunits bound by saline bridges; this structure is stabilized by $NADP^+$ and regulated by a disulphide bridge on the N-terminal of the protein (Au et al. 2000).

The cytosolic isoform is insensitive to reductants, it presents a Ki_{NADPH} = 10-20 µM and it's not regulated by Trx (Graeve et al. 1994).

The chloroplastic P1-G6PDH is inactive in photosynthetic tissues upon illumination (von Schaewen et al., 1995; Esposito et al., 2005).

P2-G6PDH is specifically localized in root plastids, but this isoform can be detected also in photosynthetic tissues (Wendt et al., 2000; Esposito et al., 2005). In the root, P2-G6PDH plays a pivotal role providing reluctant for anaplerotic metabolism, in particular during nitrogen assimilation in non-photosynthetic plastids (Esposito et al., 2003), and fatty acid synthesis (Hutchings et al., 2005).

Recently, a singular gene (named G6PD4) was identified (Wakao and Benning 2005). These studies suggested G6PD4 encoding for a non-functional enzyme, named P0-G6PDH, but in the last years different analyses revealed an important role of this protein. Meyer et al., (2011) verified - during abiotic stress - the interaction between

Arabidopsis G6PD1 and G6PD4 (P0-G6PDH), with the assembly of heterodimers thus imported into the peroxisomes at the aim to support the increased request of NADPH under stress conditions; therefore an important role for P0-G6PDH has been postulated in the stress response of the plant.

All G6PDH isoforms shared the typical motifs of dehydrogenases composed by a Rossman-fold motif on the N-terminus, and $NADP^+$ -binding site. The putative active region (YRIDHYLGKE) presents a tyrosyl-residue, which is distinctive of cytosolic isoforms, instead of a phenylalanine, characteristic of compartmented isoforms (Fig. 5).

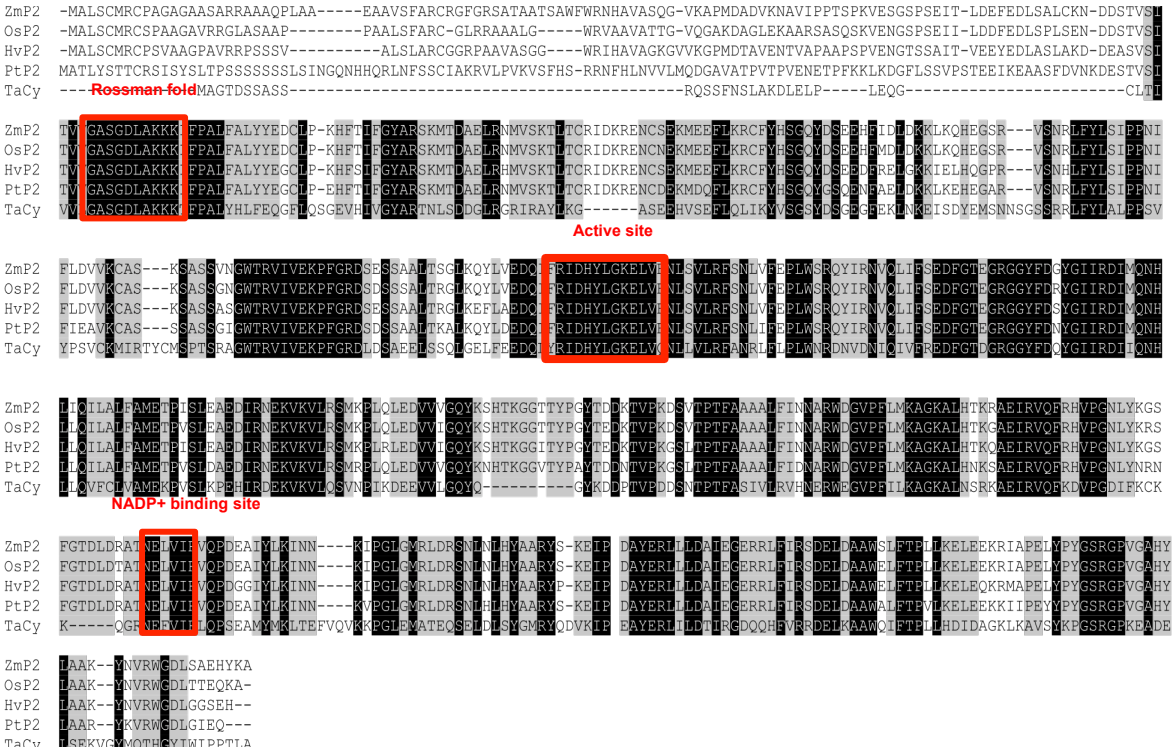

Fig. 5: Allineament of different organisms P2-G6PDH (Cardi et al. 2016).

The homotetramer is stabilized by $NADP^+$, which strongly influences the association state of the enzyme (Au et al. 2000) and when the ratio $NADP^+$/NADPH is low there is a reduction of disulphide bonds and the release of inactive monomers. It is also been observed that high levels of ATP not associated to Mg^{2+} inhibit G6PDH while the inhibitory effect is cancelled if ATP is associated with Mg^{2+}. This allowed to hypothesize the G6PDH requires ions Mg^{2+} for the stabilization of the structure: when the ATP levels not associated with the Mg^{2+} ions are too high, The ATP itself competes for Mg^{2+} by determining an inhibitory effect on G6PDH (Esposito et al. 2001).

1.5 G6PDH and different isoforms regulation

The G6PDH isoforms are subject to different regulatory mechanisms, possibly due to their different roles in plant cells.

The cytosolic isoform activity is closely dependent by the metabolites levels, and it appears to be regulated by mechanisms related to sugar sensing (Hauschild and Von Schaewen et al. 2003) (Fig. 6); more recently, it has been described an activation mechanism by phosphorylation on cyt-G6PDH by glycogen synthase kinase 3 in *Arabidopsis* (ASKα) under oxidative stress conditions (Dal Santo et al., 2012).

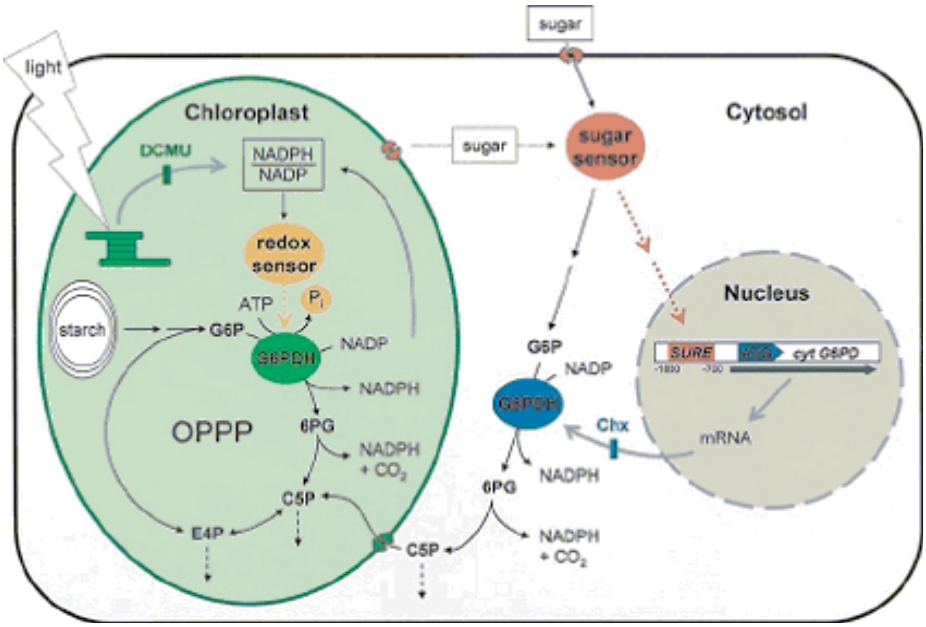

Fig. 6: Regulatory mechanisms of the different isoforms of G6PDH.

If the cytosolic isoform appears to be slightly sensitive to changes of the reductants, the activity of both compartmented isoforms is highly dependent on the ratio $NADP^+$/NADPH; (Fickenscher and Scheibe, 1986; Wenderoth et al. 1997) and thioredoxins (Nèe et al., 2009; Cardi et al., 2016).

The interaction of NADPH occurs at a different site from the binding site to $NADP^+$ (Wang et al 2008). The proposed hypothesis indicates that $NADP^+$ is important during dimers formation, and it may play a primary role in the formation of the tetramers.

The consequence is that, contrary to what was assumed previously, the $NADP^+$ is not only necessary for the catalytic activity (as substrate and eletron donor), but is involved in long-term stabilization of the tetramer (Wang et al., 2009).

The inhibition of G6PDH can be mimicked *in vitro*, by induced similar light stress, incubating the enzyme with increasing amounts of NADPH, or increasing the ratio NADPH/$NADP^+$ (Lendzian and Bassham, 1975; Esposito et al. 2001a), confirming NADPH as the main modulator for enzyme activity.

The inhibitory effect of NADPH connects the activity of the chloroplastic isoform P1-G6PDH to light exposure,, when the levels of reductants are very high and the NADPH

/ $NADP^+$ ratio increase; the same effect could be obtained when isolated chloroplasts are illuminated, and a drop in G6PDH activity was observed (Lendzian, 1980).

The inhibition by NADPH not totally explains the different regulation of the compartmental isoform of G6PDH (P1 and P2-G6PDH).

Particularly the effects of artificial reductants as the reduced dithiothreitol (DTTred) suggested that intermediates, or the final acceptor of electrons of the photosynthetic electron chain might be involved in the inhibition of the G6PDH.

These interactions, taking place between the reactions to light and the G6PDH depend on the ferredoxin-thioredoxin system, consisting of ferredoxin, ferredoxin-thioredoxin and thioredoxin reductase (FTR).

Moreover site-directed mutagenesis studies, and by construction of fusion proteins overexpressed in *E. coli* suggested that cysteine residues in the N-terminal sequence are involved in this redox regulation by the formation of a disulfide bridge: this residues are Cys^{149} and Cys^{157} in potato P2-G6PDH (Wenderoth et al., 1997); similar redox regulation has been confirmed in a number of plants, and namely in barley, where Cys^{175} and Cys^{183} have been proven as responsible of the redox regulation of P2-G6PDH (Cardi et al., 2013).

In barley plastidic isoform (P2-G6PDH) six cysteines are present, corresponsing to the highly conserved residues in G6PDH compartmented isoforms. All of them are located between the N-terminus and the center of the protein (von Schaewen *et al.,* 1995; Wenderoth *et al.,* 1997; Wendt *et al.*, 1999) (Fig. 7).

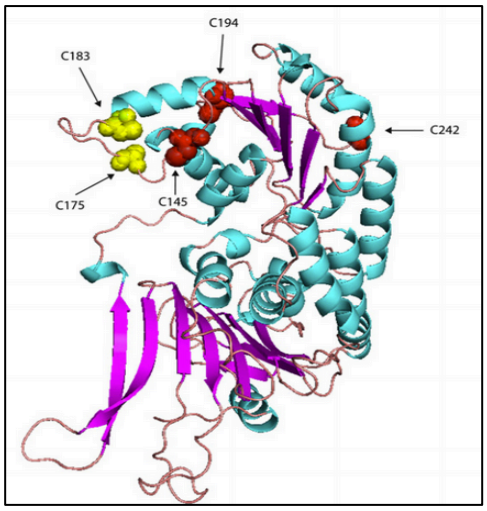

Fig. 7: predictive 3D structure of P2-G6PDH di *Populus tremula x tremuloides* (Cardi et al. 2016).

The disulphide bridge is located in the N-terminal portion of the monomer, in the proximity of the binding domain for $NADP^+$; the substitution of the disulphide-forming cysteines with serine residues completely abolishes the enzyme redox regulation (Wendt at al. 2000; Cardi et al. 2016).

1.6 G6PDH and stress

In the natural environment, many stresses as low or high temperatures, salt, drought, oxidative stress and heavy metal pollution, can occur simultaneously, and in response to these signals plants have developed different mechanism of defence.

Previous studies have shown that there is an evident association in plants between OPPP and the response to different stresses, and this association resulted in change in the activities and levels of G6PDH during exposure to various biotic (Scharte et al. 2009), and abiotic stress (Valderrama et al. 2006; Wang et al. 2008; Cardi et al. 2011, 2015; Landi et al., 2016).

Cy- and P2-G6PDHs are essential for stress tolerance: a specific increase of the cy-G6PDH activity and expression during drought stress was observed in tomato (*Solanum lycopersicum*) (Landi et al. 2016) and salt stress in wheat (*Triticum aestivum* L.) (Nemoto and Sasakuma, 2000) and in olive plants (*Olea europaea*) (Valderrama *et al.,* 2006).
Anthropic activities have greatly enhanced the number and extent of stress factors, thus increasing the damages on the flora and fauna, and, among pollutants, heavy metals are the major source of interest in the last years and for this reason a possible correlation between metals and changes in total G6PDH activity in various organisms was invastigated due to the G6PDH importance during biotic and abiotic stress.

1.7 Transit peptide analysis, and decoding of the barley P2-G6PDH sequence

In barley at least three genes encode for different G6PDH isoforms.

P2-G6PDH isoforms in both barley and poplar present a plastidic transit peptide, which in its turn, is different in these two enzymes. This may indicate different mechanisms and/or systems for entering plastids between monocots and dicot trees.

Plastidic transit peptides are formed by multiple domains, exhibiting a high degree of variability in their sequences (Emanuelsson et al., 1999). It has been shown that at least 7 different groups of plastidic transit peptides can be described, each including small repetitive amino acid sequences, required for the different steps during the import of proteins through the TIC-TOC complex on plastidic outer and inner envelopes (Lee et al., 2008). These observations complicate the comparison among different plastidic transit peptides, even among similar proteins imported into the same organelle.

Depending on the software used, the cleavage site of the N-terminal targeting sequence of *Hv*-P2G6PDH is predicted to occur at different positions: 38 for ChloroP, and 46 for Mitoprot (considering that plastidic and mitochondrial targeting sequences often share similar motifs). However, a significant identity between all these G6PDHs (plastidic and cytosolic) was only observed starting at amino acid 99 (sequence ASVSITV) on the N-terminus. Similar observations have been recently reported by Meyer et al., (2011) for *Arabidopsis* plastidic isoforms, and namely for the peroxisome-directed subunits of *At*G6PD4, presenting an unusual N-term transit peptide 152 amino-acids-long. On the other side, it should be underlined that the animal G6PDHs start in this region, thus suggesting that this region of the sequence is necessary for an active enzyme.

By bioinformatics analysis we identified a G6PDH isoforms similar to the Arabidopsis thaliana G6PD4. Moreover the *Hordeum vulgare* G6PD4 shows a probable peroxisomal targeting motif, PTS1-like, in the C-terminus.

Overall, this analysis indicates that all existing prediction programs fail to detect the right position for cleavage of the *Hv*-P2G6PDH plastidic transit peptide. While the N-term region of *Hv*-P2G6PDH is clearly different to any of the plastidic transit peptides families identified previously (Lee et al., 2008), some motifs, involved in protein import in the chloroplasts, are indeed present supporting our present hypothesis (Table 2 – S. Esposito - unpublished).

The reason might be that barley plastidic transit sequence is unusual, as it contains a rather large number of uncharacteristic acidic residues from position 59, whereas the software have been developed to screen for an enhanced presence of basic residues and counter-selection of acidic amino acids in transit peptides.

	Cab	DNAj	BCCP	PORa	GLU2	TOCC	*Hv*P2-G6PDH
T1							^{01}MALSCMRCPS^{10}
T2				SAFSV			^{11}VAAGPAVRRP^{20}
T3	KSKF	SSSSS	FPIQN	SSS	SAKLS	RPVSP	^{21}SSSVALSLAR^{30}
T3					STKTI	LTRSL	^{31}CGGRPAAVAS^{40}
T4	PNPL	NSRRK				VPFRS	^{41}GGWRIHAVAG^{50}
T4	GNVGR	NTKML					^{51}KGVVKGPMDT^{60}
T5	IRMAA	NRSKV		EQSKA	ISKGT	RSISR	^{61}AVENTVAPAA^{70}
T5		VCSSS		DFVSS	KRRNE		^{71}PSPVENGTSS^{80}
T6			PSRSS	SLRCK			^{81}AITVEEYEDL^{90}
T6			YPVVK				^{91}ASLAKDDE^{98}

Table 2 - Critical sequence motifs for protein import into chloroplasts as described by Lee et al. [38], and their comparison with first 99 aa in P2G6PDH from *Hordeum vulgare* cv Alfeo (*Hv*P2G6PDH – Accession#: AM398980).

T1- T6 represent segments of 9-12 aa residues in the putative transit peptides in which typical motifs had been previously identified and localised [38].

Cab, RbcS chlorophyll a/b binding protein, DNAJ, DnaJ-J8; BCCP, biotin carboxyl carrier protein; PORA, protochlorophyllide oxidoreductase A; GLU2, ferredoxin-dependent glutamate synthase 2; TOCC tocopherol cyclase. In the last column (*Hv*P2-G6PDH) the positions of the aminoacids residues in the transit peptide sequence are indicated by apex numbers.

1.8 Catalase and Ascorbate peroxidase

Catalase (CAT; EC 1.11.1.6) and ascorbate peroxidase (APX; EC 1.11.1.11), represent the most important enzyme responsible for the Reactive oxygen species (ROS) scavenging in plants.

ROS consist of both free radical (O_2, superoxide radicals; OH, hydroxyl radical; HO_2, perhydroxy radical and RO, alkoxy radicals), and non-radical molecules as H_2O_2, hydrogen peroxide and $1O_2$, singlet oxygen.

There is an equilibrium between the production and the scavenging of ROS in plants. This balance may be perturbed by various stress factors (Jones, 2006; Foyer and Noctor, 2005a, 2005b, 2009).

The antioxidant defence is based on a very efficient enzymatic machinery (superoxide dismutase, SOD; catalase, CAT; ascorbate peroxidase, APX; glutathione reductase, GR; monodehydroascorbate reductase, MDHAR; dehydroascorbate reductase, DHAR; glutathione peroxidase, GPX; guaicol peroxidase, GOPX and glutathione-S-transferase, GST) which is able to protect plants against oxidative stress damages.

Cat, mainly located in peroxisomes and glyoxysomes, and APx, mainly located in the cytosol and chloroplasts (Willekens et al., 1995; Takeda et al., 2000; Teixeira et al., 2004-2006) together with Glutathione peroxidase are able to efficiently remove H_2O_2, during oxidative stress (Fig. 8).

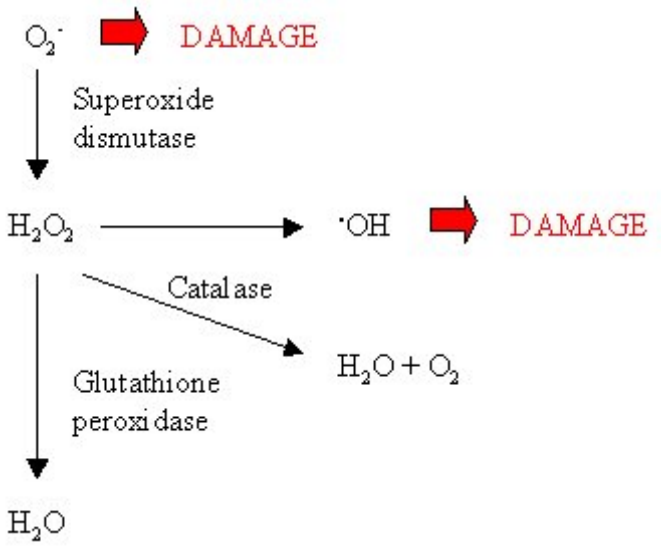

Fig. 8: ROS savaging enzymes reactions

CATs are tetrameric heme-containing enzymes catalysing the conversion of H_2O_2 into H_2O and O_2 ; this reaction is essential for ROS detoxification during stress but plays a role also in signal perception (Mhamdi et al., 2010; Hu et al., 2010; Nie et al., 2015; Liu et al., 2011). CAT isozymes have been widely studied in higher plants (Polidoros et al., 1999) as in *H. vulgare* (Azevedo et al., 1998), in *Helianthus annuus* (Azpilicueta et al., 2007), in *Brassica* (Frugoli et al., 1996) and others plants.

CAT is mainly localized in peroxisomes, and it has been demostrated it is present in leaves, cotyledons, roots, in glyoxysomes and unspecialized peroxisomes as well (Su et al., 2014); CAT has found in mitochondria too (Scandalios, 1990; Heazlewood et al.,

2004; Shugaev et al., 2011).

Otherwise, Apx belongs to the class I heme-peroxidases and is found in most eukaryotes including higher plants (Battistuzzi et al., 2001; Sharma and Dubey, 2004; Yadav et al., 2014).

APX has a higher affinity for H_2O_2 and utilizes ascorbate (AsA) as specific electron donor for the reduction of H_2O_2into H_2O in organelles including chloroplasts, cytosol, mitochondria, and peroxisomes (Groden and Beck 1979; Miyake and Asada 1996) (Fig. 9).

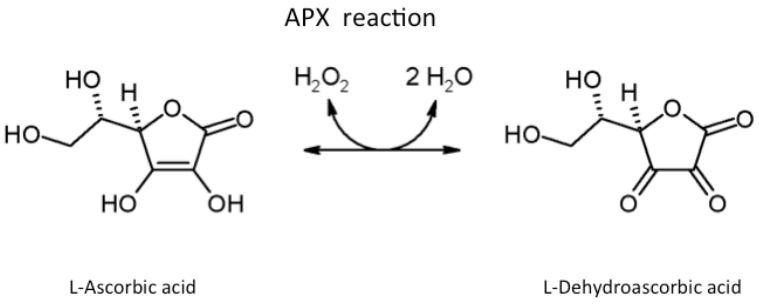

Fig. 9: apx reaction.

Different studies reveal an increase/decrease of these activities during stress; a decrease in catalase activity, related to changes in salicylic acid content during oxidative stress, were observed in rice, wheat, and cucumber seedlings (Shim et al., 2003); an increase in catalase activities, and an up-regulation of soluble ascorbate peroxidase is observed in leaves of *Pelargonium zonale* exposed to strong sunlight condition (Vidović et al., 2016); higher CAT activity were found in cadmium (Cd)-exposed *Brassica napus* (Hasanuzzaman et al., 2012b), *Oryza sativa* (Hsu and Kao, 2004), *Brassica juncea* (Mobin and Khan, 2007), *Triticum aestivum* (Khan et al., 2007), and arsenic-exposed *Triticum aestivum* seedlings (Hasanuzzaman and Fujita, 2013a).

In contrast, Cd exposure caused a decline in CAT activity (Balestrasse et al., 2001; Agami and Mohamed, 2013).

In general all these conditions are able to induce a stress response resulting in changes of the activities of these enzymes and the regulation of their levels of synthesis and/or expression.

1.9 Fumarase

Fumarase (fumarate hydratase; E.C. 4.2.1.2.) is an important enzyme of the tricarboxylic acid (TCA) cycle (Fig. 10).

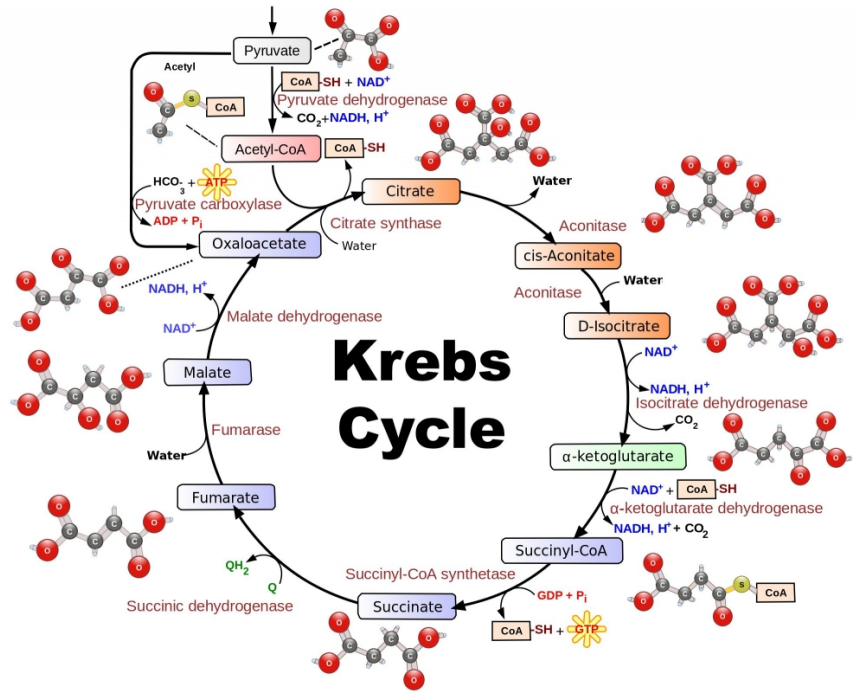

Fig .10: TCA (Krebs Cycle) reactions.

This cycle is known also as citric acid cycle (or Krebs cycle) consisting of a series of biochemical reactions to generate energy from acetyl-CoA derived from carbohydrates, fats and proteins. Fumarase catalyses the reversible hydration of fumarate to malate.

A study on purified pea fumarase revealed inhibition by physiological concentrations of pyruvate, 2-oxoglutarate and the adenine nucleotides ATP, ADP and AMP (Behal and Oliver, 1997).

Fumarase is localized in mitochondria but a localization of it in the cytosol has also been confirmed for such plants as *Arabidopsis thaliana* and maize (Eprintsev et al., 2014); in contrast, in sycamore, potato and tomato only a single gene, and single mitochondrial isoform were detected, as in rice and poplar, whose genomes present only a single gene encoding for fumarase (reviewed in Araújo et al., 2011).

A main role for fumarase during stress is reported in plant cells; in *Arabidopsis thaliana,* fumarase is essential for cold acclimation of metabolism in the cold-tolerant model varieties (Dyson et al., 2016), and during light stress (Eprintsev, 2016); in *Hordeum vulgare* (López-Millán et al., 2012), and *Beta vulgaris L.* (Sagardoy et al., 2011), leaf extracts after Fe-deficient and Zn excess stress showed an increased fumarase activity.

All these studies reveal the importance of this enzyme during the stress and the possibility of the plant to counteract the stress through changes in activity and levels of this enzyme.

1.10 NADH-GOGAT

Nitrogen assimilation into carbon skeletons represents a physiological process of a great importance for plant growth and development.

The primary assimilation of $NH4^+$ into aminoacids occurs thanks to glutamine synthetase (GS, EC 6.3.1.2) and glutamate synthase (2-oxoglutarate aminotransferase, GOGAT. In higher plants were described two isforms of GOGAT. These isoforms have different characteristic such molecular mass, kinetics, tissue distribution, and different specificity towards the reductant: Fd-GOGAT (EC 1.4.7.1), NADH-GOGAT (EC 1.4.1.14) (Suzuki and Gadal, 1982).

The Fd-GOGAT is a monomeric iron sulphur flavoprotein made by a single polypeptide chain of 150 kDa (Vanoni and Curti, 1999). Most of the Fd-GOGAT activity is located in the leaf chloroplasts and it is involved in the assimilation of NH_4^+ derived from nitrate reduction, or from photorespiration (Turano and Muhitch, 1999; Pajuelo et al., 1997).

On the other hand, NADH-dependent glutamate synthase (NADH-GOGAT; EC 1.4.1.14) is a monomeric iron sulphur flavoprotein with a molecular mass of 200–240 kDa and its activity is located mainly in the root plastids (Gregerson et al., 1993; Lea and Miflin, 2003). The reaction of the NADH-GOGAT consists in the transfer of the amide group of glutamine formed by glutamine synthetase (GS; EC 6.3.1.2) to 2-oxoglutarate to obtained two molecules of glutamate (Fig. 11).

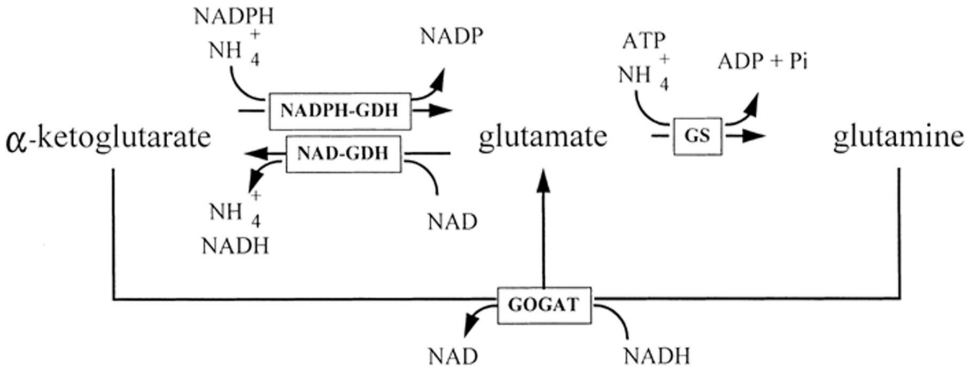

Fig. 11: NADH-GOGAT reaction.

Different studies reveal that NADH-GOGAT assimilates non-photorespiratory ammonium (Lancienet al., 2002, Potel et al., 2009) in *Arabidopsis,* and it is implicated, especially in young leaves, and grains at the early stage of ripening of rice, in the re-utilization of glutamine transported from the phloem and xylem (Hayakawa et al., 1994).

Variations in transcripts and activity of NADH-GOGAT were observed in different stress status. In the epidermis and exodermis of rice roots a specific expression of NADH-dependent glutamate synthase protein (REF?), and a variation in activity and levels of this enzyme in *Hordeum vulgare* in response to the supply of ammonium ions has been described (Esposito et al. 2005).

1.11 Phosphoenolpyruvate carboxylase

Phosphoenolpyruvate carboxylase (PEPCase, EC 4.1.1.31) is the enzyme responsible for the primary fixation of CO_2 into oxaloacetate, which is subsequently converted to malate (O'Leary, 1982) (Fig. 12).

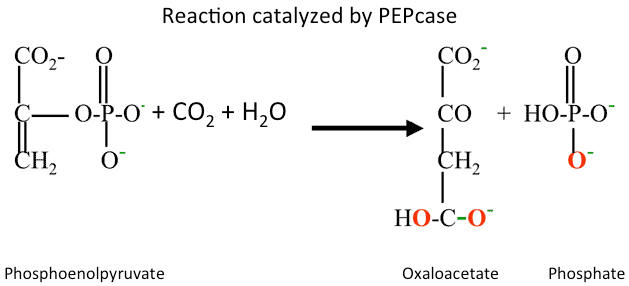

Fig. 12: Phosphoenolpyruvate carboxilase reaction.

PEPCase is present in bacteria, algae, and higher plants and in addition to its role in photosynthesis, levels and activity of pep carboxylase have been reported to vary in response to different abiotic stresses (García-Mauriño et al. 2003; Monreal et al. 2013) for replenishment of tricarboxylic acid cycle intermediates, NADPH regeneration, and recapture of respired CO, (Chollet et al., 1996; Lepiniec et al., 2003; Izui et al., 2004).

PEPCase is regulated by a phospho*enol*pyruvate carboxylase-kinase (PEPCaseK) which in turn is regulated by different stress as salinity condition. Indeed in salt-treated *Sorghum* plants an increased PEPCase-K activity and, as consequence, also of PEPcase, were observed (Echevarría et al. 2001; García-Mauriño et al., 2003) and an increase of ABA was responsible for this (Monreal et al., 2007a). The same salinity effects on PEPCase activity were also observed in *Hordeum vulgare* (a C3 plant), and *Aleuropus litoralis* (a C3–C4 intermediate plant) (Amzallag et al., 1990; Popova et al., 1995).

Moreover in C4 plants, PEPCase is controlled by a light-dependent regulatory phosphorylation process (Chollet et al., 1996; Vidal et al., 1996) but also by chilling (Friesen et al., 2016).

The fact that PEPCase has an important role in C4 and CAM plant metabolism allows this enzyme to be implicated in the adaptation to stress in different higher plants, and to be one of the principal enzymes involved in the regulation of stress conditions.

1.12 Heat shock proteins (HSP70)

Protein function is determinant for all the reaction inside the cells, but the function is influenced by how the protein is correctly folded to form a specific three-dimensional structure. The three- dimensional structure of the proteins is not determinated just by their primary structure, contributing only 50% for the correct folding (Dobson et al., 1998), but also by free energy of the constituent amino acid residues (Levitt et al., 1997) as described in principle *in vitro* studies by Anfinsen (1972 Nobel prize in chemistry) (Fig. 13). However, cells conditions as temperature, pH, salt concentration, tend to destabilise the correct final structure of the protein.

For these reasons, molecular chaperones are presents into the cells; these proteins help the correct folding of proteins, and they able to prevent the uncorrect association, or aggregation, of exposed hydrophobic surfaces of unfolded or partially folded proteins. Under stress conditions, such as heat shock, the presence of these chaperones is very important cause that allows cellular proteins to avoid and/or recover from aggregation.

Among the different chaperones a major role in the stress response is given by heat shock proteins (HSP). These proteins are located in all cell compartments (cyt, myt, clp, nucleus, ER), and are generally divided in different classes: HSP100, HSP90, HSP70, HSP60 e small HSP (with molecular weight between 17 e 30 kDa).

In particular the 70kD stress proteins comprise a ubiquitous set of highly conserved molecular chaperones that range in actual size from 68 to 110kD (Vierling, 1991; Miernyk, 1997).. Some family members could be divided in two types:

- HSC70: the 70-kD heat shock cognate which are constitutively expressed
- HSP70: the 70-kD heat shock protein which are expressed only when the organism is challenged by environmental stresses such as temperature extremes, anoxia, heavy metals, and predation

The HSP70 could be so very important during abiotic stress such as in *Elodea canadensis* (Esposito et al., 2007) and in the moss *Leptodyctium riparium* (Esposito et al., 2012).

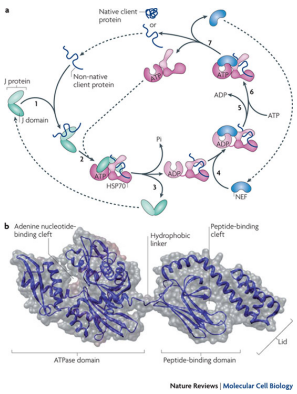

Fig. 13: Heat shock proteins conserved domanin (Nature review).

2 AIMS OF THE PROJECT

- Overexpression and purification of the recombinant poplar wt-P2-G6PDH and ser to cys mutants
- Analysis of the effects of different heavy metals on enzyme activity and kinetic parameters
- Determination of the effects of Nickel on Barley plants growth, physiological parameters, and activities of basal metabolism enzymes
- Analysis of the possible changes in G6PDH activities,occurrence and transcripts in plants after exposition to Nickel
- Analyse the subcellular localization of different barley G6PDH isoforms in *Arabidopsis* protoplasts and *N.benthamiana* leaves

4 MATERIALS AND METHOD

4.1 Induction of Gene Expression and Bacterial growth

The plastidic G6PDH sequence was identified from poplar (*Populus trichocarpa*) genome (http://www.plantgdb.org/PtGDB/) and sequenced using poplar cDNA (courtesy of J.-P. Jacquot – N. Rouhier, Nancy, France). The sequence was cloned in pET15b plasmid, and the recombinant protein was overexpressed in *E. coli* strain BL21(DE3)psBET as standard host, after transformation by electroporation at 1.8 KV, 600Ω, 3µF (BioRad Gene Pulser elettroporator).

Different bacteria colonies were tested to verify their capability to overexpress the recombinant protein. Colonies were grown in 3 ml of LB medium (10% Tripton, 5% east extract, 10% NaCl) with ampicillin and kanamycin (50 mg/L) for 4h and after for other 3h with the inductor isopropyl-b-D-thiogalactoside (IPTG-0, 1mM). Bacteria were harvested by centrifugation at 3000 rpm for 10 min, and the pellet resusped in BBF + β-mercaptoethanol for SDS-PAGE.

The colony best expressing the recombinant protein was used for bulk preparation of the enzyme . The colony was inoculated in 250 ml of sterile LB medium (10% Tripton, 5% east extract, 10% NaCl), and grown on an orbital shaker over night at 37 °C.

Aliquot of this suspension was inoculated in 1 to 3 litre(s) of LB medium containing ampicillin and kanamycin (50mg/L), until a 0.06- 0.08 O.D. (600 nm) was obtained, and grown at 37° C. After 3 hours (about 0.8 O.D – 600 nm), the growth was blocked moving the bacterial suspension at 4°C and adding ethanol 0.5% for 4 hours. Then the colture was induced for recombinant protein synthesis by adding 0.1 mM isopropyl-b-D-thiogalactoside (IPTG) at 20°C over night or to 1,1 O.D. (600 nm). Cells were then harvested by centrifugation at 6000 rpm, 4 °C for 20 minutes (Beckman Avant JA 25).

4.2 Isolation and purification of G6PDH

Cells pellet was resuspended in a buffer containing 50 mM K_2HPO_4, 50mM KH_2PO_4, 300 mM NaCl, 10 mM Imidazole, pH 7.4 by gentle shaking (Lab Line Super Mixer).

The resuspended cells were treated with 0,1% of polyethylenimine for 20 minutes, sonicated for 5 min (ON/OFF 00.05.00, Misonix Processor XL) for two cycles, and centrifuged at 16000 rpm for 45 minutes at 4°C (Beckman Avant JA 25).

The surnatant containing enzymatic activity was stored and used for purification.
Ammonium sulphate $(NH_4)_2SO_4$ was added to 70% saturation and the suspension incubated at 4°C overnight; the protein containing G6PDH activity precipitated, and after centrifugation (16000 rpm for 45 minutes at 4°C - Beckman Avant JA 25) the pellet was dissolved in 50 mM K_2HPO_4, 50 mM KH_2PO_4, 300 mM NaCl, 10 mM Imidazole, pH 8.0; the suspension was desalted by gel filtration (PD10 column - Sephadex G25; GE-Healthcare)

The *Pt*P2-G6PDH was purified by Immobilized Metal Ion Affinity Chromatography (IMAC) using 1 ml Hi-Trap column (GE-Healthcare) and imidazole elution (Cardi et al., 2013; 2016). The bound recombinant protein was eluted in a buffer containing 50 mM K_2HPO_4, 50 mM KH_2PO_4, 300 mM NaCl, 250 mM Imidazole, pH 7.4.

*Pt*P2-G6PDH eluted in a single peak, the active fractions were collected and diluted in 30 mM Tris-HCl, 100 mM NaCl, 5% glycerol, pH 8.00 and then concentrated by ultrafiltration (Diaflo Ultrafilters, Amicon) under N_2.

4.2.1 G6PDH assay

The activity of the purified enzyme was determined by assays at 25°C according to Cardi et al (2013), by measuring the reduction of $NADP^+$ to NADPH at 340nm in the presence of glucose-6-phosphate in a 1 cm cuvette in Cary 60 UV-Vis (Agilent Technologies) spectrophotometer.
The reaction mixture contained 5 mM $MgCl_2$, 150 μM $NADP^+$, and 3 mM G6P in 50 mM Tris–HCl buffer, pH 7.5. Blank was without G6P.
One unit of enzyme (U) activity defined as the amount of enzyme that reduced 1 μmol $NADP^+$ per minute, the total activity was expressed as units per mg of protein.
The purified protein was confirmed as pure by SDS-PAGE, and identified using specific antibodies by Western blotting analyses.

4.3 Proteins determination

Protein concentrations were determined according to Bradford (1976).

The Bradford protein assay is a spectroscopic procedure and a colorimetric protein assay based on the absorbance shift of the dye Comassie Brilliant Blue G-250 at 595nm. The increase of absorbance at 595 nm is proportional to the amount of bound dye to aromatic aminoacid residues present in the protein chain, and thus to the amount of protein in the sample, referred to a standard curve obtained using bovine serum albumin (BSA) as standard protein (Fig. 14).

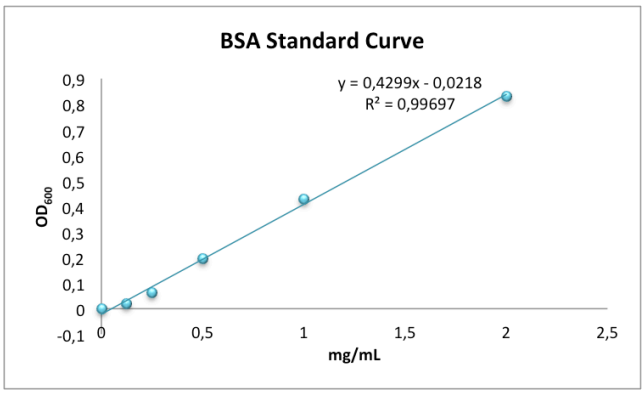

Fig. 14: BSA standard curve for proteins determination.

4.4 SDS polyacrylamide gel electrophoresis (SDS-PAGE)

SDS-PAGE was performed using Laemmli's procedure (Laemmli 1970). The acrylamide concentrations were 4% (stacking) and 10% (running), containing 10% sodium dodecyl sulphate (SDS) for stacking gel and running gel, respectively. After the run at 40mA-180V for 75min (BIO-RAD Mini-Protean Tetra System), gels were stained in a solution of 0.1% Comassie Brilliant Blue R-250, 50% methanol, 10% acetic acid and 40% distilled water by gentle shaking for 20 min. Gels were rinsed and washed in the same solution without the dye (Table 3).

Running

Percentage	10%	
N. of gels	2 gels	4 gels
H2O	5.3 ml	10.6 ml
Acrylamid 30%	6.6 ml	13.2 ml
Separating gel solution	5 ml	10 ml
Glycerol 70%	2.855 ml	5.71 ml
SDS 10%	200 µl	400 µl
APS 10%	100 µl	200 µl
TEMED	10 µl	20 µl

Staking

Percentage	4%	
N. of gels	2 gels	4 gels
H2O	3.47 ml	6.94 ml
Acrylamid 30%	1 ml	2 ml
Stacking gel solution	1.875 ml	3.75 ml
Glycerol 70%	1,078 ml	2.156 ml
SDS 10%	75 µl	150 µl
APS 10%	37.5 µl	75 µl
TEMED	7.5 µl	15 µl

4.5 Western blotting analyses

After SDS-PAGE, proteins were immediately blotted onto a 0.2 μm nitrocellulose membrane (Bio-Rad) overnight at 9V, 300 mA. The membrane was saturated by 1% non-fat milk blotting for 1h, and after three washing in TBS + 1% Tween, filters were probed with primary antisera for 1h. Antisiera against his-tag was SIGMA cat.1305538 (1:1000); antisiera against different potato G6PDH isoforms (Wendt et al 2000) was a generous gift of Prof. A. von Schawen (Munster - Germany).
Then membranes were developed with secondary antibody (anti-mouse for his tag - Sigma A9044; anti-rabbit for G6PDH - Sigma A0545, 1:80.000). Then, reacting proteins were visualized by enhanced chemiluminescence using Amersham ECL Prime kit, and images acquired by a high definition camera (Chemidoc System – Quantity One software – Bio-Rad).

4.6 *In vitro* effects of metal ions

Heavy metals salts were tested for their effects on *Pt*P2G6PDH: $CdCl_2$, $CuSO_4$, $ZnSO_4$, $NiSO_4$, $Pb(CH_2COO)_23H_2O$. Assays were carried out under standard conditions, varying the concentration of single metals.

Results were generally expressed as percentage of the control (no HM). All assays were performed in 5 replicates for each concentration.

Metal ions concentrations producing 50% inhibition (IC_{50}) were calculated from the non-linear regression graphs. The same procedure was utilized also for the *Pt*P2G6PDH mutants, where the cysteine residues present in the sequence were substituted with serine.

4.7 Plant material and growing conditions

Seeds of barley (*Hordeum vulgare*, Nure) were germinated on moistened paper for approximately 5 days. The seedlings were grown in a controlled cabinet according to Esposito et al. (2001a) at 20°C under 16-h-light/8-h-dark regime with approximately 180 μmol photons m^{-2} s^{-1}. Air was supplied continuously and the nutrient solutions were controlled for pH and adjusted daily.

Plants were grown for 7 days in optimal growing conditions in a nutrient solution at pH 6,5 (Rigano et al. 1996) (Table 4):

KH_2PO_4	0.01M
K_2HPO_4	0.01 mM
K_2SO_4	1.25 mM
$MgCl_2$	1 mM
Oligo-elements	10 mL/L
$FeSO_4$ EDTA	3.5 mg/L
$Cacl_2$	1 mM
$(NH_4)_2SO_4$	2.5 mM
H_2O	Final volume 1L

Oligoelements	
KCl	190 mg/L
H_3BO_3	80 mg/L
$CuSO_4$ x 5 H_2O	6 mg/L
$MnSO_4$	43 mg/L
$ZnSO_4$ x 7 H_2O	30 mg/L
$(NH_4)_6Mo_7O_{24}$ x $4H_2O$	1 mg/L

After 7 days barley plants were exposed to different heavy metals. The plants were treated at different concentrations (0.5 mM, 1 mM, 2 mM) of metals, and at given times, samples were collected for measurements (Fig. 15).

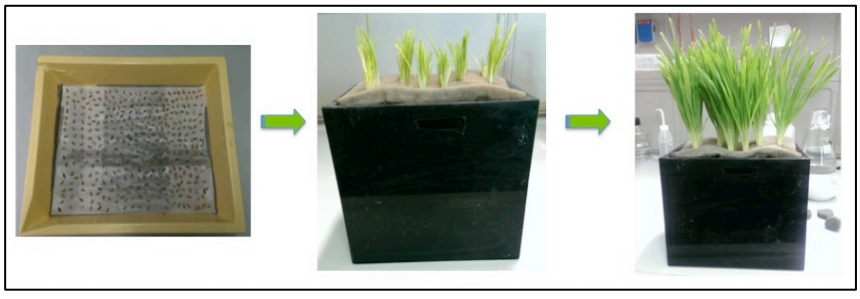

Fig 15: Steps of idroponic growth

4.8 Proteins extraction and G6PDH activity determination

Extracts for determination of enzymatic activity were prepared from 0.3 g of leaves or roots. The plants were washed with distilled water and then cut in small slices for protein extraction. Samples were mechanical homogenized (Tyssue Lyzer, Quiagen) at 50 Hz (2 min - 5 times cycle) in ice-cold extraction buffer different for each protein (1:2 ratio W/V – see after). Homogenates were centrifuged at 13000 rpm for 20 min two times and the supernatant fraction was utilised for analyses.

Extracts for determination of G6PDH enzyme activity and protein content were prepared in Tris-Hcl 50 mM, $MgCl_2$ 5 mM, EDTA 4 mM, 10% glicerol, pH 7.9 extraction buffer.

G6PDH activity assays were run as previously described (par. 4.2.1); protein determination and western blotting procedure have been described previously (par. 4.3 and 4.5, respectively).

4.9 Determination of catalase activity

Catalase activity was extracted in 50 mM Tris-HCl, 0.1 mM EDTA, 0.2% Triton X-100, 1 mM PMSF, 2 mM DTT, pH 7.
About 0.5 g of plant roots/leaves were grind in a cold mortar and pestle using liquid nitrogen and then suspend in a homogenization buffer solution (1:3 ratio). The resultant suspension was centrifuge at 14000 rpm for 30 min at 4°C. The surnatant containing activity was utilized for the determination of the catalase rate.
In this protocol, CAT (EC 1.11.1.6) activity was estimated according to Beers and Sizer (1952), measuring the initial rate of disappearance of H_2O_2 at 240 nm. The assay was carried out under standard conditions in 90 mM of K-PO4 buffer (pH 7) and 0,06% H_2O_2.
The decrease in H_2O_2 was observed at 240 nm (10 seconds intervals) for 180 seconds. The H_2O_2extinction coefficient (E) = 39,4 $mM^{-1}cm^{-1}$at 240 nm and 1 nmol H_2O_2 $ml^{-1}min^{1}$ was defined as 1 unit of CAT.

4.10 Determination of ascorbate peroxidase activity

APX (EC 1.11.1.11) activity was measured according to Nakano and Asada (1981), monitoring the decrease in absorbance at 290 nm of ascorbate oxidized.
The extraction buffer was 50 mM Na-P Buffer (pH 7.0), 2% PVPP, 0.1 mM EDTA, 2 mM Ascorbate.

The reaction mixture contained 30 mM KH_2PO_4 buffer (pH 7.0), 0.1 mM EDTA, 0.5 mM ascorbate and 0.06% H_2O_2. During the assay the reduction in ascorbate concentration was observed at 10 seconds intervals for 3 min at 290 nm.

4.11 Determination of fumarase activity

Samples were homogenized in extraction buffer (50 mM Hepes-KOH, pH 5 mM $MgCI_2$, 1 mM EDTA, 5 mM DTT, 1 mM PMSF, 10% glycerol, and 0.1% Triton X-100).

Fumarase assay were performed monitoring the conversion of L-Malate in Fumarate + H_2O. A reaction mixture of L-malic acid was prepared by utilizing 7 mg/mL of L-malic acid in 100 mM KH_2PO_4, pH 7.6; the solution was brought at pH 7.6 with 1N of KOH.

The increase of absorbance were measured at 240nm at 25°C for 10 minutes

48.3 mM L-malic acid. The blank were done just with buffer without the sample. In a 3 mL reaction mix, the final concentrations were 96.7 mM potassium phosphate,

One unit of enzyme (U) activity was defined as the amount of enzyme that reduced 1μmol $NADP^+$ per minute, the total activity was expressed as units per mg of protein.

4.12 Determination of NADH-GOGAT activity

NADH-GOGAT activity was assayed monitoring the conversion of 2 x L-glutammate + $NAD^+ + H^+ \rightleftarrows$ L-glutammine + 2-oxoglutarate + NADH by observing NADH oxidation to NAD^+ at 340 nm.

The proteins extraction was done in KH_2PO_4–KOH 25 mM, EDTA 1 mM, cysteine 1mM, FAD^+ 25 µM, pH 8.8.

The assay mixture contained 50 mM KH_2PO_4–KOH, pH 7.5, 10 mM 2 oxo-glutaric acid, 10 mM Gln, 1 mM NADH, 1 mM amino-oxyacetate, and extract. The reaction was started by adding glutamine. The activity was expressed as µmol oxidized NADH $min^{-1}mg^{-1}$ protein.

4.13 Determination of Phospho*enol*pyruvate Carboxylase activity

The PEPcase extraction was done in Tris-HCl 100 mM, $MgCl_2$ 10 mM, 20% glicerol, DTT 5 mM, pH8.

Phospho*enol*pyruvate carboxylase assay was performed based on the principle that:

$PEP + HCO_3^- \rightarrow$ Oxaloacetate + Pi (made by PEP carboxylase)

Oxalacetate + NADH → Malate + NAD^+ (made by Malic Dehydrogenase)

During the assay the formation of oxaloacetate is monitored spectrophotometrically as a decrease in A_{340} resulting from the oxidation of NADH. The assay was performed in 50 mM Tris-HCL pH 7,5; 18 mM $MgCl_2$; 0.18 mM NADH; 0.18 mM $NaHCO_3$; 0.5 U MDH and 0.9 mM PEP.

The enzimatic units were obtained recorded first the decrease in A_{340} to establish a blank rate (spontaneous NADH oxidation) and after the addition of PEP. One unit of enzyme is defined as the quantity of enzyme able to oxidize one micromole of NADH per minute at 25°C per mg of protein.

4.14 HSP70 extraction

To evaluate the effects of heavy metals stress, the levels of HSP70 were checked.

Samples were taken at given times at different concentrations of heavy metals. The protein were extracted in 25 mM Tris-HCl pH 7.4, 10 mM EDTA, 1 mM β-mercaeptoethanol and 2 mM PMSF. The levels of HSP70 monitored by western blotting analyses utilizing antisiera against 3 different isoforms: mitochondrial, cytosolic and chloroplastic HSP70 (1:1000 in TBS, Agrisera). The secondary antibody was anti-rabbit conjugate RFLP (1:160000 in TBS, Sigma).

4.15 RNA isolation from leaf material

Total RNA was extracted as described by Sokolowsky (1990) from fresh barley leaves to obtain total fraction of cDNA. About 200 to 400 mg fresh leaves material was harvested and freezed in liquid nitrogen.

The material was directly homogenized in a precooled tube with mini pistil (4.9 mm). After addition of lysis buffer (1:2 ratio), and PCI (25:24:1) (Phenol, Chloroform, Isoamyl alchol), samples were shaken for 20 min on an overhead shaker, and then centrifuged for 10 min at 13.000 rpm (Eppendorf 5415D). The upper phases were mixed with same volume of PCI and centrifuged for 10 min at 13.000 rpm (Eppendorf 5415D).

The upper phase was brough to 3 M LiCl, mixed, taken on ice for 2h, and centrifuged for 10 min at 4°C and 13.000 rpm. The pellet was resuspended in 0.1% DEPC H_2O plus 0,3M sodium acetate, pH 5.2 and 70% ethanol, mixed, and taken for 30 min at -70°C. The sample was centrifuged for 10 min at 4°C and 13.000 rpm and the pellet obtained was washed with 70% ethanol. After a drying step at room temperature, the pellet was resolved in suitable amount of 0.1% DEPC H_2O and stored at -80°C.

Lysis buffer:	0.6 M NaCl; 10 mM EDTA; 100 mM Tris; 4% SDS; adjust to pH 8.0 with HCl
PCI:	25 vol. phenol; 24 vol. chloroform; 1 vol. isoamyl alcohol

Total RNA was extracted from leaves of barley plants at different times of treatment; RNA integrity was checked on denaturating agarose gel 0.8% (Fig 16).

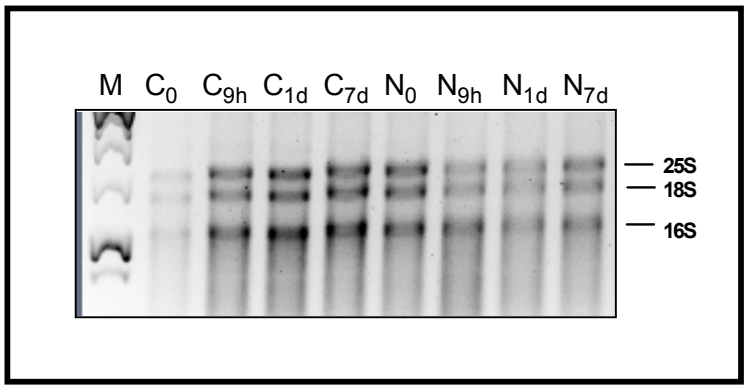

Fig. 16: Total RNA on 0,8% denaturating agarose gel.

Agarose gels observation confirmed the suitable quality of the total RNA. The gel showed the three expected bands of the ribosomal subunits 25S, 18S, and 16S.

A specific,ready-to-use kit was utilised for cDNA preparation (QuantiTect Reverse Trasciption Kit, Quiagen).

4.16 Real Time-PCR analyses

The *Hordeum vulgare* genes analysed were: cytosolic G6PDH isoform (cy-G6PDH; MLOC_7841); plastidial G6PDH isoform (P2-G6PDH MLOC_18415.1), inactive G6PDH isoform (P0-G6PDH MLOC_79070.2), ascorbate peroxidase (APX AJ006358.1), catalase (CAT U20778.1), heat shock proteins 70 (HSP70 L32165.1).

Triplicate quantitative assays were performed using an ABI 7900 HT (Applied Biosystems, Foster City, CA, USA) and Platinum SYBR Green qPCR SuperMix (Life Technologies, Carlsbad, CA, USA).

Leaf samples of plant grown under control conditions were used as calibrators; α-TUBULIN-2 (Y08490.1) served as endogenous reference gene. Quantitation of gene expression was carried out using the $2^{-\Delta\Delta Ct}$ method as in Livak & Schmittgen (Livak and Schmittgen, 2001). For each sample, mRNA amount was calculated relatively to the calibrator sample for the same gene. Primers for each gene is given in Table 5.

cyt G6PDH_frw_realT	GGCAAGCTGAAGGCTGTTT
cyt G6PDH_rev_realT	GGTCTGCATGTACCCAACCT
P2G6PDH_frw_realT	ATCAGCATCATCTGCGAGTG
P2G6PDH_rev_realT	ACCTCTTGTTAGGGCAGCAG
P0G6PDH_frw_realT	ATTTCATCACGTCCCTGGCA
P0G6PDH_rev_realT	TCGGGTAGGTCACGTAAAACC
cat_frw_realT	CGACGACAAGATGCTGCAGT
cat_rev_realT	TGGTTGTTCTTGAAGCCGC
hsp70_frw_realT	GCGTTGAGATCGAGTCCCTCTT
hsp70_rev_realT	CCCATGGTCTTGCGGAAAA
apx_frw_realT	CGGAGCTTTTGAGTGGTGACA
apx_rev_realT	CCGCAGCATATTTCTCCACAA
alfatub_frw_realT	CTCCATGATGGCCAAGTGTGA
alfatub_rev_realT	ATGTCGCTTGGTCTTGATGGT

Table 5. Forward and Reverse primers utilised for qRT-PCR analyses.

4.17 Water content (WC)

WC is the total of water present in plant tissues; it is the amount of water in the leaf relatively to its dry weight. The WC resulted from the formula:

WC (g/g) = (FW-DW)/DW

Where:

FW: fresh weight

DW: dried weight

4.17.1 Relative water content (RWC)

RWC is the water content of a given amount of a leaf relative to its fully hydrated or fully turgid state. It indicates the hydration state of the leaf. The RWC is done from the formula:

RWC = (FW-DW)/(TW-DW)
Where:
FW: fresh weight
DW: dried weight
TW: turgid weight

The fresh weight (FW) of 3 to 5 leaves was rapidly determined soon after detaching from plants grown hydroponically in control conditions. The leaves were then hydrated for 3-4 hours by floating in a Petri dish in distilled water to determine the turgid weight (TW); then the same leaves were dried overnight at 70^{o} C for the dried weight (DW) (STF-N 52, Falc).

4.18 Determination of leaf pigments

Determinations of chlorophyll-a, chlorophyll-b, carotenoids levels were obtained to calulate the variation, and abundance, of the photosintetic pigments after 1 mM Nickel treatment.

Concentrations of pigments were analysed spectrophotometrically (Zhang e Kirkham, 1996): samples from different treatments were weighted and cut in slices, and immersed in 5 mL of 80% of pure acetone for seven days at 4°C in the dark. After centrifugation, spectrophotometric analyses were done at different wavelength: 663.2, 648.8 e 470.0 nm.

Absorbance values obtained allowed the determination of the pigments concentrations in µg/ml of surnatant using the following formulas:

[chl a] µg ml-1 = (12.25 · A663.2) - (2.79 · A648.8)

[chl b] µg ml-1 = (21.50 · A648.8) - (5.10 · A663.2)

[car] µg ml-1 = [(1000 · A470.0) - (1.82 [chl a] + 85.02 [chl b])] / 198

To evaluate the pigment content respect to fresh weight unit (FW) of plants, the value were expressed in µg g^{-1} by the following formula:

[Pigment] µg g^{-1} = (Vsurn. / FW) · [pigment] µg ml^{-1}

4.19 Growth variation and inhibition test

The inhibition of growth induced by heavy metal treatments was measured at different times of exposure: measurements were taken both considering the weight of the whole plant and separately for roots and leaves.
Growth inhibition (GI) was calculated by the formula:
$\%GI = [1 - (HM_{WT}/HM_{ctrl})] * 100$
Where:
HM_{WT}: average weight of plants exposed to HMs
HM_{ctrl}: average weight of control plants

4.20 RAPD analyses

Leaves from barley plants were analysed for RAPD markers. The variability in leaves was investigated using different primers supplied by Operon Technologies Inc. (Alameda, Calif., USA). Total cellular DNA was extracted from 0.4 g by Isolate II Plant DNA kit (BioLine).

DNA concentration in the samples was determined spectrometrically and integrity was checked on 1,5% agarose gels (Fig 17).

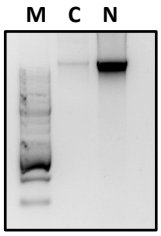

Fig. 17: Agarose gel showing the integrity of the control and treated DNA plants.

RT-PCR for DNA amplification was performed in a volume of 25 µl, containing the reaction buffer: 10 mM Tris-HCl pH 8.0, 50 mM KCl, 1.5mM $MgCl_2$ plus 200 µM of each dNTP, 0.8 µM 10-base primer, 25 ng of template DNA, and 2 units of Taq DNA polymerase.

DNA amplifications were performed using a thermal cycler (Bio-RAD T100). The cycle used involved one preliminary step of denaturation, followed by 40 cycles of denaturation - annealing – elongation, following this scheme:

94°C for 5 min

94°C for 1 min
36°C for 1 min
72°C for 2 min
} 40 cycles

72°C for 5 min.

PCR products were separated on 1.8% agarose gels by electrophoresis run in 1X TBE buffer (0.089M Tris-borate and 0.2mM EDTA; Table 6), and visualised with DNA loading buffer red (Bioline).

TEB 10X
Tris-base 108g
Boric Acid 55g
EDTA 0,5M pH 8.0 40 ml
V. tot. 1L

Reproducibility of RAPD procedure was checked by repeating the analyses of samples 3 times. Only bands showing consistent amplification were discussed.

4.21 Comet Assays

To determine possible DNA strand breaks, comet assays were performed on leaves and roots of barley plants.

About 150 mg of tissue were cut with a sharp blaze in 1.5 mL of Tris 400 mM, pH 7.5 for 15 min to allow the protoplast release.

The cellular suspension was then filtered with 20 µm Miracloth and at 500 µl suspension was added 500 µl LMA (1% low melting agarose in Dulbecco's PBS).

On a microscope slides, covered by 1% NMA (normal melting agarose), were added 80 µl of the mix (suspesion+LMA) and stored for 5 min at 4°C.

Cells lysis was obtained with a lysing buffer (2.5 mM NaCl, 100 mM EDTA, 10 mM Tris, 1% Triton X100, 10% DMSO, pH 10) for 1h at 4°C.

The microscope slides were washed 2 times with 400 mM Tris-HCl pH 7.5 and then put for 15 min in the electrophoretic buffer (Na_2EDTA 1 mM, NaOH 300 mM, pH>13) to allow the DNA release. After the 15 minutes an electrophoresis was mede on these samples, 25 min at 25 V, 300 mA. The slides were removed from electrophoresis chamber, rinsed and neutralized in 400 mM Tris-HCl, pH7,5.

DNA was visualized by fluorescence microscopy (Nikon Eclipse E1000) after staining with a 50 µg DNA-binding dye (DAPI, AppliChem) for 3 hours. Comets observed were analysed by ImageJ and Casplab software.

4.22 Gradient-PCR

Total RNA was extracted from fresh barley leaves. To obtain the cDNA a ready-to-use kit was utilized (QuantiTect Reverse Trasciption Kit, Quiagen). The cDNA obtained was used to perform a gradient-PCR with specific primers in order to amplify the sequence for P2-G6PDH and P0-G6PDH (Table 7). For the amplification a Fusion DNA Polymerase and a specific buffer for sequence reach in GC was used (Phusion High-Fidelity DNA Polymerase, ThermoFisher Scientific).

Name	**Sequence**	**Restriction enzyme**	**Comment**
Hv_P2_s_XbaI	NNTCTAGAATGGCGCTCTCCTGCATGAGG	XbaI	Tm:67.48°C GC:61%
HvP2-StopasXhoI	WWCTCGAGGTGTTCCGAGCCGCCCA	XhoI	Tm:65.41°C GC: 70%
Hv_P0_s_XhoI	NNCTCGAGATGGTTACGACAGTCCTCCTCG	XhoI	TM:64.00°C GC:54%
HvP0-StopasNco	NNCCATGGAGCAGCCATCATCCCATCG	NcoI	TM:62.67°C GC:57%

PCR conditions were determined as:

	65µl rxn	**Final conc.**
H_2O	Add to 65µl	
5X GC Buffer	13µl	1X
10mM dNTPs	1.3µl	200 mM
10µM Forward primer	2.6	0.4 µM
10µM Reverse primer	2.6	0.4 µM
cDNA	100 ng	
Phusion pol	1µl	0.004U/µl

The DNA amplifications were performed using a thermal cycler. The cycle used consisted in one first step of denaturation followed by 40 cycles of denaturation/annealing/elongation.

98°C for 30 sec

98°C for 10 sec
62°C for 15 sec } 40 cycles
72°C for 50 sec

72°C for 5 min.

PCR products were separated by electrophoresis on 1% agarose gels, run in 1X TAE buffer.

TAE 50X
Tris-base 242gr
Glacial acetic acid 57.1gr
EDTA 0,5M pH 8.0 100 ml
V. tot. 1L

4.23 Cloning into pBSK

Bands obtained from gradient-PCR were purified using a specific kit (NucleoSpin- Gel and Clean up, Macherey-Nagel). The purified products were cloned into pBSK empty vector by blunt-ends ligation using 41.2 ng of vector and 134 ng of insert.

The protocol was as follows:

pBSK	41.2 ng
Insert	134 ng
50% PEG4000	2 μl
10X T4 ligase buffer	2 μl
T4 ligase	0.2 μl (5U)
H_2O	Add to 20 μl

Samples were incubated for 1h at room temperature and then the mixtures were used for the transformation of chemically competent cells.

4.24 Transformation of *E. coli*

E.coli strain XL1blu was used as standard host. Competent cells were transformed by thermic shock using the ligation mixture. The competent cells were thawed at RT and maintained on ice; the ligation mixture was added to each sample and let for 30 min on ice. Then cells were incubated for 90s at 42°C; resuspended in 0.8 mL of ΨB without antibiotics, and put on a termoshaker for 1h at 37°C at 800rpm. Cells were harvested by centrifugation for 3 min at 3000 rpm, and plated on YT-plates +Amp + tetracycline + IPTG. Colonies result visible after 1d at 37°C.

ΨB-Medium

Tryptone	2%
Yeast extract	0.5%
$MgSO_4$ (M.w 246.48 g/mol)	16.26 gr
KCl (M.w 74.56 g/mol)	1.492 gr
pH 7.6 with KOH	

YT-Medium

Tryptone	8.0 g/l
Yeast extract	5.0 g/l
NaCl	2.5 g /l
pH 7.0 with NaOH	
For plates add: Agar (1.5%)	15 g/l

4.25 Plasmid-Mini-Preparation from *E. coli*

Plasmid miniprep was made using a manual protocol from *E.coli* in order to ascertain the correctness of sequence insertion into the plasmid. Briefly, 1.5 mL bacteria suspension was centrifuged for 2 min at 7.000 rpm, the supernatant discarded and the pellet resuspended in 200 µL solution 1 by vortexing. 200 µL of solution 2 and 200 µL solution 3 were added and solution obtained was inverted 6 - 8 times without vortexing.

Samples were incubated for 10 min on ice, centrifuged for 10 min at 13.500 rpm, 4°C and the supernatant transferred in a new tube with 450 µL isopropanol; after mixing thoroughly, this was centrifuged for 10 min at 13.500 rpm, 4°C. The supernatant was discarded and the pellet after a washing in 300 µL 70% ethanol was centrifuged for 5 min at 13.500 rpm at RT; after drying samples were resuspended in 30 µL H_2O.

Solutions:

Solution 1:	50 mM Tris-HCl, pH 8
	10 mM EDTA
	RNAse (0.1 mg/mL)
Solution 2:	0.2 M NaOH
	1 % SDS
Solution 3:	3 M Potassium acetate
	Set pH 4.8 with glacial acetic acid

4.26 pBSK enzyme digestion

The correct insertion of the full length P2-G6PDH and P0-G6PDH was checked by enzymatic digestion of the mini-prep frm the *E.coli* XL1 transformation. The correct enzymes were selected using digestion informatics analyses (NEBcutter software tool). The plasmid pBSK + P2G6PDH was cut by a single digestion with HindIII or SacI while the plasmid pBSK + P0G6PDH was digested with XbaI, SacI or EcoRI. Digestions were made by incubating the enzyme at 37°C for 1h, and the fragment obtained were visualized on 1% agarose gel. Only the plasmids showing the correct bands pattern were utilized for the sequencing.

4.27 Subcloning of P2-G6PDH and P0-G6PDH behind the reporter

To obtain a reporter fusion proteins behind the GFP a initial PCR was made with the pBSK plasmids containing the nucleotidic P2-G6PDH and P0-G6PDH full-length sequences (Table 8). For the amplification a Phusion DNA Polymerase and a specific buffer for sequence reach in GC was used (Phusion High-Fidelity DNA Polymerase, ThermoFisher Scientific).

Name	**Sequence**	**Restriction enzyme**	**Comment**
Hv_P2_s_XbaI full	NNTCTAGAATGGCGCTCTCCTGCATGAGG	XbaI	Tm:67.48°C GC:61%
Hv_P2 _as_BHI full	WWGGATCCCTAGTGTTCCGAGCCGCCCA	BamHI	Tm:67.0°C GC:65%
Hv_P2mat_s_Spe	NNACTAGTGGAGCGTCAGGCGACCTTG	SpeI	Tm:65.96°C GC:68%
Hv_P2mat _as_BHI	WWGGATCCCTAGTGTTCCGAGCCGCCCA	BamHI	Tm:67.0°C GC:65%
Hv_P0_s_Spe full	NNACTAGTATGGTTACGACAGTCCTCCTCG	SpeI	TM:66.9°C GC:50%
Hv_P0_as_BHI full	NNGGATCCTCAGCAGCCATCATCCCATC	BamHI	TM:62.56 GC:55%

Table 8: primers for P0-G6PDH and P2-G6PDH amplification

The PCR condition were as follow:

Component	**65µl rxn**	**Final conc.**
H_2O	Add to 65 µl	
5X GC Buffer	13 µl	1X
10mM dNTPs	1.3 µl	200 mM
10µM Forward primer	2.6 µl	0.4 µM
10µM Reverse primer	2.6 µl	0.4 µM
pBSK	5 ng	
Phusion pol	1 µl	0.004 U/µl

DNA amplifications were performed using a thermal cycler (T100 Bio-Rad).

The thermal cycle used was one first step of denaturation following by 35 cycle of denaturation/annealing/elongation. The annealing temperatures were: 60°C for the P2-G6PDH isoforms and 53°C for the P0-G6PDH.

98°C for 30 sec

98°C for 10 sec

60°C/53°C for 15 sec } 35 cycle

72°C for 50 sec

72°C for 5 min.

PCR products were separated by electrophoresis on 1% agarose gels, run in 1X TAE buffer.
The bands obtained were purified from the agarose gel by a NucleoSpin-Gel and Clean up from Macherey-Nagel. Purified products were cloned into pGFP_NX empty vector by sticky-ends ligation.
The product for P2-G6PDH full length was cut by double digestion with XbaI and BamHI, the P2-G6PDH mature with SpeI and BamHI; P0-G6PDH was cut by BamHI and SpeI.
The digestions were obtained by incubation with enzymes at 37°C for 1h for the P2-G6PDH while for the P0-G6PDH was performed first 1h digestion with BamHI and then, after the 1h, a digestion with SpeI for only 10 minutes.

For the ligation were used 60ng of vector, previously digested with SpeI and BamHI, and 100 ng of insert as described in table 9.

pGFP_NX	60 ng
Insert	100 ng
50% PEG4000	2 μl
10X T4 ligase buffer	2 μl
T4 ligase	0.2 μl (5U)
H_2O	Add to 20 μl

Table 9: ligation mixture

Samples were incubated for 1h at RT, then the mix were used for the transformation

of *E.coli* strain XL1 blue. Transformed bacteria were utilized for the purification of the plasmids containing the nucleotidic sequence for P2-G6PDH and P0-G6PDH isoforms, using a kit (Nucleo Spin Plasmid Easy Pure, Macherey Nagel).
The correctness of the plasmid insertions were controlled by digestion with specific enzymes:

- pGFP_NX+P2full: digested with XbaI and SacI
- pGFP_NX+P2mat: digested with SpeI and BamHI
- pGFP_NX+P0full: digested with XbaI

Digested fragments were visualized on 1% agarose gel.

4.28 Subcloning of P2-G6PDH and P0-G6PDH in front of the reporter

The reporter fusion proteins in front of the GFP/OFP were obtained by enzymatic digestion of the pBSK plasmids containing the nucleotidic sequences for the P2-G6PDH and P0-G6PDH full length. The plasmid pBSK + P2-G6PDHwas digested with XbaI and XhoI, while the pBSK + P0-G6PDH was digested with XhoI and NcoI. The digested fragments were visualized on 1% agarose gel and the bands purified from the agarose gel, and ligated in pGFP_NX and pOFP_NX. For the ligation 60ng of vector were used, digested with the correct enzyme in the presence of 100 ng of insert. The products of the ligation were used to transform *E.coli* strain XL1 blue and the purified plasmids containing the nucleotidic sequence for the P2-G6PDH and P0-G6PDH isoforms were digested to control the correct insertion. The plasmids pGFP_NX+P2-G6PDH (pOFP_NX) were digested with HindIII while the plasmids pGFP_NX+P0-G6PDH were digested with XbaI.

The digested fragments were visualized on 1% agarose gel.

4.29 Protoplast isolation from leaf tissue (tobacco, *Arabidopsis*)

Seeds of tobacco and *Arabidopsis* were germinated on sterile medium (1/2 Murashige and Skoog basal medium - MS medium), 1% sucrose and 0.8% agar, pH 5.5 in Petri dishes for several days, exposed to a photoperiod of 16 hours. When the plant seedlings were visible, these were transferred in a sterile box with the same medium until protoplast extraction. (Fig. 18).

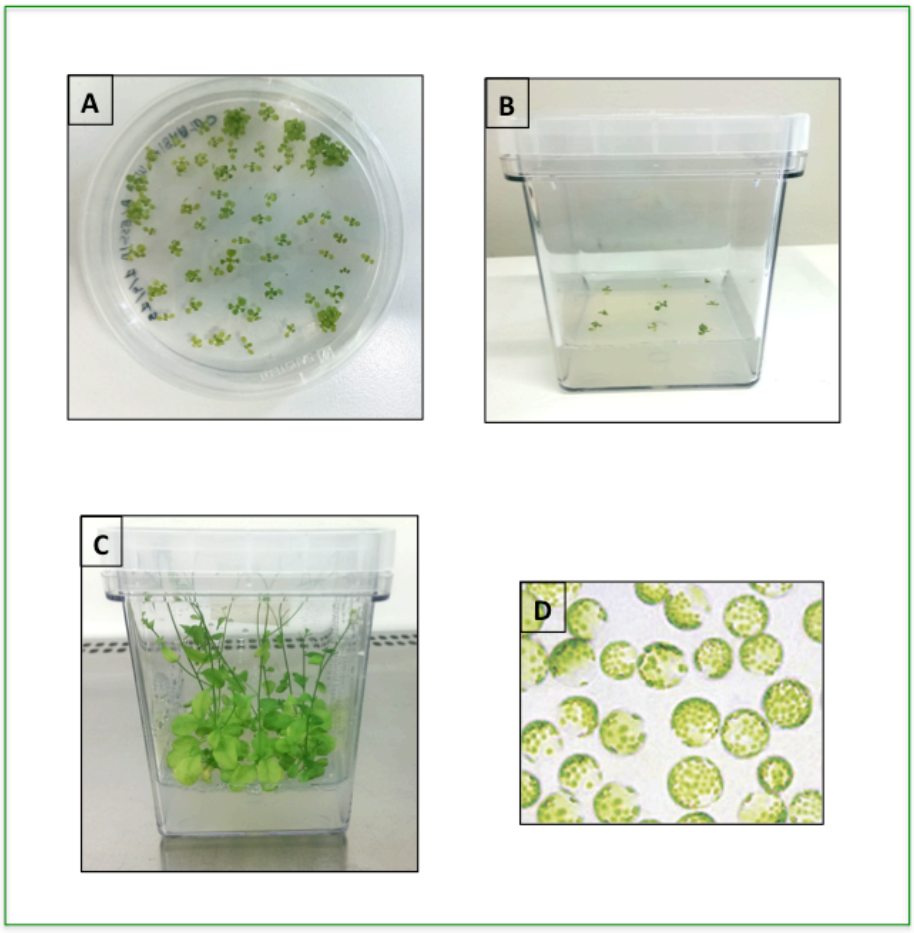

Fig .18: A) *Arabidopsis* seeds; B) rosettes; C) young plants; D) protoplasts

Young leaves from 3 to 4 week old plants grown on sterile MS medium, 1% sucrose were harvested into a sterile Petri dish with 5 ml osmoticum (0.5 M mannitol for tobacco, and 0.45 M mannitol for *Arabidopsis*).

The tissues were cut with a sharp razor blade into thin, ca. 1 mm wide strips, and leaves placed right-side-up in a fresh Petri dish to float on 20 ml osmoticum for pre-plasmolysis for 1h at RT. The osmoticum was removed, replaced with 12 ml of enzymatic solution and incubated in darkness for 12h - 16h at 21-25°C (no shaking).

The next morning the Petri dish was quickly shaken to release protoplasts, and the maceration state and intactness were checked under an optical microscope.

The protoplast suspension was filtered through a 125 µm mesh over 63 µm mesh combination into a glass container. The filtration device was raised with 8 ml 0.2 M $CaCl_2$ using a 10 ml wide-bore pipettes to saved protoplast.

The protoplast solution was centrifuged for 5 min at 60 *g* in a swing-out rotor at 15°C.

The protoplasts obtained were washed for 2-times in 6 ml 0.5 M (0.45 M for tobacco protoplast) mannitol plus 3 ml 0.2 M $CaCl_2$, mixed by gentle inversion, and centrifuge again for 5 min at 60 *g*.

The pellet was then resuspended in 10 ml W5 medium (artificial sea water) and protoplasts counted with a haemocytometer (e.g. Neubauer: Volume = 0.1 µl).

After 1 h on ice the solution was centrifuged (as above), the supernatant discarded, and the protoplast number adjusted to 1.67 million/ml with ice-cold Mannitol-Mg solution ManMg (= 500000/300 µl).

4.30 Protoplast transfection for transient gene expression with plasmid DNA

30 µg of plasmid DNA (1 µg/µl in TE) were placed in the centre of small Greiner Petri dishes and mixed with 300 µl protoplast suspension.

500 µl of PEG solution were dropped from a distance of ca. 5 cm on protoplast-DNA mixture, and the solution was incubated for 30 min at RT (transfection).

Successively, (every 5 min) the sample was diluted with a total of 7 ml of W5 medium (i.e. + 0.5 ml, + 1 ml, + 2 ml, + 3 ml = 6.5 ml), transferred into fresh screw-cap glass tubes and centrifuged for 5 min at 60 *g* in a swing-out rotor at 15°C.

The transfected protoplasts were resuspended in 3 ml Gamborg's B5 medium (with hormones), transferred into small Petri dishes, and incubated at RT over night (or longer) in the dark. Gene expression was controlled at different time points by CLSM.

Solutions for transient gene expression in protoplasts:

Enzyme solution:

- 0.5 M mannitol for tobacco *(0.45 M for Arabidopsis)*
- 10 mM $CaCl_2$
- 1% Cellulase (Onozuka R-10, Serva)
- 0.25% Macerozyme (Onozuka R-10, Serva)

(stir in cold room, sterile-filtrate (0.2 µm) and store at -20°C.)

0.2 M $CaCl_2$

W5 medium:

- 145 mM NaCl
- 125 mM $CaCl_2$
- 5 mM KCl
- 5 mM Glucose
- pH 5-6, autoclave

ManMg solution:

- 0.5 M mannitol
- 15 mM $MgCl_2$
- 0.1% MES
- pH 5.7 with 0.1 N KOH, sterile-filtrate (0.2 µm)

PEG solution:

- 0.4 M mannitol
- 0.1 M $Ca(NO_3)_2$
- 0.1% MES
- pH 8 with 0.1 N KOH
- add 40 g PEG 6000
- sterile filtrate (0.2 µm) and freeze at -20°C

Gamborg's B5 medium:

- 3.17 g/L B5 complete (Duchefa, Haarlem, NL)
- 0.5 M glucose *(*0.45 M for *Arabidopsis)*
- pH 5.7 with 0.1 N KOH,

sterile filtrate store at -20°C

B5 hormone additions:	Tobacco (for 50 ml $B5_T$)	*Arabidopsis (for 50 ml $B5_A$)*
2.4D (1 mg/ml H_2O)	0.1 mg/L = 5 µl	1 mg/L = 50 µl
BAP (1 mg/ml EtOH)	0.2 mg/L = 10 µl	0.15 mg/L = 7.5 µl
NAA (1 mg/ml DMSO)	1 mg/L = 50 µl	-

4.31 Binary vectors

Binary vectors were prepared to analyse the subcellular localization of the isoforms in whole plant by agro-infiltration. The pGFP_NX (pOFP_NX) + G6PDHs isoforms were digested with specific enzymes to obtain fragments containing the whole nucleotidic sequences of different G6PDH isoforms plus the sequence for GFP/OFP, and finally subcloned in pGPTVII-HYG.

P2-G6PDH full length the plasmid was cut by double digestion with XbaI and EcoRI ; P0-G6PDH the plasmid was cut by HindIII and EcoRI.

The digestions were obtained by incubating the enzymes at 37°C for 1h, EcoRI was added 10 min before the end of 1h digestion. Fragments were visualized on 1% agarose gel, purified and ligated in pGPTVII-HYG.

For the ligation were used 65 ng of vector, previously digested with appropriate restriction enzyme, and 80 ng of insert. The products of the ligation were used to transform *E.coli* strain XL10. A control PCR was performed to verify the correct insertion of sequences in the plasmids after purification from the transformed bacteria. The PCR conditions were as follows:

Component	**65µl rxn**	**Final conc.**
H_2O	Add to 65µl	
5X Buffer	13µl	1X
10mM dNTPs	1,3µl	200mM
10µM pNosT primer	2.6	0.4 µM
10µM p35S primer	2.6	0.4 µM
vector	10ng	
Taq	1µl	0.004U/µl

Conditions:

98°C for 3 min

98°C for 30 sec

62°C for 30 sec 35 cycles

72°C for 2,30 min

72°C for 7 min.

PCR products were observed on 1% agarose gels and corrects plasmids were utilized to transform *Agrobacterium* competent cells.

4.32 Transformation of *Agrobacteria*

The *Agrobacteria* competent cells were thawed at RT and kept on ice. At each sample wad added about 1 µg DNA, mixed and incubated for 5 min on ice. Cells were freezed in liquid Nitrogen (5 min), and incubated for 5 min at 37°C; then 1 mL of YT without antibiotics was added, and the samples were incubated for 2 - 4 h at RT (preferentially at 28°C). Finally cells were harvested by centrifugation and plated on YT-plates + Kanamycin (25mg/L) + Rifampicin (100mg/L).

Colonies were visible after 2 d at 28° C.

YT-Medium

Tryptone	8.0 g/l
Yeast extract	5.0 g/l
NaCl	2.5 g /l

pH 7.0 with NaOH

For plates add

Agar (1.5%)	15 g/l

4.33 Agro-infiltration of tobacco leaves

The transformed *Agrobacteria* were inoculated with 3 mL YT + Kanamycin (25mg/L) + Rifampicin (100mg/L) and let roll over night (O/N) at 28°C. The same procedure was used also for 19K strain. 1 mL of the O/N culture were inoculated in 50 mL YT + AB + 500 µL 1M MES pH 5,6 plus freshly prepared 10 µL of 100 mM acetosyringone in DMSO, and incubated O/N at 28°C under gentle shaking. The cells were harvested by centrifugation for 15 min at 3500 rpm.

Agrobacteria were resuspended in buffer 10 mM $MgCl_2$; 10 mM MES, pH 5.6 and 100 µM Acetosyringone until OD_{600} was taken to 1 (for 19K-strain to 2) and then the *Agrobacteria* were incubated in the dark for 2-3h. The suspension was mixed 1:1 with the 19K-strain and infiltrated into the tobacco leaves using of 1 ml syringes. *N. benthamiana* plants were cultivated under normal conditions. After 2 days of growth, small leaf slices were analysed under the CLSM (Fig. 19).

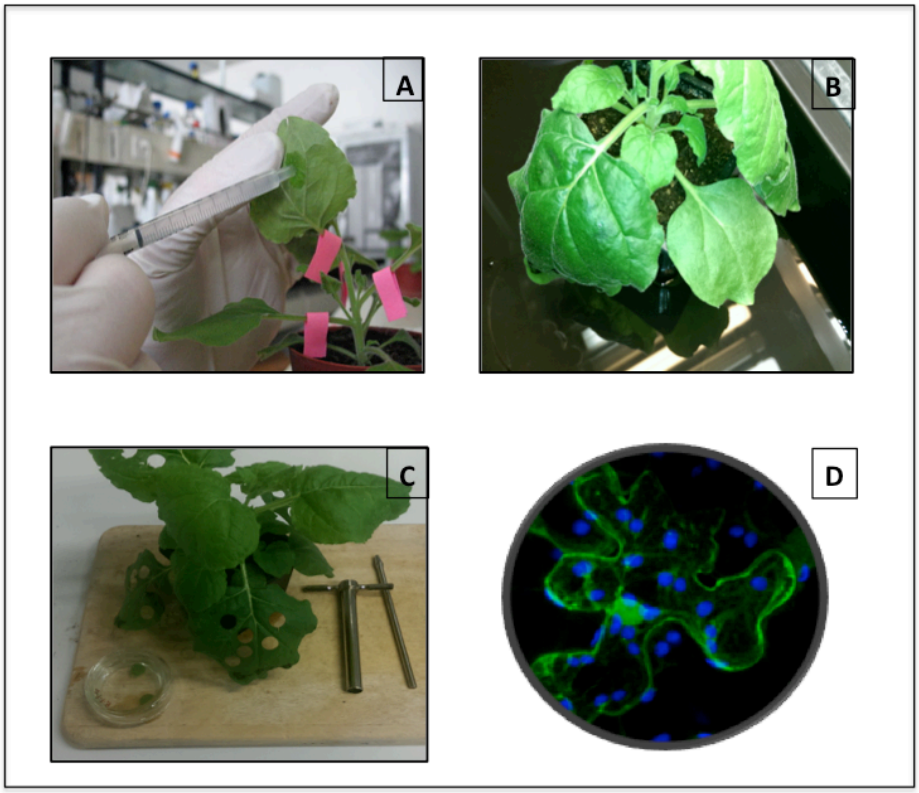

Fig. 19: A) Agro-infiltration of N. benthamiana leaves; B) N. benthamiana plant; C) cutting of leaves slices; D) CLSM analyses

4.34 Statistical analysis

Each experiment was made in at least five replicates. Values were expressed as mean ± standard deviation (SD). The statistical significance of qRT-PCR and enzymatic assay was evaluated through Student's t-test ($p \leq 0.05$, at least).

5 RESULTS

5.1 Overexpression of G6PDH isoforms

E.coli strain BL21(DE3)psBET was used as a standard host; competent cells were transformed with pET15b vector containing the sequence for the P2-G6PDH from *Populus trichocarpa* (*Pt*P2-G6PDH).
Positive colonies were utilised for a test to verify the expression of the recombinant protein by the transformed bacteria (Fig. 20).

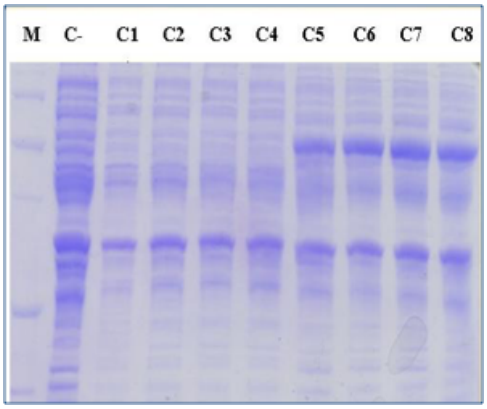

SDS gel showing a protein of the expected MW corresponding to P2 G6PDH. M: Markers; C-: Control (*E. coli* without transformed plasmid); C1,C2,C3,C4: different colonies without IPTG; C5,C6,C7,C8: transformed colonies after induction with IPTG.

Those colonies best expressing the recombinant protein were utilised to grow a large scale culture (1 to 3 litres) for enzyme purification.
A rapid procedure for the purification of recombinant *Pt*P2-G6PDH was utilised.
The purification protocol consisted in a gel filtration step, followed by Immobilized Metal Ion Affinity Chromatography (IMAC). The elution of the recombinant protein was obtained using buffer containing 250mM Imidazole. After IMAC, the recombinant protein was judged sufficiently pure by SDS-PAGE and western blotting (Fig. 21) and utilised for following measurements.

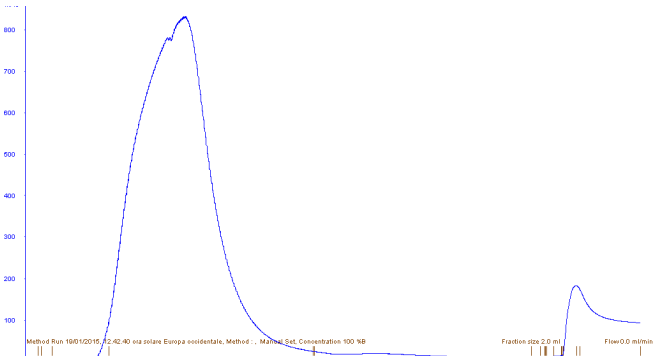

Fig. 21: I Immobilized Metal Affinity Chromatography (IMAC) profile eluating from a HiTrap Ni column (1 ml – GE Healthcare) using buffer with K_2HPO_4 50mM, KH_2PO_4 50mM, imidazole 250mM, NaCl 300mM, pH7,4.

The specific activity of the purified recombinant enzyme was 8000 U/mg protein.
Both SDS-PAGE and immunoblotting with antisiera against the his-tag indicated a highly pure enzyme preparation (Fig. 22).

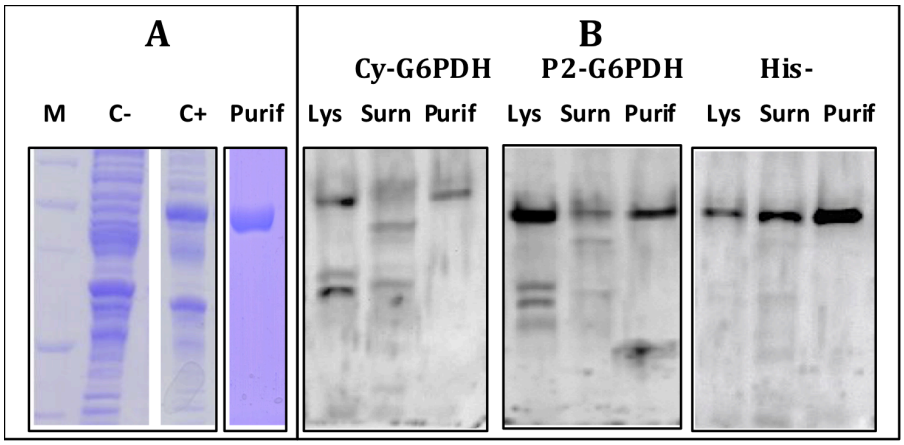

Fig. 22 – Electrophoretic analysis of *Pt*P2-G6PDH. A: SDS gels showing a protein of the expected MW corresponding to P2 G6PDH. M: Markers; C-: Control (*E. coli* without transformed plasmid); C+: transformed colonies after induction with IPTG; P: purified protein after IMAC. B: Immunoblotting using antisera versus Cy-G6PDH Ab (potato); P2-G6PDH (potato); His-tag. Lys: bacterial lysate; Surn: soluble fraction; Purif: purified protein (as in A).

5.2 *In vitro* inhibition assays

The recombinant *Pt*P2-G6PDH-wt activity was tested in the presence of different heavy metals: Cd^{++}, Cu^{++}, Zn^{++}, Ni^{++}, Pb^{++} in order to investigate their possible action as inhibitors (Fig. 23), and IC_{50} values were calculated after 1h of incubation with metals (Table 10).

The most toxic of the metals tested was copper, with a IC50 <26 μM, while the less effective was Lead, with a IC50 about 100-fold higher.

Metal ions	IC_{50} (mM)
Cu^{++}	0.0257
Zn^{++}	0.050
Cd^{++}	0.123
Ni^{++}	0.881
Pb^{++}	2.821

Table 10: IC_{50} values after 1h of incubation with heavy metals

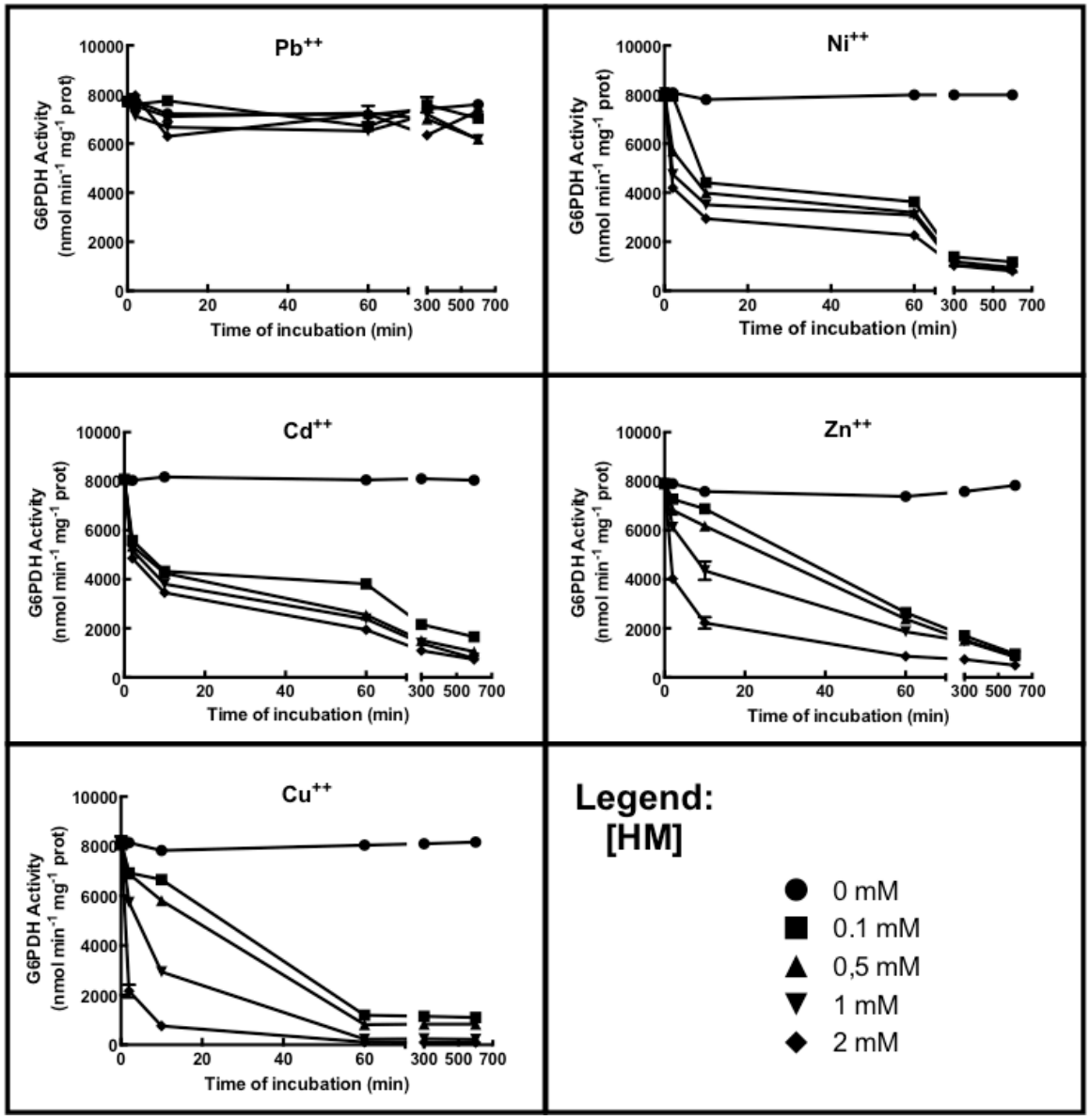

Fig.23: The graph showed the effects of heavy metals on G6PDH activity (activity% versus time of incubation with each metal concentration)

The effects of HMs on *Pt*P2-G6PDH activity could be divided in three groups:

Pb^{+2} did not show any substantial effect on *Pt*P2-G6PDH activity at all the concentrations tested.

Ni^{++} and Cd^{++} showed similar effects: after 10 minutes 40-52% (Ni^{++}), and 45-65% (Cd^{++}) inhibition was observed; then a slow decrease in activity continued up to 10h when the inhibition was reduced to less than 10-15% of the initial value.

Finally, Zn^{++} and Cu^{++} induced a progressive decrease time and concentrations dependent, even if at different extent: 2 mM Zn^{++} caused a rapid 50% decrease after 1

minute which continuously lowered to 13% after 10 hours; 1 mM Cu^{++} after 10 minutes induced a 40% decrease in the activity d and at 2mM the residual rate was only 10% of the initial value. After 10h the activities were below 15% in all the conditions and essentially null at 1-2mM for both Cu^{++} and Zn^{++}.

These results would suggest both a direct effect of specific HMs on enzyme structure and functionality, and / or a competition of HMs with the physiological element widely known as an essential cofactor of G6PDH reaction, Mg^{++}.
Thus, the $Km_{Mg^{++}}$ was calculated on highly desalted preparation of the recombinant enzyme. These measurements indicated a $Km_{Mg^{++}}$ = 90 µM (Figure 24).

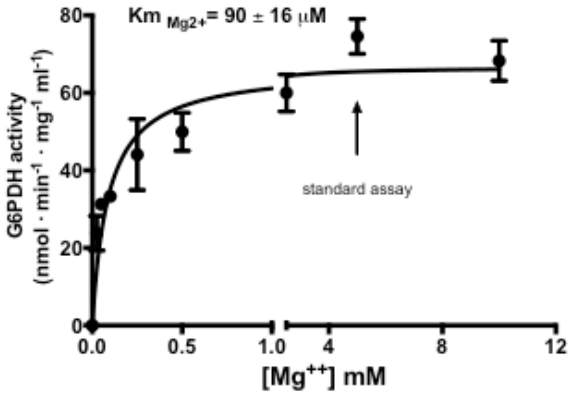

Fig 24: $Km_{Mg^{++}}$ of the *Pt*P2-G6PDH

The effects of the metals were observed in the presence of saturating (5 mM) and sub saturating (0.5-2.5 mM) Mg^{++} in the presence of different HMs, in order to establish the competition with the magnesium, if any, of the HMs tested (Fig. 25).

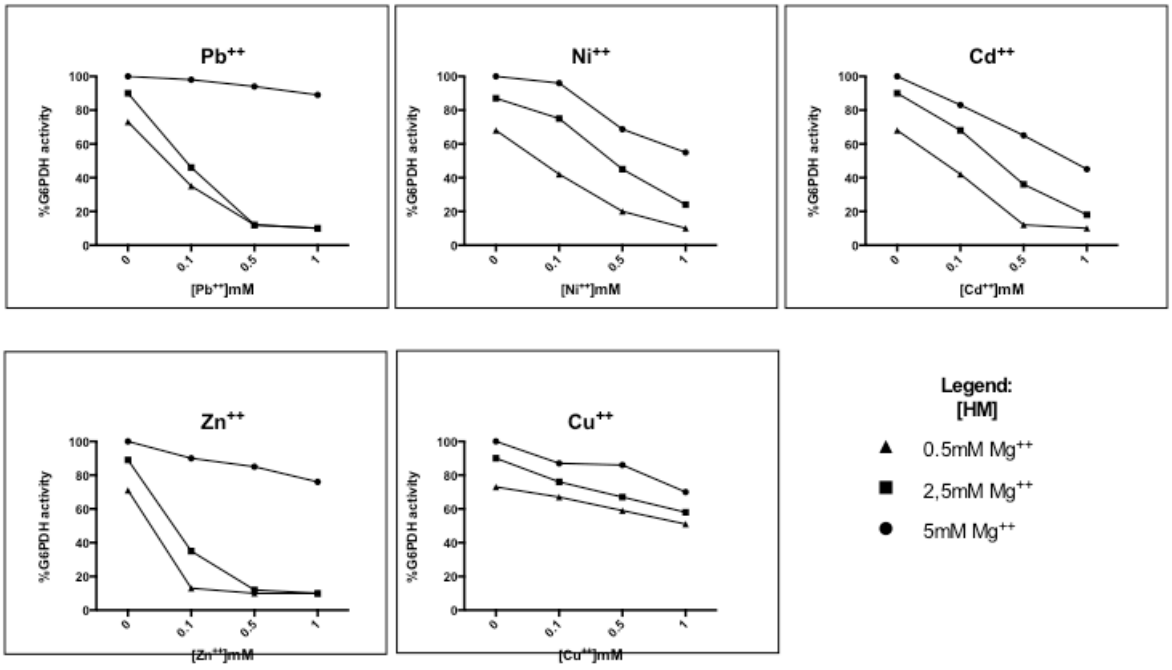

Fig. 25: The graph showed the effects of heavy metals on G6PDH activity at different magnesium concentration.

Except for Cd^{++} and Ni^{++}, all the metals exerted a limited inhibition of *Pt*P2-G6PDH activity when saturating Mg is present.

Pb^{++} and Zn^{++} had the worst effects on enzyme activity when the magnesium concentration is sub-saturating, resulting in a substantial loss of activity at 0.1 mM. Ni^{++} and Zn^{++} showed milder effects; anyway, a continuous loss of activity rate was observed with both metals.

Interestingly, Cu^{++} inhibition was the lighter among all HMs tested.

5.3 Purification and incubation of *Pt*P2-G6PDH mutants

Cysteine to serine mutants of *Pt*P2-G6PDH were available in the laboratory, and obtained as described in Cardi et al., (2016); these recombinant proteins were tested – as for wt enzyme - with the different HMs, in order to verify if specific cysteine residues, highly conserved in the G6PDH sequence, may have a role in the inhibition by metals of enzyme activity.

The mutant enzymes C145S, C242S, and C194S were generally unaffected (less than 50% inhibition after 10 min) by most of the metals tested up to 1 mM; noticeable inhibition was observed only at 1-2 mM Cu (C145S), and with lead and copper (C194S). All these mutagenized enzymes exhibited metal inhibitions lower than 50%.

In contrast, the disulphide-bridge cysteines mutagenized enzymes C175S and C183S were both promptly and severely inhibited by all HMs (Fig. 26). A comprehensive table of the effects of metals on cysteine mutant enzymes after 1 min of exposure was shown (Table 11):

Pb^{2+} did not show appreciable effects on *Pt*P2-G6PDH-wt; and on C242S and C194S at all the levels tested, except with 2 mM Pb^{2+}. On the contrary, C175S, C183S and C194S mutagenized enzymes showed a decreased G6PDH activity on lead exposure.

Ni^{2+}, Cd^{2+} and Zn^{2+} caused a decrease in activity despite of the HM concentration used and time intervals tested. The most marked effect was obtained for C175S, C183S and C194S mutants, where incubation with HMs induced a over 80% inhibition of G6PDH.

Cu^{2+} is the strongest inhibitor of enzyme activity: the effect is rapid, causing a strong decrease in enzyme activity after just few minutes; in disulfide mutants C175S and C183S a total inhibition of G6PDH activity was observed after 10 min at 0,5 mMCu^{++}.

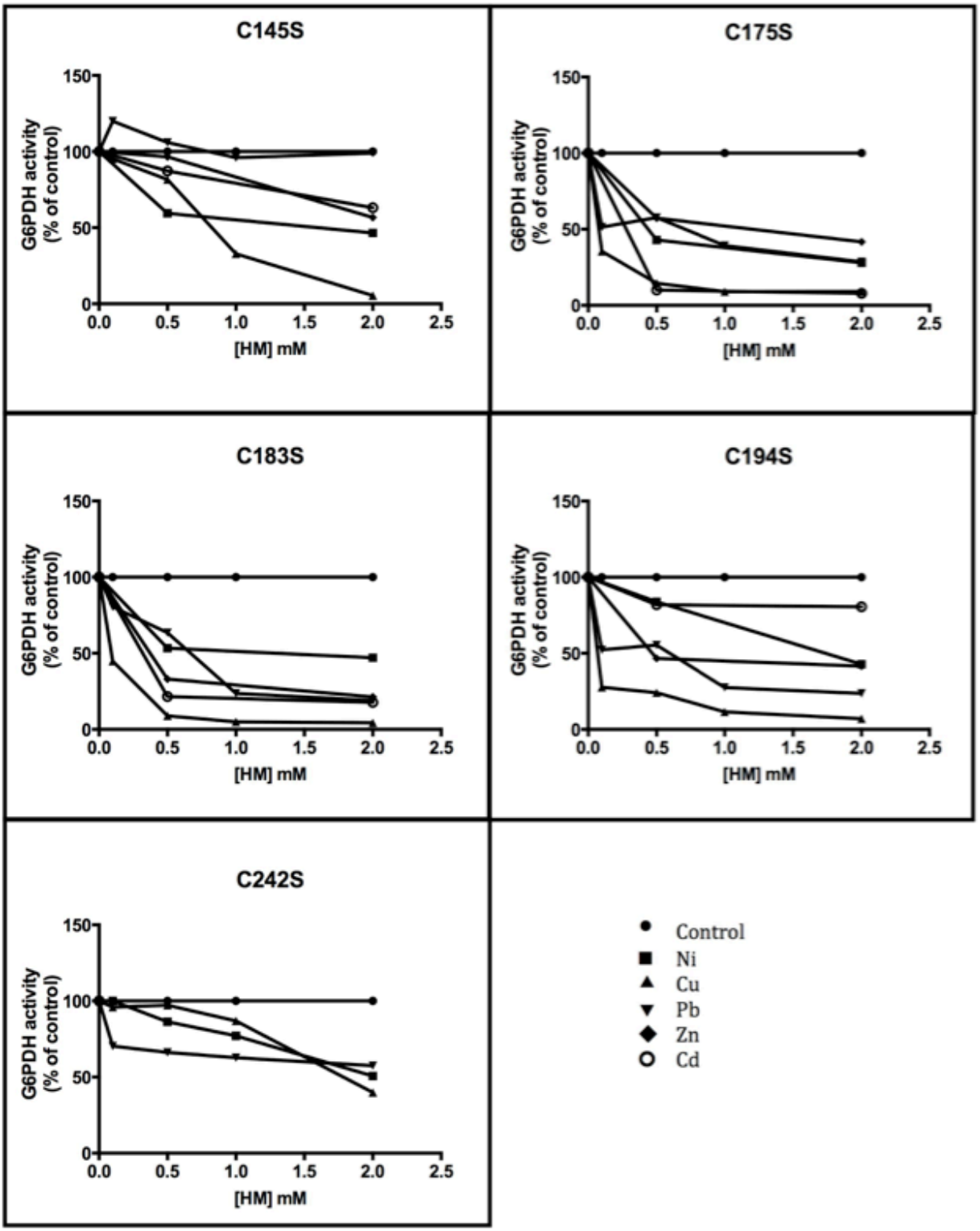

Fig. 26: %G6PDH activity of several cys to ser mutants after incubation with differents Heavy metals.

				Regulatory Cysteines			
	[HM]	*WT*	*C145S*	*C175S*	*C183S*	*C194S*	*C242S*
	0	100	100	100	100	100	100
		100%	71%	18%	19%	56%	75%
Pb	0,1 mM	98	99	60	80	80	80
	1 mM	100	100	54	24	64	60
Ni	0,1 mM	98	98	52	53	80	89
	1 mM	55	89	43	32	60	60
Cd	0,1 mM	79	80	29	22	83	80
	1 mM	73	60	24	14	63	60
Zn	0,1 mM	90	80	26	33	80	80
	1 mM	76	60	25	12	60	60
Cu	0,1 mM	94	80	24	45	80	80
	1 mM	70	60	23	5	60	60

Colors Legend

	100≤90 %		59≤50 %		19≤0 %
	89≤80 %		49≤40 %		
	79≤70 %		39≤30 %		% WT (CxxxS)
	69≤60 %		29≤20 %		

Table 11: G6PDH activity assays on wt e mutants of PtP2-G6PDH after incubation with different heavy metals

5.4 G6PDH activity in *Hordeum vulgare* plants

In order to assess the effects of heavy metals on whole living plants, *Hordeum vulgare* plants grown in hydroculture were treated with differents heavy metals at differents concentrations. At given times barley plants were collected, and G6PDH assays were performed (Fig. 27).

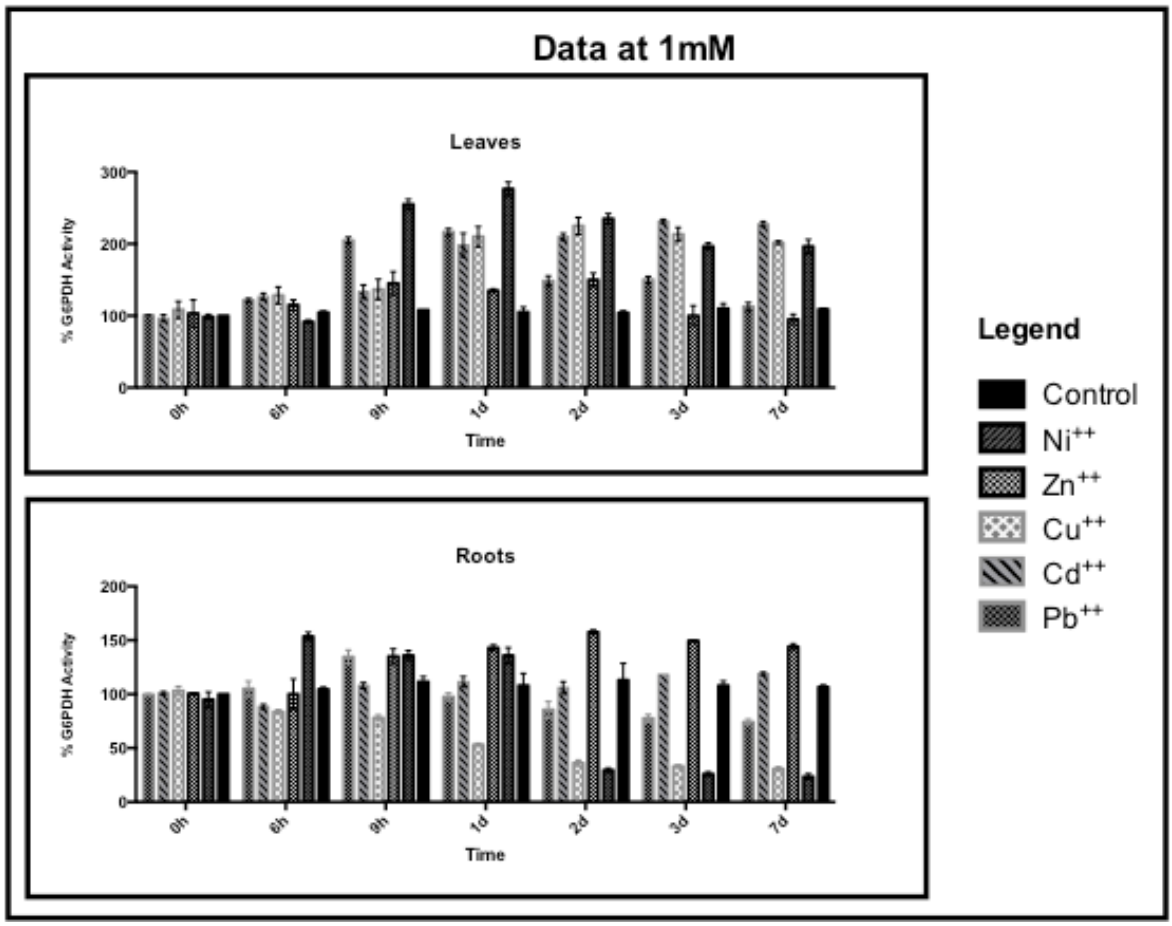

Fig. 27: The graph shows changes in G6PDH activity after incubation of barley plants with 1 mM of each heavy metals (activity% versus time of incubation).

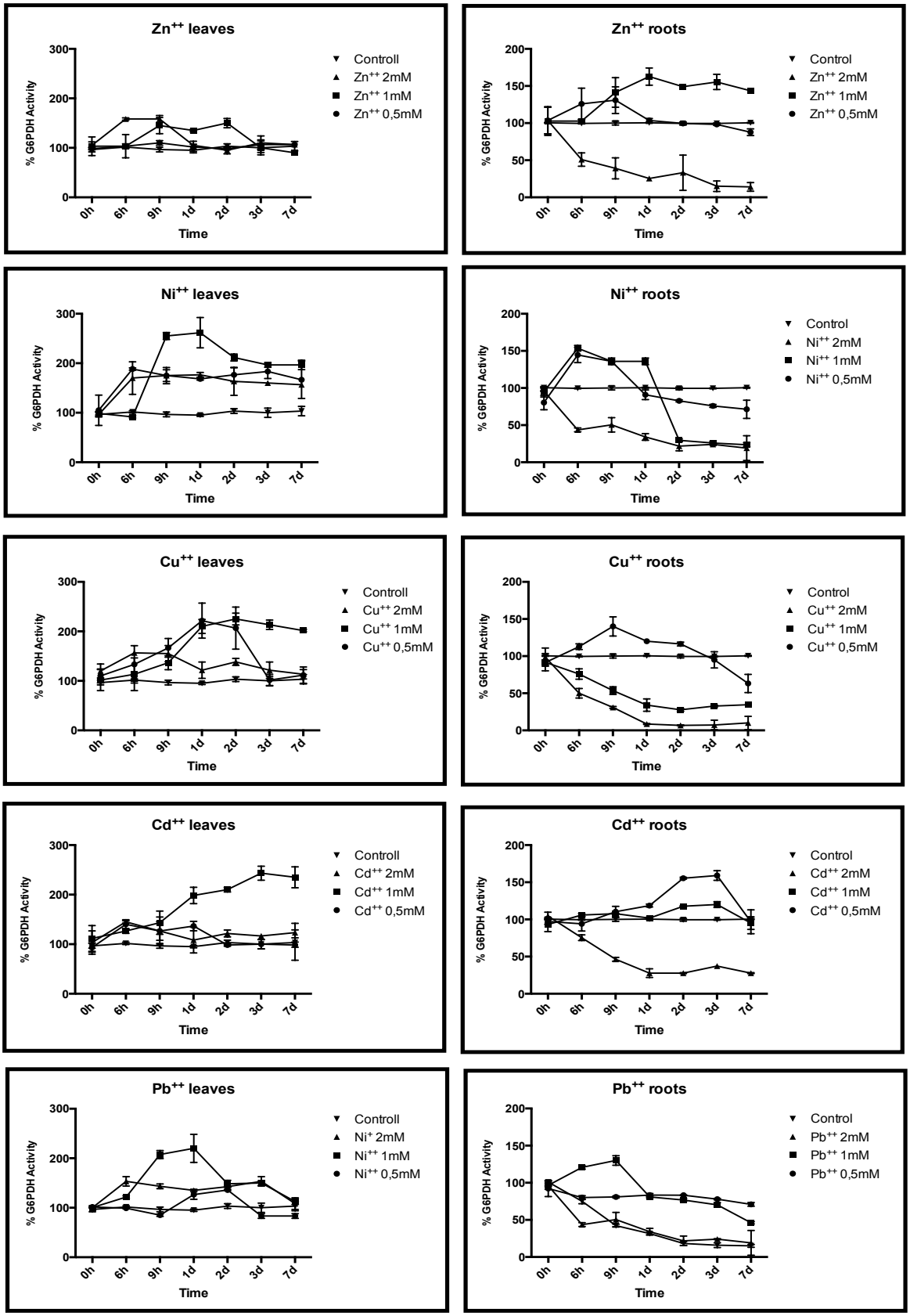

Fig. 28: The graph shows changes in G6PDH activity after incubation of barley plants with different heavy metals (activity% versus time of incubation with each metal concentration.

Total G6PDH activity in barley leaves was 30 ± 4 nmol * min^{-1} * mg^{-1} prot.; in the roots enzyme rate was 110±8 nmol * min^{-1} * mg^{-1}prot (Fig. 28).

Generally, in the leaves HMs exposure resulted in a limited - but evident - increase with some elements, whereas in the roots a general detrimental effect was observed.

Specifically, among the metals tested, in the leaves Ni^{++} and Cd^{++} were those causing most evident changes in G6PDH activities, 2.5-fold increase and 2.3-fold, at 1 mM after 1 d, respectively; Cu^{++} induced a 2 -fold increase up to 7d at 1 mM. Zn^{++} caused a negligible effect, and a low increase in G6PDH activity was observed only at 2 mM, after 6 to 9 hours.

In the roots, Cu^{++} and Cd^{++} caused a severe decrease in G6PDH activity, the residual rate was less than 40% after 1d at 1-2 mM; lead and zinc did not showed major effects up to 2 mM, when their toxic effects lowered G6PDH activity at less than 50% after 1d. Interestingly, Ni^{++} induced an increase of enzyme rate at 1-2 mM within 1 day; after that G6PDH activity crashed at less than 30%.

5.5 Measurements of different enzymatic activities in barley plants

In order to estimate if heavy metals were able to cause changes in different enzymes involved in basal metabolism, activity assays were performed on barley plants exposed to Nickel, the metal causing the higher inhibition effects on *Pt*P2-G6PDH.

The assays were made after exposing plants to 1 mM Ni, the level resulting the major variation of *Pt*P2G6PDH activity in plants during the stress.

5.5.1 Catalase and ascorbate peroxidase activities

Catalase (EC 1.11.1.6) and ascorbate peroxidase (EC 1.11.1.11) activities were estimated to assess the ROS scavenging capability during oxidative stress induced by Ni (Fig. 29).

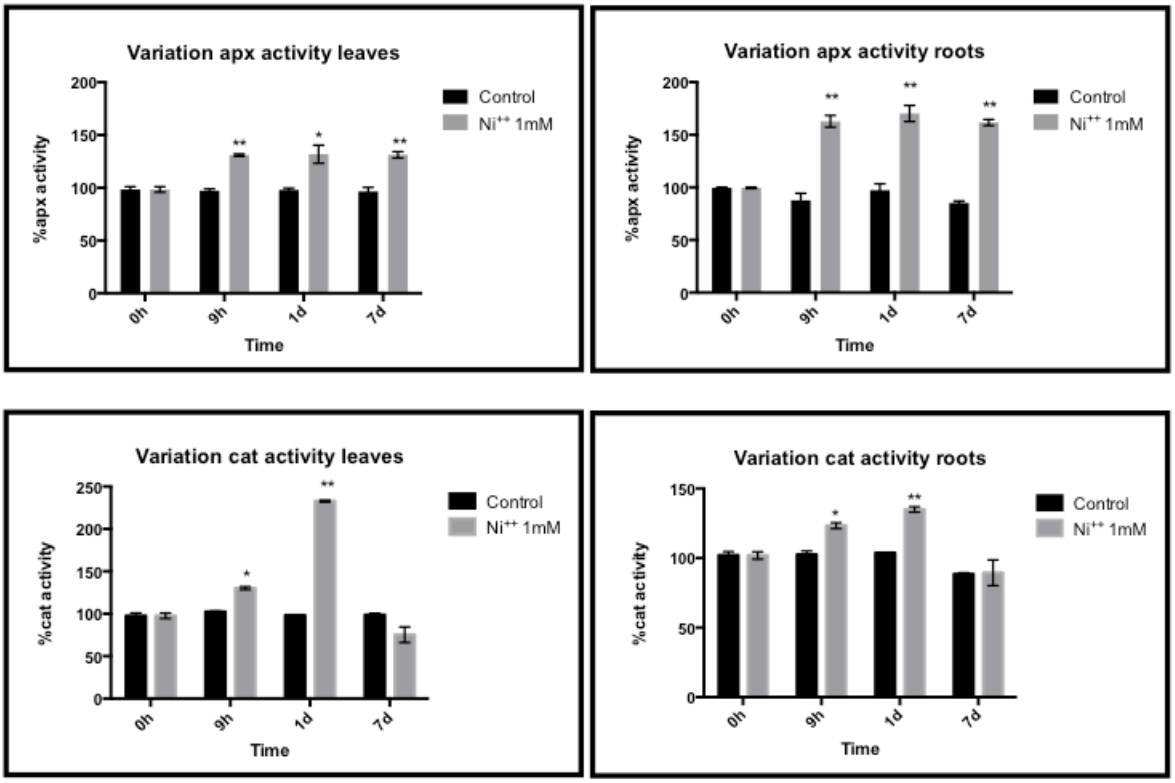

Fig. 29: The graph shows changes in Cat and apx activities after incubation of barley plants with 1mM Nickel (activity% versus time of incubation with metal).

Basal catalase activity (control = 100%) was 583.4 ± 10,7 nmol * min^{-1} * mg^{-1} prot in the roots, and 643.9 ± 15,2 nmol * min^{-1} * mg^{-1} prot in the leaves. An increase of about 20% in the activity was observed in both leaves and roots after 9 hours of Ni exposure; after 1d, a 2.3-fold increase was detected in the leaves; in the roots the activity increased slightly to return to the basal value after 7d.

Differently, apx activity immediately raised by 50-60% after 9h with respect to the control plants (basal activity: 108 ± 10 nmol * min^{-1} * mg^{-1} prot); in the leaves, enzyme rate increased by 30-40% with respect to the basal rate (126.92 ± 2,4 nmol * min^{-1} * mg^{-1} prot) within 1d.

5.5.2 NADH-GOGAT activity determination

NADH- Glutamine oxoglutarate aminotransferase (NADH-GOGAT- EC 1.4.1.14) was utilized as marker of nitrogen metabolism during Ni^{++} stress (Fig. 30).

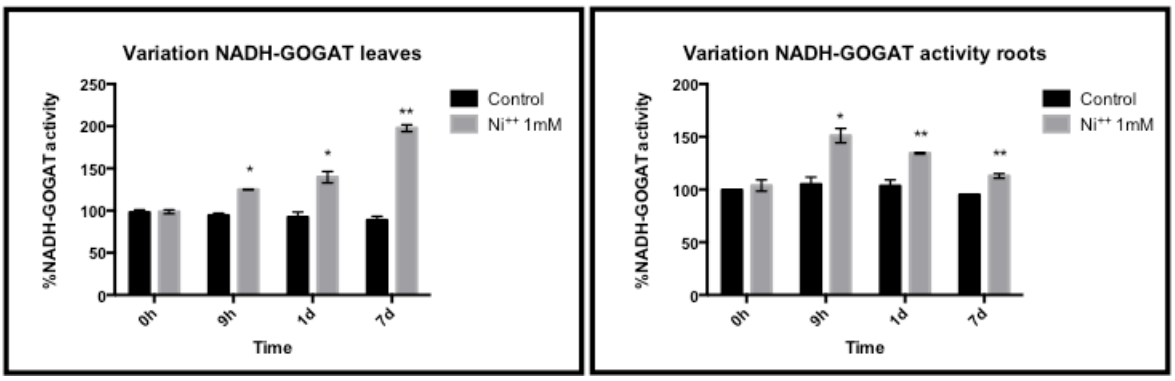

Fig. 30: The graph shows changes in NADH-GOGAT activity after incubation of barley plants with 1mM Nickel(activity% versus time of incubation with metal

Enzyme rate increased by 50% with respect to the initial value (10295 ± 40 nmol min^{-1} mg^{-1} prot) in barley roots after 9h exposure to Ni. After 1d, the activity gradually returned to the initial condition.

In the leaves, activity gradually and continuously increased: after 7 days the activity was about 80% higher than the basal activity (793 ± 17.4 nmol min^{-1} mg^{-1} prot in the leaves).

5.5.3 Phospho*enol*pyruvate Carboxylase Assay

PEPcase (EC 4.4.4.31) was utilized as marker of dark CO_2 fixation metabolism during Ni^{++} stress (Fig. 31).

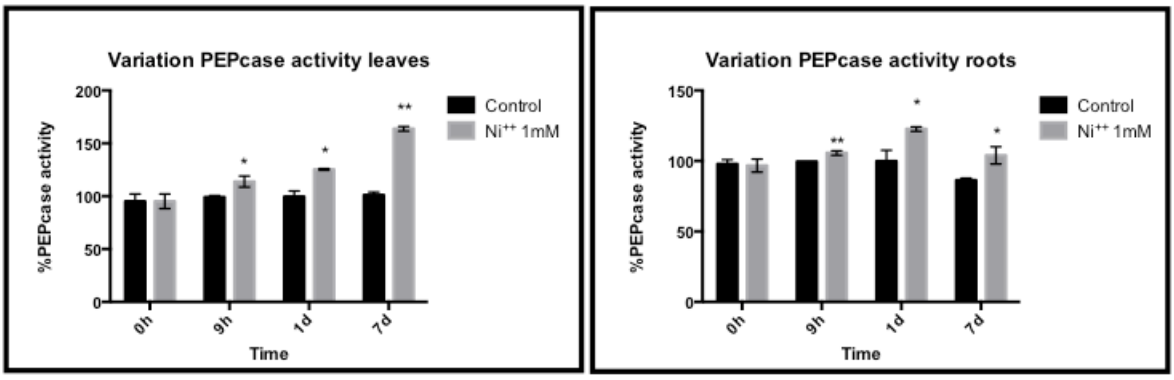

Fig. 31: The graph show changes in PEPcase activity after incubation of barley plants with 1mM Nickel (activity as % versus time of incubation)

The basal phospho*enol*pyruvate carboxylase activity (PEPcase EC 4.4.4.31) (= 100%) was 45 ± 1 nmol * min^{-1} * mg^{-1} prot in the roots, and 27.7 ± 1.4 nmol * min^{-1} * mg^{-1} prot in the leaves.

The exposure to Ni^{++}, differently from the other enzymes tested, caused few changes in PEPcase activity in the roots while a gradual increase was observed in the leaves, where the final activity was 60% higher than in control plants.

5.5.4 Fumarase assay

The effects of Ni^{++} on mitochondrial TCA were monitored by fumarase activity (Fig 32).

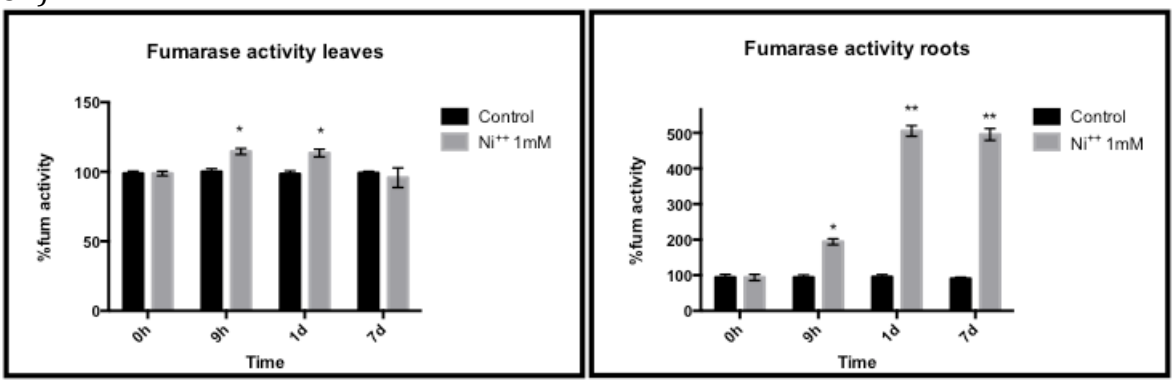

Fig. 32: The graphs show changes in Fumarase activity after incubation of barley plants with 1 mM Nickel (activity as % vs time of incubation with metal)

The effects of Ni^{++} on mitochondrial TCA were monitored by fumarase activity.

Basal activity (= 100%) was 85 ± 5.5 nmol * min^{-1} * mg^{-1} prot in the roots, and 128.5 ± 1.5 nmol * min^{-1} * mg^{-1} prot in the leaves.

A drastic increase of fumarase activity was especially detected in the roots, where activity increased by 400% just after one day; in the leaves a modest 15% increase was, observed.

5.6 Western Blottings

The possible correlation between variations in enzyme activities and abundance of the proteins levels was investigated by western blotting analyses on both leaves and roots of barley plants exposed to 1 mM Nickel. In order to quantify the results, reacting bands were measured by densitometric analysis using Quantity one tools.

5.6.1 Determination of G6PDH levels

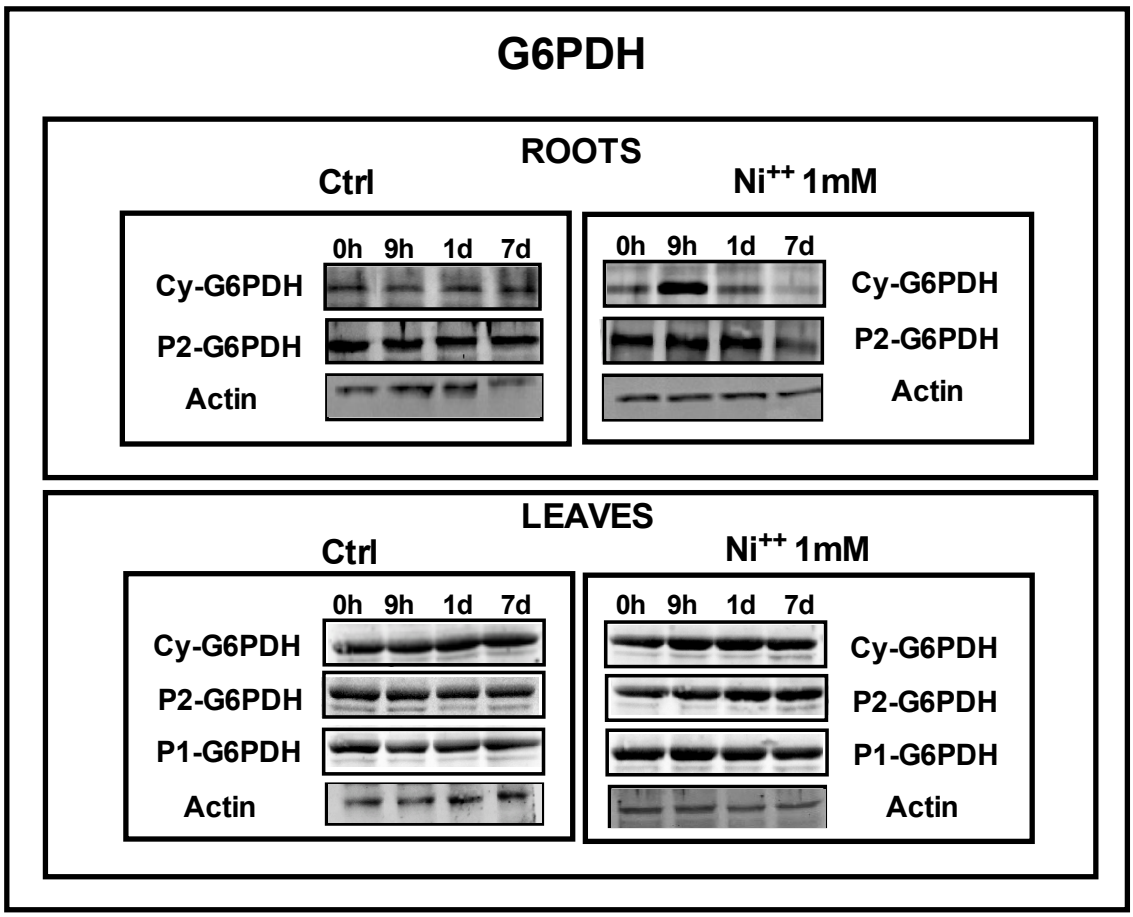

Fig. 33: Western Blotting analyses with antisiera direct against the different G6PDH isoforms in barley leaves and roots.

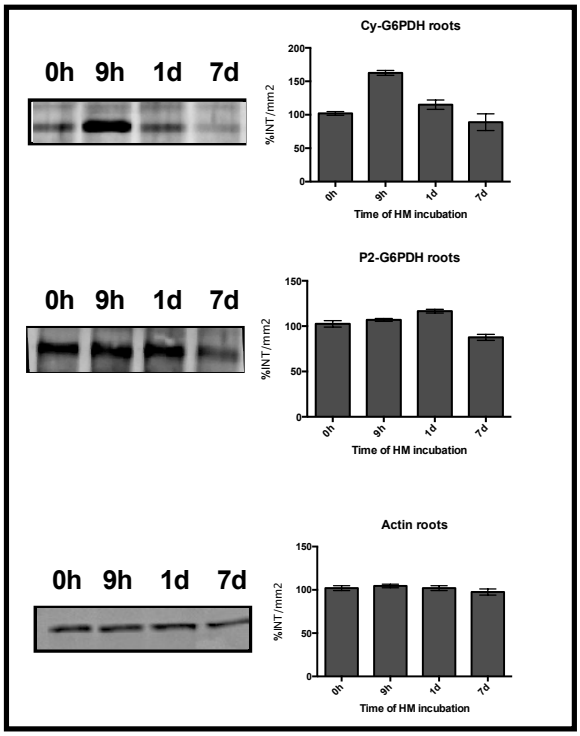
Cy-G6PDH roots
0h 9h 1d 7d
%INT/mm2
Time of HM incubation
P2-G6PDH roots
0h 9h 1d 7d
%INT/mm2
Time of HM incubation
Actin roots
0h 9h 1d 7d
%INT/mm2
Time of HM incubation

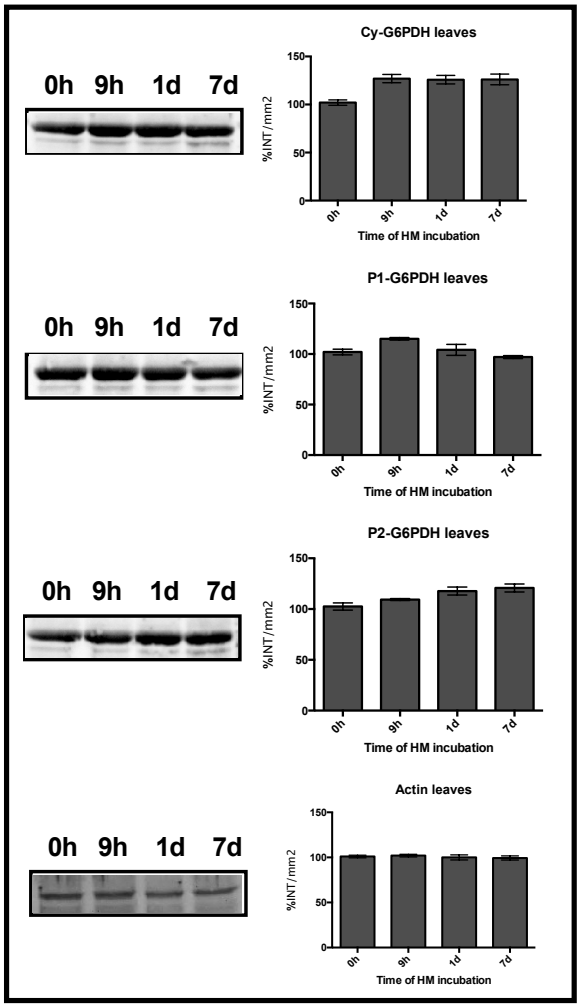
Cy-G6PDH leaves
0h 9h 1d 7d
%INT/mm2
Time of HM incubation
P1-G6PDH leaves
0h 9h 1d 7d
%INT/mm2
Time of HM incubation
P2-G6PDH leaves
0h 9h 1d 7d
%INT/mm2
Time of HM incubation
Actin leaves
0h 9h 1d 7d
%INT/mm2
Time of HM incubation

Fig. 34: Densiometric analyses of the resulted bands of the western blotting using antisiera against the G6PDH isoforms.

Western blottings revealed changes in the occurrence of the three G6PDH isoforms in both roots and leaves of barley plants exposed to 1 mM Ni^{++} (Fig. 33-34).

In the leaves, P1-G6PDH levels slightly increased in the first 24h; similarly, P2-G6PDH levels increased slowly, but continuously, up to the 7th day; in contrast, a rapid 35% increase in Cy-G6PDH occurrence was observed after 9h and maintained in the following period.

In the roots, a prompt increase of cyt-G6PDH was observed after 9h, but also rapidly the levels of the cytosolic isoform returned to the basal levels. As in leaves, a continuous and constant increase of detectable P2-G6PDH was observed, even if in the roots its levels slightly declined at 7d at 80% of the initial values.

5.6.2 Determination of different enzymes levels

Wesyern blottings analyses were utilized to determine the levels of the others enzymes tested in barley leaves (Fig 35-36).

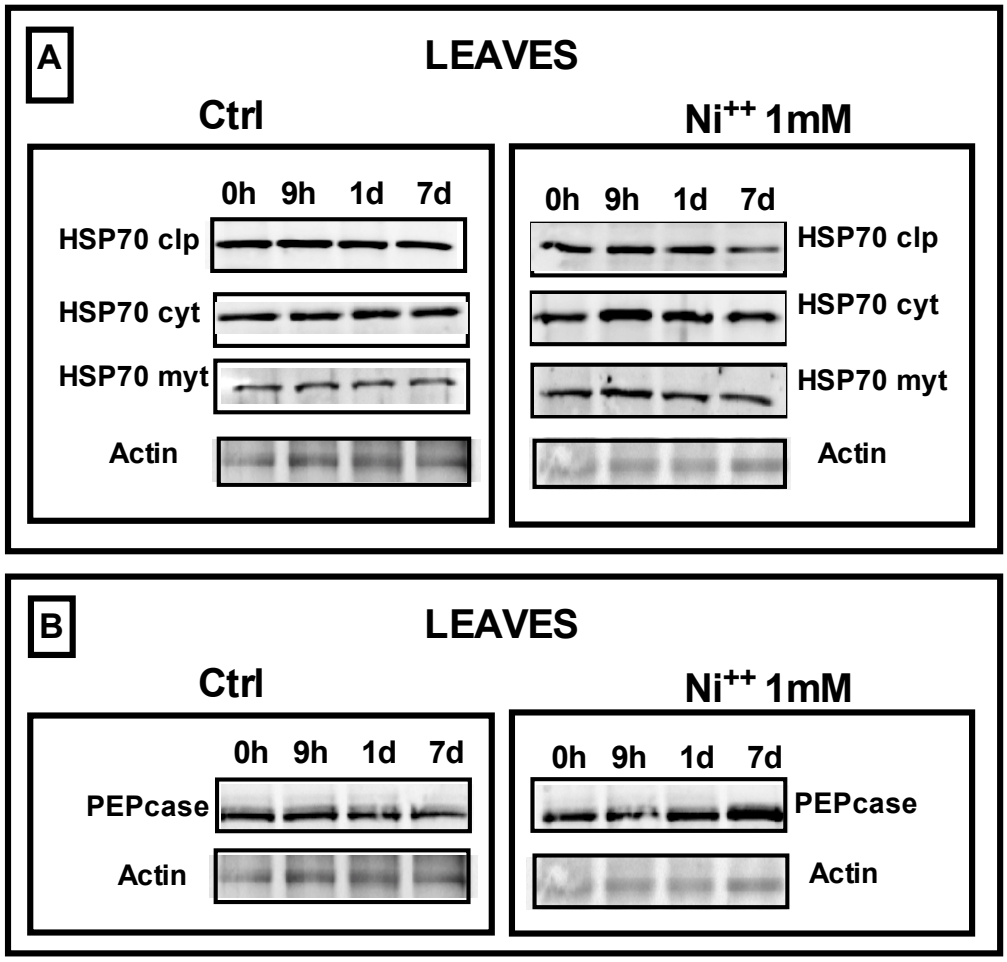

Fig. 35: Western Blotting analyses with antisiera direct against the different HSP70 isoforms (A) and against PEPcase (B) in barley leaves.

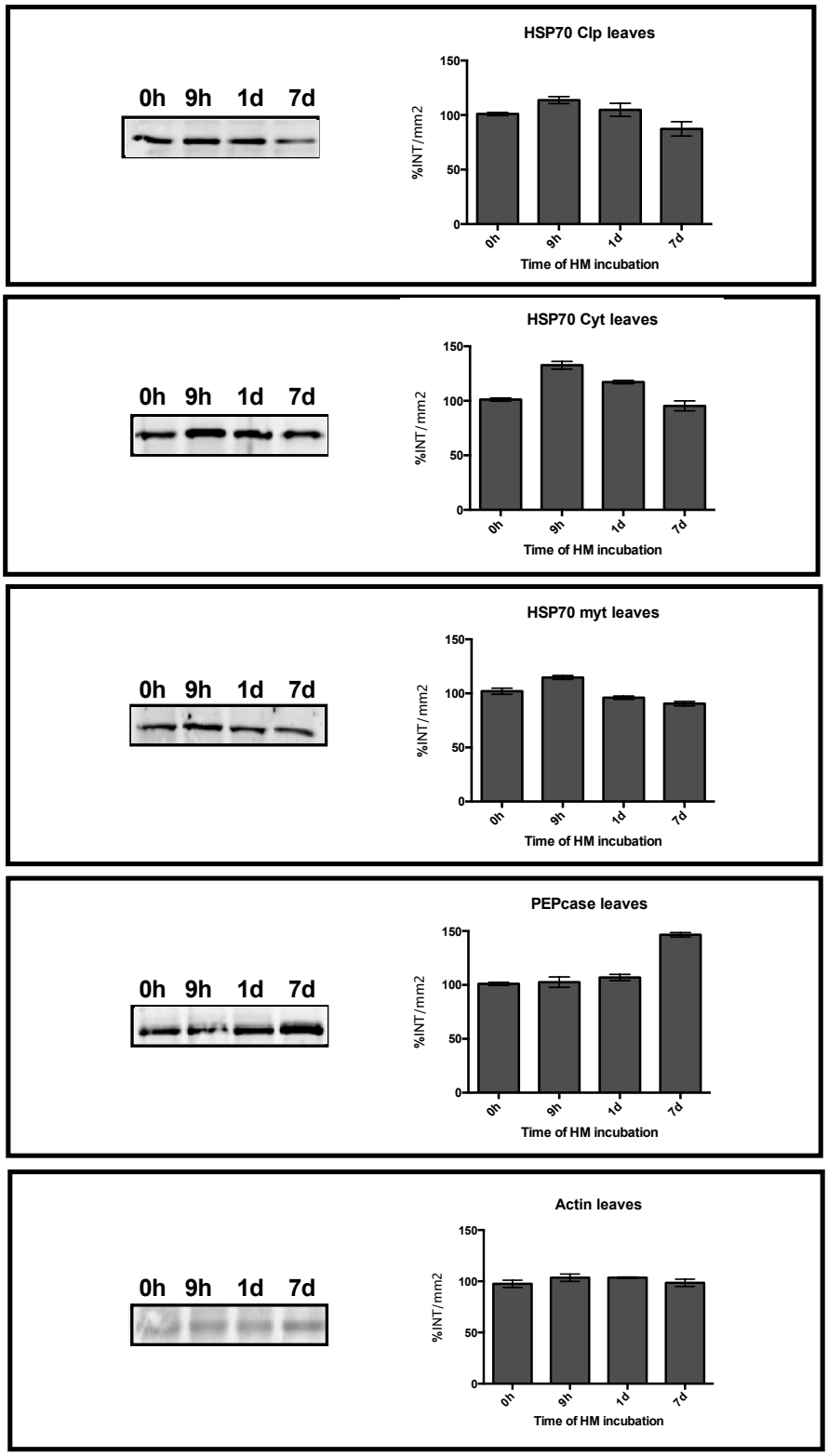

Fig. 36: Densiometric analyses of the resulted bands of the western blotting using antisiera against the HSP70 isoforms and against PEPcase.

Due to the availability of antisera discriminating the different Hsp70 isoforms, western blottings were made in order to investigate the possible changes in the different HSP70 isoforms in barley leaves extracts exposed to 1 mM Ni^{++}.

The cytosolic isoform was the HSP70 most affected by the metal: a prompt 35% increase of cytHSP70 band was observed in Ni-exposed plants after 9h. In contrast, only slight increases, less than 15%, were observed in both mithocondrial and chloroplastic HSP70 isoforms in the first 24h.

Differently, PEPcase levels remained unchanged upon Ni exposure, increasing by 40% only after 7 days of treatment.

5.7 qRT-PCR

The changes observed in acivities of different enzymes, and in the occurrence of proteins, strongly suggest possible variations in the expression of relative genes. Therefore, qRT-PCR analyses were done using specific primers fordifferent genes (expressed as fold-change with respect to control) in the leaves of *Hordeum vulgare* plants exposed to 1 mM Ni^{++} for 7 days (Fig. 37).

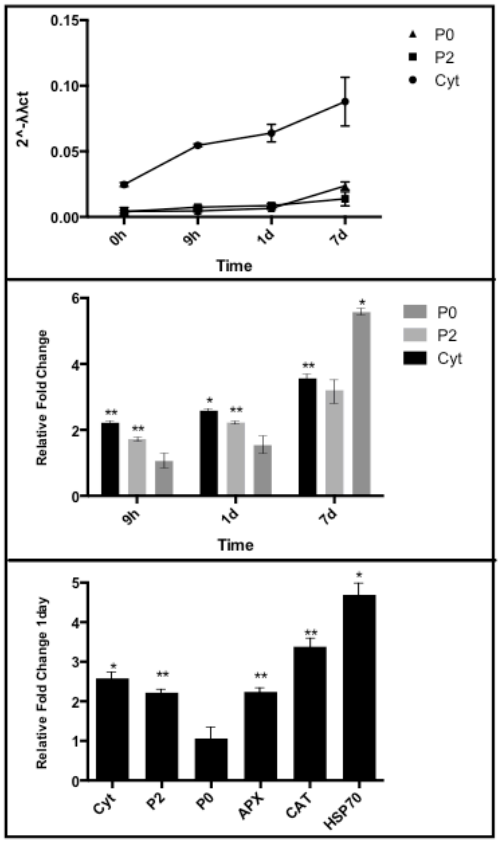

Fig. 37: qRT-PCR of differents Hordeum vulgare genes after exposition to 1mM Nickel.

The expression of Cy-G6PDH increased 2-fold after 1d after Ni^{++} exposure, and up to 3-fold after 7d. A similar behaviour was observed for P2-G6PDH also.

Interestingly, P0-G6PDH slowly increased in the first part of the experiment, while after 7d a massive 5-fold increase in the expression of this gene was observed.

Regarding others genes tested, a general increase was observed in both APX (2-fold) and catalase (3-fold); intriguingly, HSP70 genes increased more than 5-fold, indicating a prompt response to stress by the plant cell (Fig. 37).

5.8 RAPD analyses

RAPD analyses were made to determine if the presence of Ni^{++} was able to induce genotossic damage by breakages in the DNA.

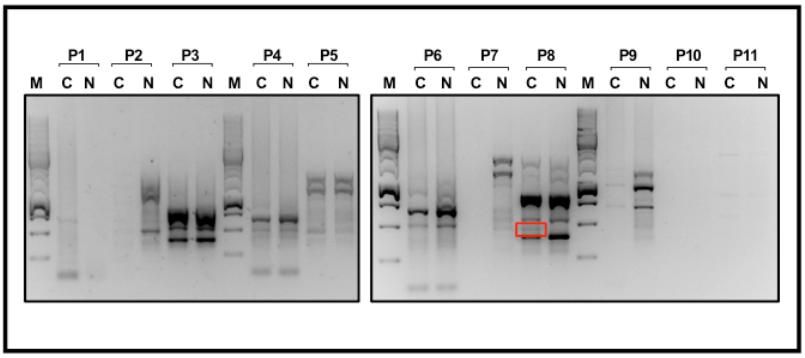

Fig. 38: Agarose gel of the RAPD analyses of the control and treated DNA plants.

Among 11 primers pairs tested, only one pair, p8, revealed the presence of a different amplification pattern with respect the control plants (Fig. 38).

5.9 Comet assay

Comet Assay analyses were also made to verify the presence of point mutations in the DNA of the treated plants.

Observations were made on leaves and roots: comets obtained (Fig. 39) were analyzed by ImageJ, and Open Comet software to determine % DNA in comet heads and %DNA in comet tails, and to calculate their incidence in the population (Table 12).

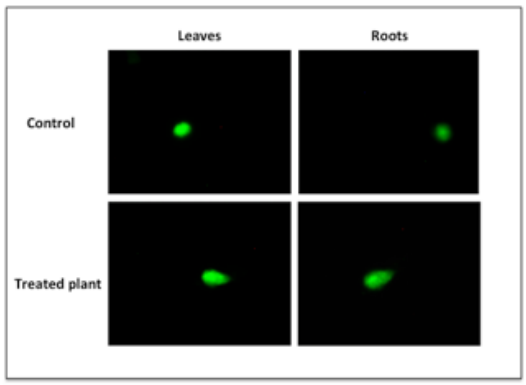

Fig. 39: Comet obtained after tratment with 1mM Nickel

	% Head DNA	% Tail DNA	% Comets on total nuclei
Roots	72%	28%	9%
Leaves	87%	13%	7%

Table 12: %DNA obtained with Open Comet software

5.10 Analyses of the growth factor

The impact of Ni^{++} was tested by monitoring different parameters as water content, growth variation, and pigments content (chlorophyll-a, chlorophyll-b, carotenoids).

5.11 Growth variation

The measure was obtained considering the weight of the total plant and considering separately the different part of the plant (roots, leaves).

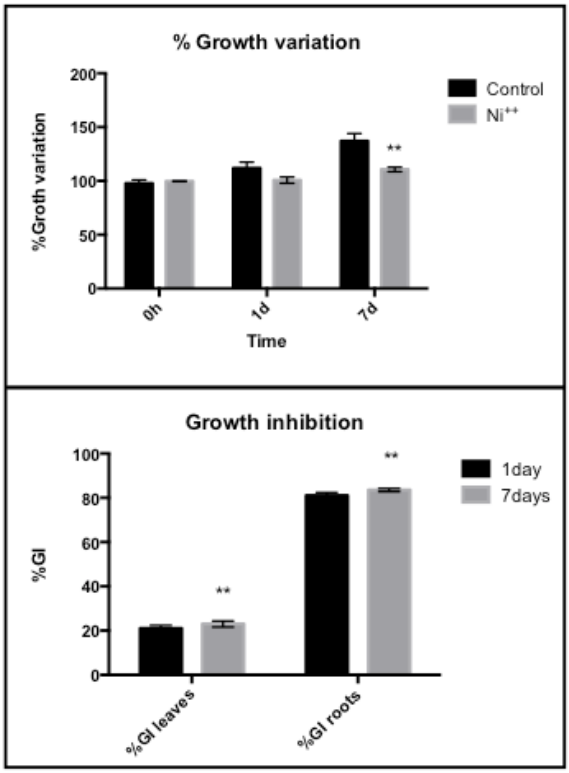

Fig. 40: Variation of growth, and growth inhibition with 1mM Nickel

Figure 40 suggests that the presence of Ni^{++} was able to induce a slowdown in the growth of treated plants. After 1d, the growth was 6% slower than in control plants, and this decrease increased up to less 17% after 7d of Ni^{++} exposure, compared to the control plants. Particularly most of the inhibition was observed in the roots, where Ni^{++} induced 80% of the total inhibition.

5.12 Water content

Water content (WC) and relative water content (RWC) were measured at different times after Ni treatment. The content was quantified by calculating the ratio between the weights of treated plants to their fully hydrated, turgid state.

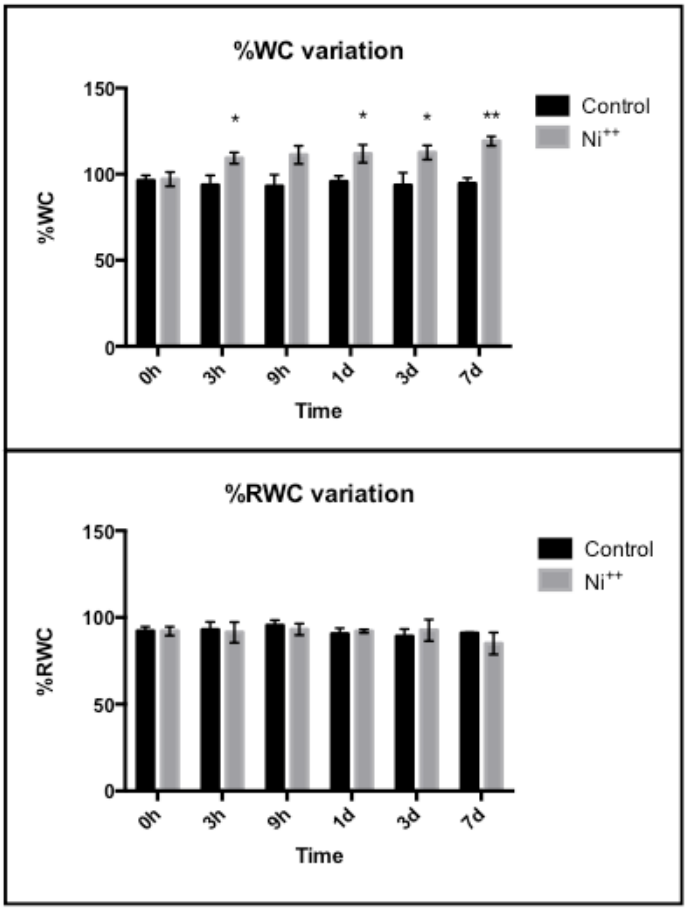

Fig. 41: Variation of WC and RWC in control plant and treated plant with 1mM Nickel

A big difference between WC and RWC was observed (Fig. 41), suggesting that the water content was different if the weight of the plant is compared, or not, to its turgid weight. The graph showed no apparent differences in RWC, while an increase of the percentage of WC was observed in treated plants. These results may indicate that Nickel did not induce changes in plants turgid state (% RWC did not change), and so in their hydration state but just in the capability to absorbing more water.

5.13 Pigments content

Analyses of the pigments content were performed after exposure of barley plants to 1 mM Ni^{++}.

Under HMs stress, sensible changes in photosynthetic pigments are able to cause major changes in both quantity and quality of the chloroplasts ETC.

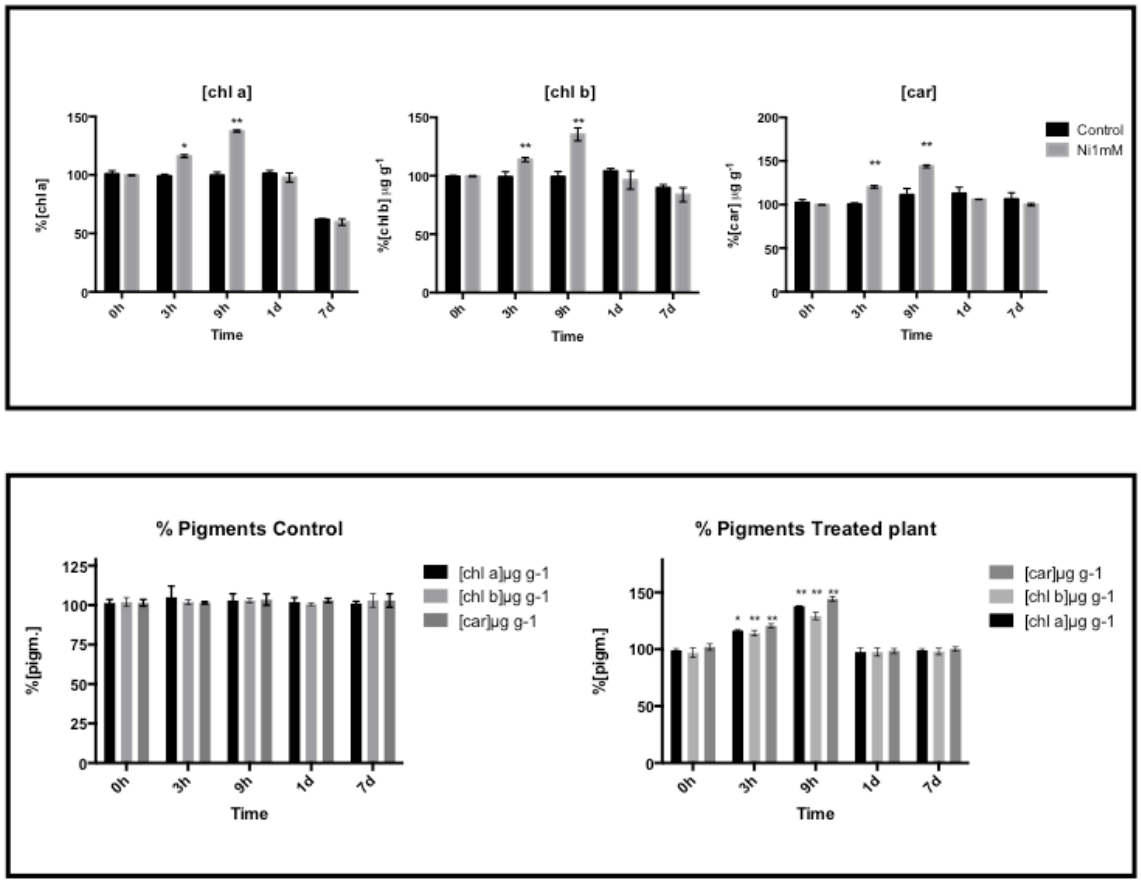

Fig. 42: The graphs show the variations of photosynthetic pigments levels.

Ni exposure induced variations in the levels of different photosynthetic pigments: chl-a, chl-b and carotenoids reached the highest values after 9h of treatment (Fig. 42).

Carotenoids increased by 50% after 9h, while chl a and chl b raised their levels by 40 and 30%, respectively.

5.14 RNA extraction and Gradient-PCR

Total RNA was extracted from young barley plants treated in optimal condition in order to obtain the different constructs necessary to determine the subcellular localisation of P2-G6PDH and P0-G6DPH.

RNA was retrotrascribed to cDNA and a Gradient-PCR was performed with specific primers to obtain the correct sequences. Samples were loaded on 1% agarose gel revealing the correct amplification of the sequences (Fig. 43),

These sequences were purified from the gel and ligated in pBSK vector.

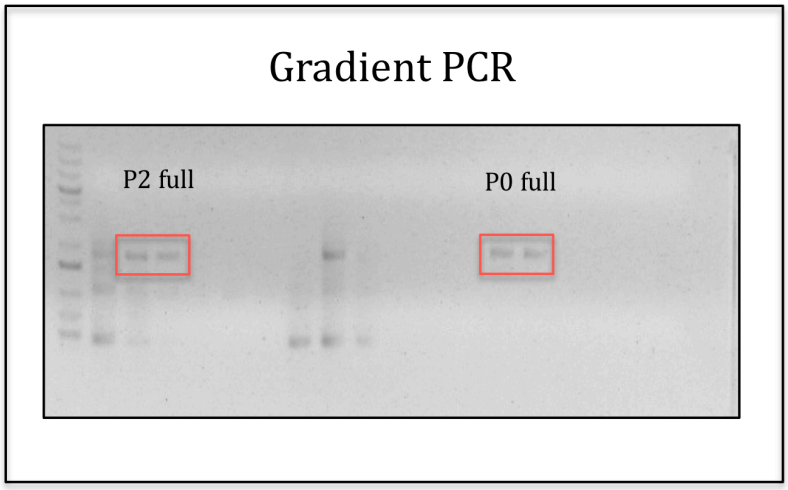

Fig. 43: 1% agarose gel of samples obtained from the gradient PCR

The ligation mix were utilized to transform competents cells of *E. coli* strain XL1-blu. Vectors were purified by miniprep from these colonies, digested and tested to verify the correct insertion of P2-G6PDH and P0-G6PDH sequences into pBSK vector (Fig. 44)

Vectors revealing the correct right insertion of the sequences into pBSK, were sequenced for a final check.

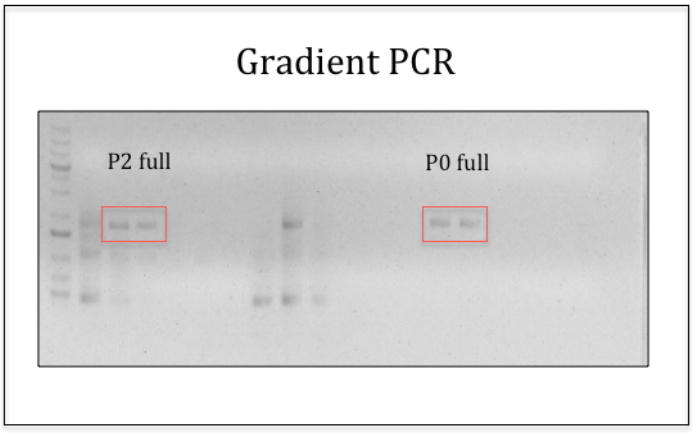

Fig. 44: 1% agarose gel of samples obtained from digestion after miniprep purification.

5.15 Cloning of *Hv*-G6PD2; *Hv*-G6PD0 (behind reporter)

To obtain all the different reporters fusion proteins, the pBSK vectors containing the sequences for P0-G6PDH and P2-G6PDH were utilized to get amplification of fragments to insert in pGFP_NX vectors behind the reporter (GFP) (Fig. 45).

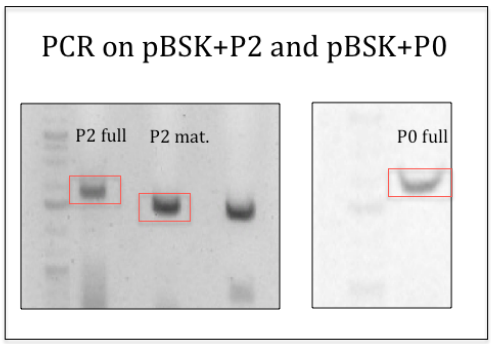

Fig. 45: 1% agarose gel of the products obtained from the PCR on pBSK+P2 and pBSK+P0.

Bands obtained were purified from the gels, and the products inserted into pGFP_NX. Again, transformation of competent *E. coli*, miniprep and digestion tests were performed, in order to check the correct insertion into the vector (Fig. 46).

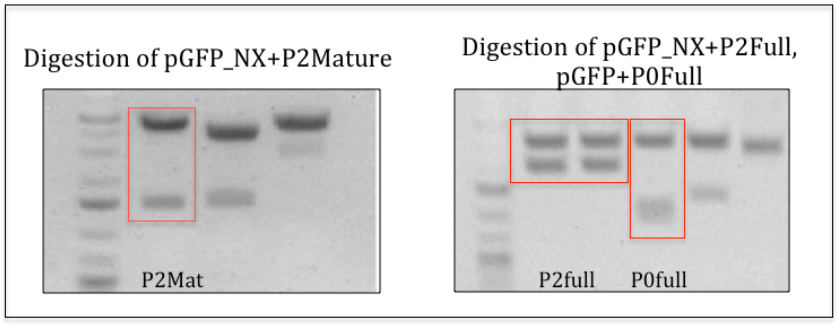

Fig. 46: 1% agarose gel of the samples pGFP_NX+P2 mature and full lenght after digestion.

5.16 Cloning of *Hv*-G6PD2; *Hv*-G6PD0 (in front of the reporter)

The cloning of the G6PDH sequences "in front" of GFP/OFP required a different strategy: the protocol consisted in the digestion of pBSK+P2 and pBSK+P0 vectors in order to cut out the specific fragments to insert into pGFP_NX/pOFP_NX in front of the reporter (GFP-OFP) (Fig. 47)

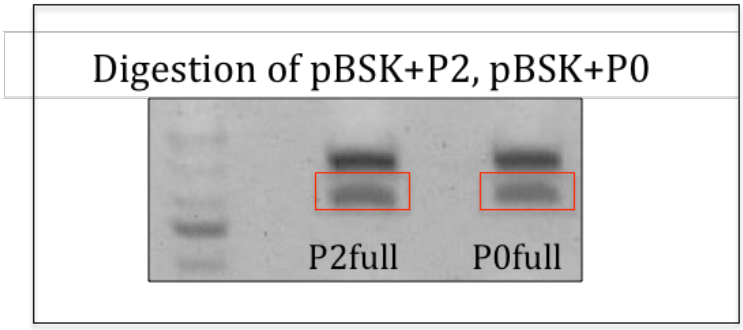

Fig. 47: 1% agarose gel of the samples obtained from the digestion of pBSK+P2/P0.

The bands obtained were purified from 1% agarose gels, and subcloned in the reporter vectors. As standard procedure, the ligation mixture was utilized to transform *E. coli* and the vectors obtained after miniprep were digested and tested (Fig. 48). The correct vectors were utilized to investigate the subcellular localization of P2-G6PDH and P0-G6PDH in *Arabidopsis* protoplasts.

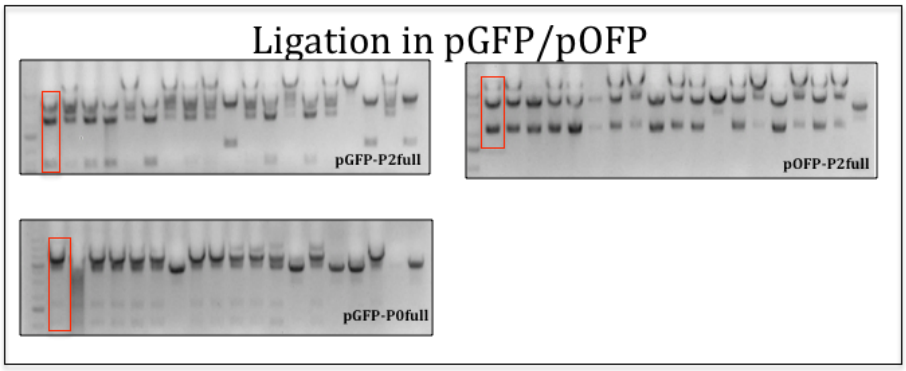

Fig. 48: Digestion of the vectors obtained from the miniprep after transformation of *E.coli*.

5.17 Arabidopsis thaliana growing and protoplast extraction and transfection

Seeds of *Arabidopsis thaliana* were germinated on sterile MS medium with a photoperiod of 16 hours. When rosettes were visible, plantlets were transferred in a sterile box until protoplast extraction. *Arabidopsis* protoplast were transfected with the different reporter vectors in order to determine the subcellular G6PDH localization. Here follow the results of these experiments:

- **P2-GFP + OFP-Lac50 & P2-OFP + GFP-Lac50:** *Hv*P2-G6PDH with GFP (or OFP) fused to the C-terminal end, is targeted to chloroplasts of cells isolated from sugar grown plants (Fig. 49).

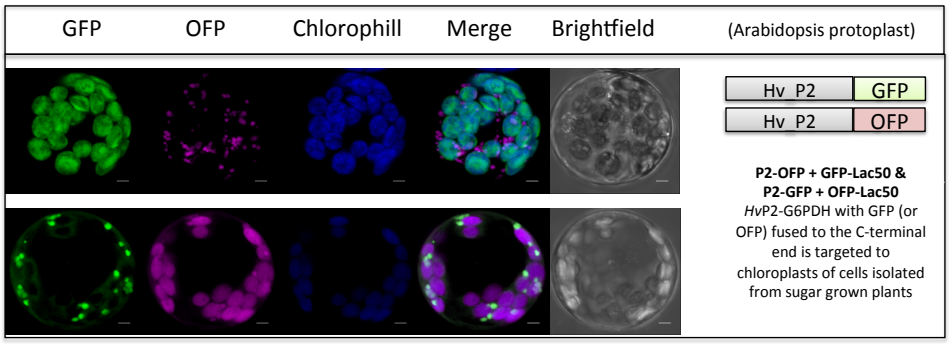

Fig. 49: P2-GFP and P2-OFP in *Arabidopsis* protoplasts

- **GFP-P2 + OFP-Lac50:** *Hv*P2-G6PDH with GFP fused to the N-terminal end, retaining the transit peptide, partially co-localized with the peroxisome marker (Fig. 50).

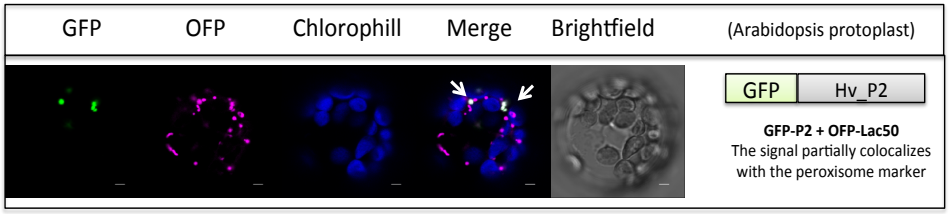

Fig. 50: GFP-P2+OFP-Lac50 in *Arabidopsis* protoplasts

- **GFP-P2mat + OFP-Lac50:** Interestingly, *Hv*P2-G6PDH with GFP fused to the N-terminal end, without the transit peptide ("mature" *Hv*P2-G6PDH), was localized in the cytoplasm (Fig. 51).

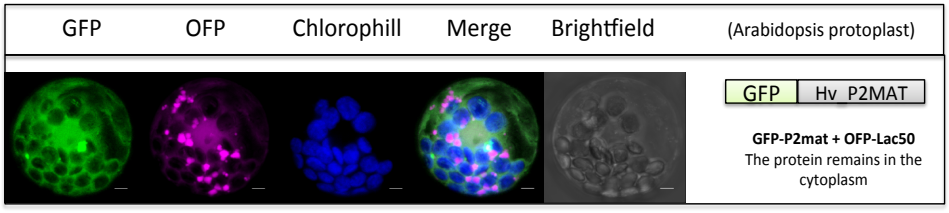

Fig. 51: GFP-P2 mature +OFP-Lac50 in *Arabidopsis* protoplasts

- **P0-GFP + OFP-Lac50:** *Hv*P0-G6PDH with GFP fused to the C-terminal end was targeted to chloroplasts (Fig. 52).

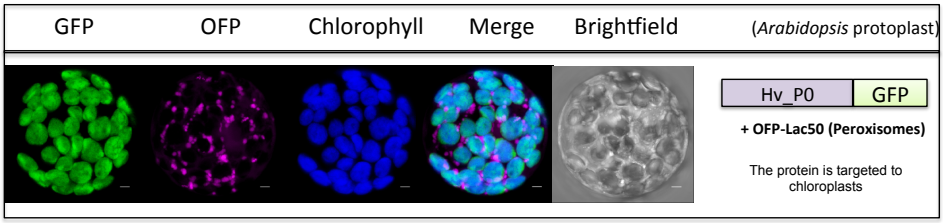

Fig. 52: P0-GFP+OFP-Lac50 in *Arabidopsis* protoplasts

- **GFP-P0 + OFP-Lac50:** In contrast, *Hv*P0-G6PDH with GFP fused to the N-terminal end remained in the cytosol (Fig. 53)

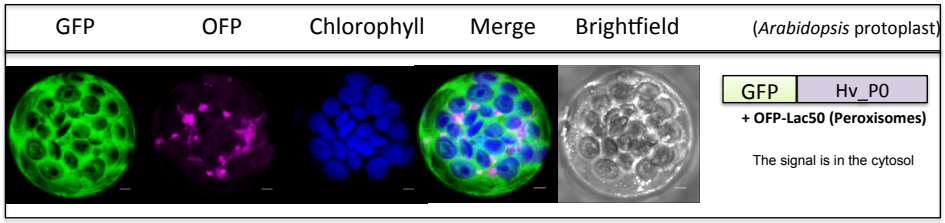

Fig. 53: GFP-P0+OFP-Lac50 in *Arabidopsis* protoplasts

- **GFP-P0mat + OFP-Lac50:** Mature (devoid of the transit peptide) *Hv*P0-G6PDH with GFP fused to the N-terminal end, remained in the cytosol as well (Fig. 54)

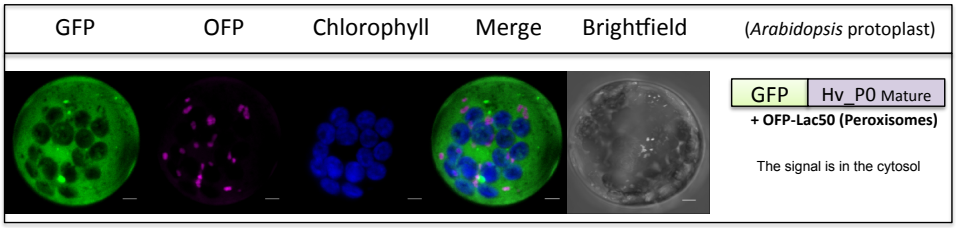

Fig. 54: GFP-P0 mature +OFP-Lac50 in *Arabidopsis* protoplasts

5.18 Protoplast co-transfection

The same constructs were utilized also to analyse the sublocalization after co-transfection and so to determine if the presence of the P0-G6PDH was able to determine variation in P2-G6PDH localization.

- **P2-OFP + P0-GFP:** Both *Hv*P2-G6PDH with OFP fused to the C-terminal, and *Hv*P0-G6PDH with GFP fused to the C-terminal end, localized in the chloroplast stroma (Fig. 55).

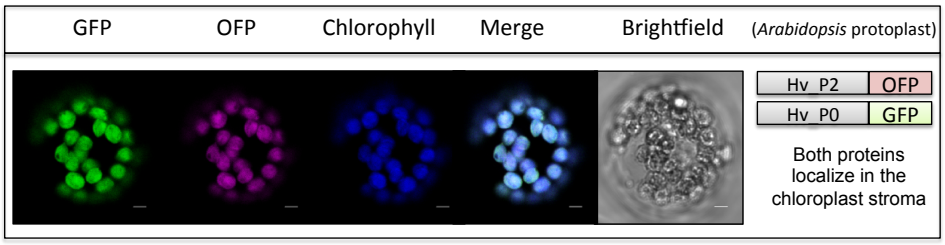

Fig. 55: cotransfection P2-GFP + P0-GFP in *Arabidopsis* protoplasts

- **P2-OFP + GFP-P0:** *Hv*P2-G6PDH with OFP fused to the C-terminal localized in the chloroplasts, and *Hv*P0-G6PDH with GFP fused to the N-terminal end localized in the cytosol, as they did in the single transfection experiments (Fig. 56).

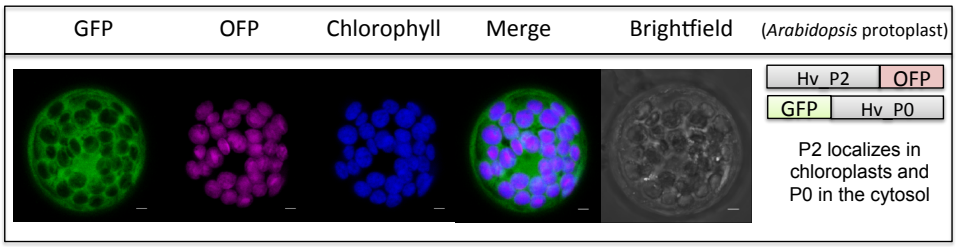

Fig. 56: cotransfection P2-GFP + GFP-P0 in *Arabidopsis* protoplasts

5.19 Binary vectors

To obtain the binary vectors for the agro-infiltration of *N. bentamiana* leaves, the reporter fusion plasmids containing P2-G6PDH and P0-G6PDH were digested by specific enzymes to obtain fragments constituted by GFP/OFP + P2-G6PDH/P0-G6PDH. These fragments could be inserted directly into the pGPTVII-GFP-HYG vectors.

To this aim, pGFP_NX (pOFP_NX) plus P2-G6PDH were digested with XbaI and EcoRI; while the pGFP_NX plus P0-G6PDH were digested with HindIII and EcoRI.

The fragments were purified and ligated into the pGPTVII-GFP-HYG vectors and utilyzed to transform *E.coli* XL10. In order to check the correct insertion of the sequences, PCR with p35S promoter primers, and pNosT terminator primers were done on the vectors after isolation from transformed *E.coli* XL10 colonies (Fig. 57).

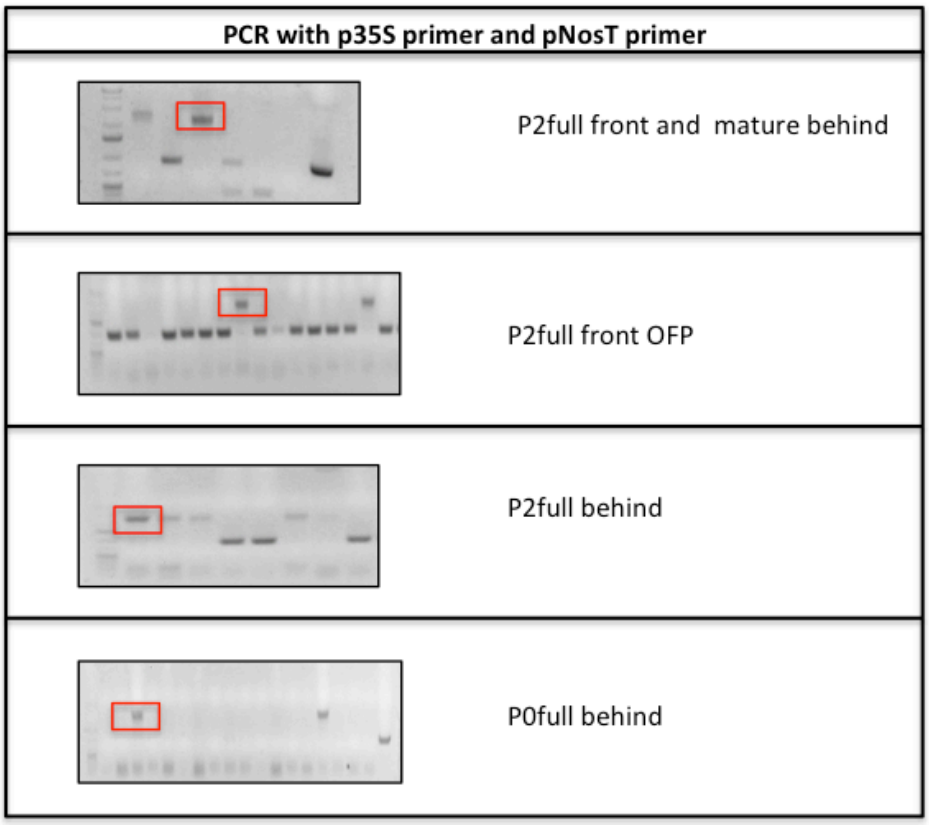

Fig. 57: 1% agarose gel of the products obtained from PCR with p35S primer and pNosT primer.

5.20 Agro-infitration

The vectors were utilised for the *Agrobacteria* transformation and the subsequent Agro-infiltration of *N.bentamiana* leaves.

After the agro-infiltration, plants were grown for two days under optimal conditions and then leaf slices were utilized for CLSM analyses.

- **P2-GFP & P2-OFP:** *Hv*P2-G6PDH with OFP or GFP fused to the C-terminal localized in the plastids of epidermal, heterotrophic cells (Fig. 58).

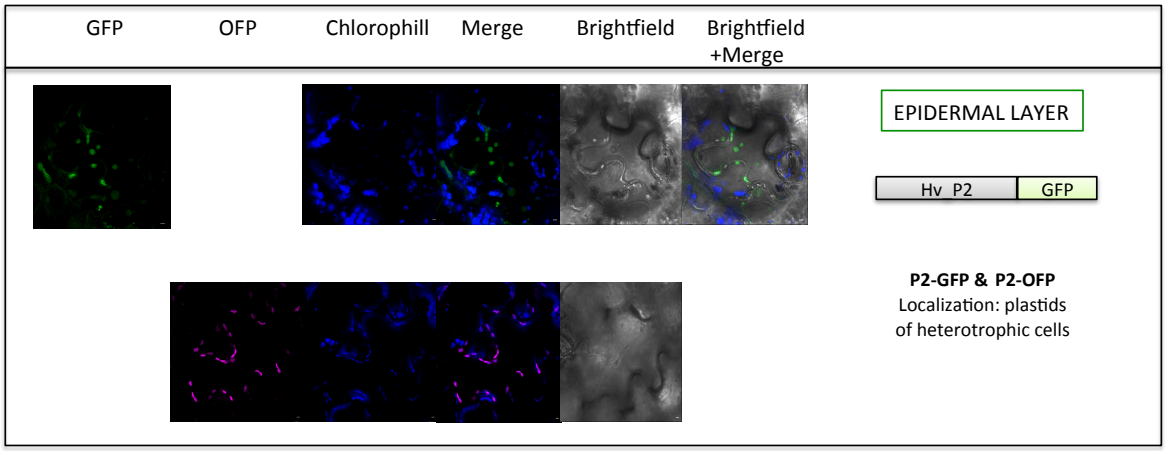

Fig. 58: P2-GFP in *N. benthamiana* leaves epidermal layer

- **P2-GFP:** In contrast, *Hv*P2-G6PDH with GFP fused to the C-terminal localized in the cytosol of mesophyll, photoautotrophic cells (Fig. 59).

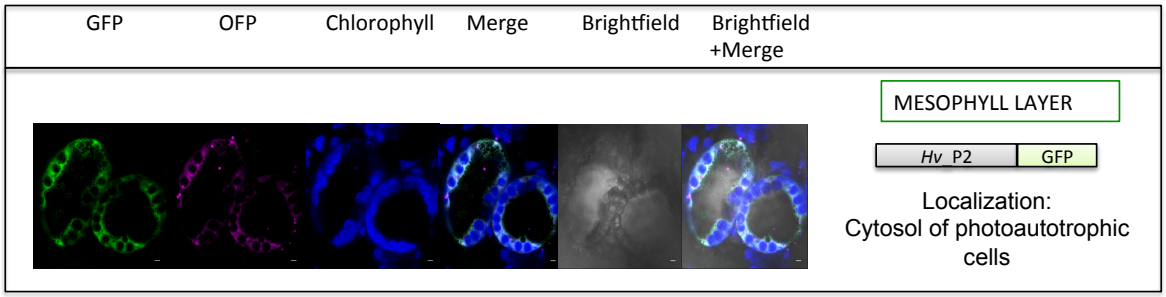

Fig. 59: P2-GFP in *N. benthamiana* leaves mesophill layer

GFP-P2mat + OFP-Lac50: *Hv*P2-G6PDH with GFP fused to the N-terminal end, without the transit peptide ("mature" *Hv*P2-G6PDH), was localized in the cytosol of epidermal, heterotrophic cells. The OFP-Lac50 construct clearly indicated that "mature" *Hv*P2-G6PDH was not directed into peroxisomes (Fig. 60).

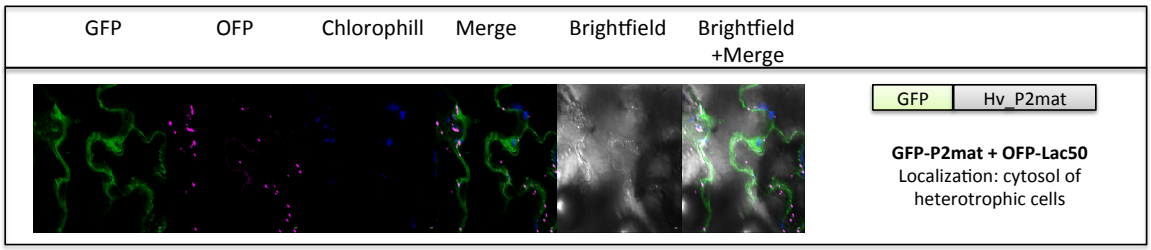

Fig. 60: GFP-P2 mature in *N. benthamiana* leaves

- **GFP-P2 + OFP-Lac50:** Intriguingly, a partial co-localization with peroxisomal marker was observed for *Hv*P2-G6PDH with GFP fused to the N-terminal end, retaining the transit peptide (*Hv*P2-G6PDH) (Fig. 61).

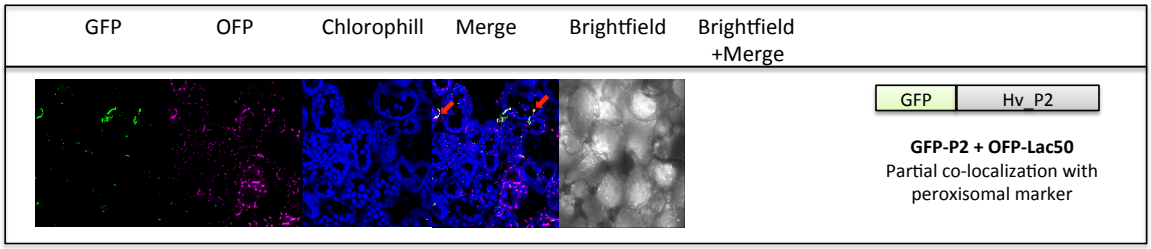

Fig. 61: GFP-P2 in *N. benthamiana* leaves

- **GFP-P0 + OFP-Lac50:** *Hv*P0-G6PDH with GFP fused to the N-terminal end, localized in the cytosol of mesophyll, photosynthetic cells (Fig. 62)

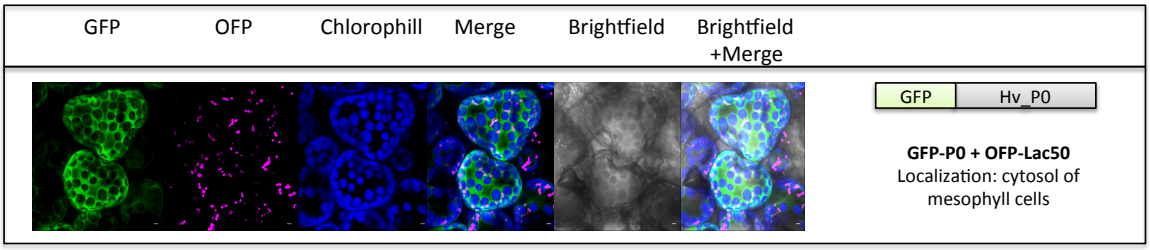

Fig 62: GFP-P0 in *N. benthamiana* leaves

- **GFP-P0 + P2-OFP:** *Hv*P0-G6PDH with GFP fused to the N-terminal end localized in the cytosol of mesophyll, photosintetic cells, while *Hv*P2-G6PDH with OFP fused to the C-terminal localized in the plastids of etherotrophic cells, chloroplasts of mesophylls cells and in peroxisomes (Fig. 63)

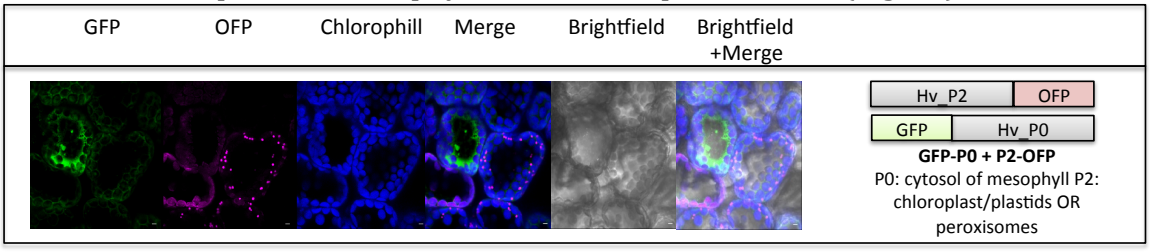

Fig. 63: GFP-P0 + P2-GFP in *N. benthamiana* leaves

6 Discussion

The recombinant plastidic isoform P2-G6PDH from *Populus trichocarpa* was overexpressed and produced in *E.coli*, and purified homogeneity by IMAC. The purified wt, his tagged enzyme had a specific activity of 8000 U/mg protein.

The kinetic properties of *Pt*P2-G6PDH resembled those observed for the recombinant isoform in potato (Wendt et al 2000), P2-G6PDH purified from barley roots (Esposito et al 2001a); and recombinant barley P2-G6PDH, with and without the his-tag (Cardi et al., 2013). At this regard, it should be underlined that the his-tail did not affect the main kinetic properties of this enzyme, as previously demonstrated for barley P2-G6PDH (Cardi et al., 2013).

Our results suggest that Cu^{+2} was the most powerful inhibitor of P2-G6PDH in the long-term: the inhibition potentials could described by the following sequence: $Cu^{++} > Zn^{++} > Cd^{++} > Ni^{++} > Pb^{++}$.

This sequence is similar to the sequence obtained by thermodinamics experiments reviewed by Dudev and Lim (2014), and previous results on based on carbonic anhydrase II (Zn-protein) which showed, the metal ion affinities increase in the order $Mn^{++} < Co^{++} < Ni^{++} < Zn^{++} < Cu^{++}$ (McCall and Fierke, 2004).

Moreover many enzymatic activities require Mg^{++} for activation and stability (Christensen et al 2005), and G6PDH has been widely known as stabilised by Mg^{++} (Esposito et al. 2001) for this reason the recombinant enzyme for *P.trichocarpa* was desalted in order to eliminate all Mg^{++} present. Effectively, this desalted preparation showed a null activity in the presence of $NADP^+$ and G6P, and the activity can be observed only when Mg^{++} was added, resulting in a $Km_{Mg^{++}}$ of 90 μM. Under standard assay conditions, Mg^{++} is in a large excess (5 mM, about 55-fold Km value), and exceeds of about 30-fold $NADP^+$ concentration; thus it is expected that magnesium should stabilize both $NADP^+$ and NADPH, allowing both the free access to the active site, and the release of the reduced cofactor. Basically, the reactions utilising di-nucleotides phosphates - such as NAD^+ and $NADP^+$ - are stabilised by Mg^{++}, due to the effects on the ADP that is half of these molecules, which are facilitated in their access/release from enzyme active site. Theorically, it can be supposed that a lack of Mg^{++} could results in a subtraction of available $NADP^+$ for the reaction.

A further point is given by $[NADP^+]$, largely exceeding the Km_{NADP+} (at least 10 fold); in this case, it can be supposed that under the standard activity assay the substrate $NADP^+$ never limits enzymatic reation.

On the other hand, the large excess of Mg vs $NADP^+$, and the high concentration of free, available Mg^{++} (which can be considered constant), seem not to exclude a possible competition of divalent cations utilised in this study vs Mg^{++}, causing the observed inhibition.

Due to the inhibition observed under standard conditions by HMs, it could be asked if specific metals could interfere with Mg^{++} docking, and thus $NADP^+$ binding.

So it should be argued how G6PDH is affected by the presence of HMs under sub-optimal Mg^{++} levels.

The sequence of binding of the cofactors and substrates to plant G6PDHs, as established previously (Cardi et al 2013; Castiglia et al 2015), follows a sequential mechanism in which the substrate G6P and the cofactor $NADP^+$ can bind indifferently as first in the active site.

To determine if this inhibition by HM is caused by the competition between metals and the essential Mg^{++}, inhibition activity experiments at different levels of Mg^{++} were performed.

The data reveal different effects of the metals affecting the enzyme rate.
Lead did not limitate G6PDH activity at saturating magnesium levels (5 mM); intriguingly, this behaviour sensibly changed when magnesium concentration is below the saturation. Indeed lower levels of Mg^{++} caused an activity decrease of the recombinant *Pt*P2-G6PDH, over 50% at 0,1 mM HM. These effects could be supposed as exerted on the functional enzyme, whose structure resulted promptly lost in the presence of these metals but could be ascribed also to a competition with Mg^{++}.
Zn showed effects compatible with a possible Mg^{++} competition. The zinc at 5mM magnesium is not able to determine activity variation at the beginning of the incubation period at 5mM Mg^{++} but when the Mg concentration is lower the Zn is able to determina a decrease of enzymatic activity.
Thus, it can be suggested a possible competition of these metals with Mg^{++}.
At this regard Dudev and Lim (2014) demostrate by chemical analyses between two cations exhibiting the same charge and similar R_{ion}, the metal ion that is a better electron acceptor binds more favourably to the same ligand. Thus Mg^{++} and Zn^{++} share the same charge and similar ionic radii; therefore, Zn^{++} is a better charge acceptor than Mg^{++} , and a Zn^{++} complex is more favourable - and more stable - than the corresponding Mg^{++} complex with the same ligands.
Therefore, all Mg^{++} - binding pockets are susceptible to replacement by Zn^{++}; to avoid this, the cell physiology is forced to maintain high concentrations of Mg^{++} in order to privilege Mg^{++} among other dications (e.g., Zn^{++}), and maintaining the cytosolic concentration of Zn^{++} at 10^{-8} M or less.
So when assays were made under subsaturating Mg^{++} levels, both Zn^{++} and Pb^{++} immediately inhibited the enzyme, indicating a direct competition with magnesium as soon as it was lower of a largely exceeding concentration.
Cu^{++}, instead, cause less than 10% inhibition at 0.1 mM, and more than 75% inhibition at 2 mM after 1 min.
The effects of Nickel and Cadmium were very similar: immediately both induced a 35-50% inhibition in 1 min after exposition to metals - independently by concentration of magnesium. These effects are both dose, and magnesium independent: the graphs show that inhibition at sub optimal magnesium concentrations gradually increased, indicating that the poisoning effects of Ni and Cd are not competitive with Mg^{++}, and possibly affected enzyme structures weakened by Mg^{++} deficiency, and thus difficultly binding $NADP^{+}$. It should be remembered that $NADP^{+}$ is both a substrate, and a stabilizer of the enzyme: G6PDH requires a second, structural NADP+ for its stability (Wang et al., 2008). The assessed notion is that the structural NADP+ is necessary for the second dimerization to form a tetrameric enzyme, but these co-factor apparently does not affect G6PD activity. Thus, the 4 subunit stage would more stable, and apparently more active that dimers.
Therefore, it can be argued that Ni and Cd affect the structure of the active enzyme without competiting with Mg^{++}, and possibily altering the structure of the enzyme and the $NADP^{+}$ binding.
Moreover, the utilization of cys to ser mutants of the enzyme would help to understand the nature and extent of HMs effects of *Pt*P2-G6PDH. These data could also suggest the regions on the enzyme that might play an important role in the protein inhibition.
The data reveals that only Ni^{++}, ineffective at 0.1 mM, caused on wt enzyme activity an appreciable inhibition (50%) at 1 mM; among the cys-to-ser mutants, C145S seemed a quite stable enzyme, which did not appear affected seriously by HMs, only 40%

inhibition was seen at 1 mM with some elements (Table 11); at this regard it should be noted that this mutant maintained the same level of activity, and kinetic parameters, as WT (Cardi et al., 2016), suggesting that this residue is not particularly involvet in the functionality of the enzymatic reaction even if this cys is quite near to the disulfide bridge, and somewhat influencing $NADP^+$ access to the active site.
Other two mutants, C194S and C242S were essentially identical, showing a 40% inihibition at 1 mM with all the metals. For these preoteins, the inhibition by 40 % at 1 mM lead is intriguingly, and it should be remembered that these enzymes showed the loss of NADPH inhibition (Cardi et al., 2016) suggesting that these cys are involved in the general structuring of the enzyme for the binding of the substrate; as confirm, the putative 3D structures suggested that these residues are buried in the enzyme structure, and quite far from the catalytic site.
More interestingly, the mutants in the cysteines involved in the disulphide bridge, C175S and C183S (Cardi et al., 2016) were severely inhbited by metals. It should be underlined that these mutants show a limited activity, less than 20% with respect to the rate measured in the WT enzyme, fully compatible with a reduced G6PDH (inactive form). This would reinforce the notion that the disulphide strongly stabilizes the enzyme structure, and possibly the access to the $NADP^+$ site: the mutants mock the reduced, inactive state of plastidial G6PDH, and thus metals could exerte a further inhibition of the enzyme activity, avoiding the binding of co-factor (or alternatively the stabilisation of $NADP^+$ by Mg^{++}).
Computer modelling of reduced plastidial G6PDH, based on the crystal structure of the human enzyme (Au et al. 2000), indicated that the two regulatory cysteine residues are positioned in a loop situated near the NADP+-binding domain (Nèe et al 2009). Furthermore, a conserved arginine residue (corresponding to Arg131 in AtG6PDH1, Nèe et al 2014) is involved in the coordination of the phosphate group of $NADP^+$. This disulfide bridge would influence the position and structuring of the loop, for the binding the 2-phosphate of $NADP^+$; in our experiments the metals could have a facilitated access to the $NADP^+$ binding site because of the substitution of cyt to ser on this loop.
Interestingly, the drastic effect of copper on all the cys-mutants could be explained by the evidence that a given aa ligand generally interacts with di-cations following the first-row transition-metals sequence: Co^{++}, Ni^{++}, Cu^{++}, and Zn^{++}, and more favourably with Cu^{++}, due to the most negative interaction energy. Intriguingly, cys shows a predilection for the Cu^{++} (Dudev and Lim, 2014) and for this reason all the cys-G6PDH mutants are deeply affected from the Cu^{++} presence (also C145S, C194S, C242S).
These inhibitions may cause some important physiological changes as reducing production of NADPH, which plays important role in the regeneration of reduced glutathione (GSH), and therefore overwhelming antioxidant defence mechanisms.
The exposure of plants to metals of course induces more general effects on the physiology of plants, thus a set of experiments directed to investigate the damages induced by HMs had been designed.
Heavy metals (HM) represent one of the most dangerous sources of pollution in ecosystems. These metals could be accumulated in the environment and could be absorbed and/or accumulated by different living organisms (Pinto et al. 2004; Cho et al, 2003), and particularly in plants (Arya andMukherjee, 2014; Esposito et al., 2007; Basile et al., 2010).

Heavy metals accumulation is able to induce a number of toxic effects in plant cells, namely ultra structural, physiological, and biochemical damages (Esposito 2012; Basile 2015).
Among heavy metals, Nickel represents one of the elements more utilised by the industry, and so it is widely present in the environment due to this anthropic impact (Dos Reis et al., 2017).
In this study, Nickel effects were analysed on barley (*Hordeum vulgare)* plants grown under controlled condition in order to observe the damages caused by the exposure to 1 mM of this metal up to 7 days.
The results obtained show a general plant stress conditions such an 80% inhibition of root growth; a similar if less effective damage was observed in leaves (minus 20% of growth), similarly as previously described for *Brassica* after treatment with heavy metals (Ebbs et al., 1997; John et al., 2009).
Generally, the first visible effect of heavy metal toxicity is the decrease in roots length and changes in their morphology; this is not unexpected, due to the evidence that root apparatus is the first part of the plant in contact with the soil pollutants as demonstrated in *Brassica juncea* (Feig et al., 2013) and *B. oleracea (*Barrameda-Medina et al., 2014).
The exposure to heavy metals caused variations in the photosynthetic apparatus, namely in pigments, as described in different studies: Gupta *et al.* (2009) showed chlorophylls and carotenoids increased under Cromium stress in *B. juncea*. This increase is, moreover, correlated to the PSII activity due to a stabilization of the oxygen evolving complex (OEC) due to metal ions.
The data in barley plants suggest an increase of chl-a, chl-b and carotenoids levels after few hours of exposure to Nickel. After 9h pigments levels were increased by 50% with respect to control plants. This increment could be due to defence mechanism to protect the photosynthetic apparatus, as happens in Arabidopsis thaliana after mild ammonium stress (Sanchez-Zabala et al., 2015).
This plant response is possibly due to the different roles played by different pigments: the carotenoids are involved in the protection of the photosynthetic apparatus from possible photooxidation (Cheminant et al., 2011): in fact these pigments strongly increased in the plant during Ni exposure. Moreover, the stress response machinery increases both chlorophyll-a/b, present in the antennas, possibly to protect the reaction centers, and chlorophyll-a synthesis, the primary pigment involved in light absorption.

Another parameter important for plants growth is the water content; WC can be directly or indirectly regulated under stress conditions (Kramer and Boyer; 1995).
In this study, barley plants treated with Ni did not show any appreciable change in their hydration status (% RWC). As shown by Aroca et al. (2001) for tolerant corn plants, unalteration of the hydration state could be related to leaf transpiration rate that did not change during the exposure to low temperatures.
Differently from their hydration state, the ability of the plants to take up water increased upon HM stress. This has been described in *Arabidopsis*, and it has been supposed to be regulated – at least partially - by aquaporins (PIPs) under salinity (Javot et al., 2003; Postaire et al., 2010). Several studies show that the determination of a generic mechanism for water content adjustment by PIPs is particularly difficult to define, because the expression of PIPs genes during salt stress results in a down-

regulation of 15 genes, an up-regulation of 13 and a non-adjustment of 9 genes in *Phaseolus vulgaris* and *Zea mays* L. (Aroca et al., 2007; Ruiz-Lozano et al., 2009).
Changes induced by Ni exposure in primary metabolism were analysed by measuring the activity of pivotal enzymes of main metabolic pathways as G6PDH, catalase, NADH-GOGAT, PEPcase, fumarase and ascorbate peroxidase.
One of the main effects of heavy metals is to induce an oxidative stress in plants causing an imbalance of the antioxidant system (Keunen et al., 2011). As expected, some of the key enzymes involved in ROS scavenging, as APX and CAT, strongly increased their activities both in roots and leaves. CAT activity raised by 30% in the leaves after one day; similarly, APX activity was 40% higher than in control plants. These data may justify the increase of H_2O_2 observed as result of oxidative stress (Gill et al. 2015).
Similarly, the expression of genes for CAT and APX greatly increased following exposure to nickel. These results are similar to those shown Banik et al. (2016) in which increase expression of CAT and APX was observed upon salt stress.
Previous studies have shown an association between OPPP and the response to different stress, due to an increase in activity and levels of G6PDH during exposure of plants to various biotic and abiotic stresses (Scharte et al. 2009; Cardi et al. 2011, 2015; Landi et al., 2016). The exposure of *Hordeum vulgare* plants to 1 mM nickel confirmed G6PDH activity and occurrence increase after 9h of treatment. Particularly Western blotting analyses and results of qRT-PCR demonstrated a great increase in the expression and synthesis of the cytosolic isoform. Similar results were obtained previously during the exposure of plants of *Hordeum vulgare* to nitrogen deficiencies (Edwards et al., 2001b).
In another study (Esposito et al., 2005) a close correlation between variation of G6PDH and activities of NADH-GOGAT has been proposed, due to the providing by OPPP of reductants needed for the activity of glutamine oxoglutarate aminotransferase. The data here shown confirmed a 80% increase of NADH-GOGAT upon Nickel stress in leaves and roots of treated plants.
In addition an increase in the expression of different G6PDH isoforms, as P2-G6PDH and Cy-G6PDH was observed by RT-qPCR. This increase resembles that of activites over time, confirming that the cytosolic isoform is the bulk of the activity as shown before in plants of *Hordeum vulgare* (Esposito et al. 2001b). The isoform P0-G6PDH, increased after 7d of treatment with Ni, indicating a role of this isoform in the long-term stress response. Particularly, it can be argued that the increase in a P1-G6PDH isoform could result in the combination with P0-G6PDH, to form a heterodimers directed inside the peroxisomes, in order to activate a peroxisomal cycle supporting the increase of NADPH request under stress conditions (Mayer et al. 2001).
Other studies have shown variations in PEPcase activity during abiotic stress: Hatzig et al. (2010) found that an increase in PEPcase activity is linked to the metabolism of organic acids upon salinity. Similarly, in this research, PEPcase activity increased by 60% in the leaves of stressed plants. In the roots the increase in PEPcase activity was observed as well, although after 7 days enzyme rate returned to the initial values. This increase may be associated with the accumulation of organic anions (malate and citrate), as in sugar beet plants exposed to high Zn (Sagardoy et al., 2011).
Intriguingly, fumarase activity changed in a different pattern: in the leaves, Ni exposire caused only risible changes (+15%), while in the roots the enzyme activity increased 4-fold, indicating a major response in mitochondria under metal stress. This increased activity could be justified by a raise in both malate and citrate levels in

the roots, as demonstrated in *B. oleracea* under Zn stress (Barrameda-Medina et al. 2014). These organic acids are needed to facilitate the transport of metals in the leaves (malate); and / or complexing the metal for sequestration in the vacuoles (citrate); or generally simply to protect the cell, by maintaining metal ions homeostasis (Blasco et al., 2015).
Western blotting analysis with antibodies directed against different isoforms of G6PDHs and HSP70s, and antibodies directed against the PEPcase showed that nickel is able to induce increase in proteins levels, possibly to counteract the effects of the metal stress.
To assess if these increases could be related to an increase in the expression of corresponding genes, a qRT-PCR analysis has been done, confirming an actual correspondence between levels of activity, amount of protein and expression levels.
As expected, HSP70 isoforms are the genes more changing, showing an activation by 4.69 fold. The effects of HMs stress on HSP70 have been shown previously on *Lemna minor* exposed to cadmium and lead (Basile et al 2016), and on the moss *Leptodyctium riparium* (Basile et al., 2011). These increases, observed *in vitro*, can be related to the levels of metals in polluted river waters (Basile et al 2012; 2015); and polluted air as in *Conocephalum conicum* (Marchantiales) (Basile et al 2013).
These results have been confirmed by experiments in this study, where it was observed an increase in both the transcripts and occurrence of different HSP70 isoforms using specific antibodies; in particular, Western blottings suggest that cytosolic isoform is majorly expressed with respect to chloroplastic and mitochondrial HSP70 isoforms.
The presence of heavy metals is able to induce genotoxic effects in plants: it has been demonstrated that exposure to cadmium and aluminum induced a DNA deterioration in a number of plants, such as *Lactuca sativa* (Monteiro et al., 2012), *N. tabacum* (Tkalecetal., 2014), *V. faba and A. cepa* (Arya and Mukherjee, 2014) and *Hordeum vulgare* (Acharyetal., 2012b). These data are comparable to those obtained in *Hordeum vulgare* upon Nickel stress.
Both RAPD analysis and Comet assays showed a present, even if slight, genotoxic damage as reported by Achary et al. (2012b) for barley exposed to aluminum.
In conclusion, as a result, a stress response based on increase of many enzymes activity involved in ROS scavenging in response to stress was observed in all subcellular compartments and a metabolic cascade of enzymatic activities is turned on to counteract stress.
Further studies are needed to better clarify some aspects of this complex set of responses to the nickel stress, in particular to identify the most important sites of the nickel accumulation in leaves and roots tissues, and to verify the synthesis of certain compounds typically used for intracellular detoxification by some metals (such as cadmium), for example phytochelatins and metallothionines.
Moreover the western blotting analyses made on *Hordeum vulgare* leaves demostrated an increase of the P2-G6PDH also in leaves and for this reason we invastigated the leaf subcellular localization of the plastidial isoform and it's possibile interaction of the P2-G6PDH and P0-G6PDH in *Arabidopsis* protoplasts and in *Nicotiana benthamiana* leaves.
The experiments reveals the *Hv*P2-G6PDH with GFP (OFP) fused to the C-terminus end is addressed to chloroplasts of protoplasts from sugar grown cells of *Arabidopsis*. In the agro-infiltration experiments in *Nicotiana benthamiana* leaves the protein can

be found in heterotrophic plastids in the epidermis, and in the cytosol of mesophyll cells.
In *Arabidopsis* protoplasts (sugar grown cells), when GFP are fused to the N-terminus the bulk of the signal is found in the cytosol, but in part it can be localised within peroxisomes (partial co-localization with peroxisomal marker), identified by a specific fluorescent signal.
Thus we can assess that usually *Hv*P2-G6PDH is directed to heterotrophic plastids.
The apparently unexpected evidence of a cytosolic localization within mesophyll cells is probably due to the missing recognizing of the peculiar heterotrophic transit plastidial peptide by chloroplastic Tic-Toc systems in mesophyll cells (Jarvis 2008).
When the N-term is blocked by GFP, *Hv*P2-G6PDH is localised partially in the peroxisomes. From this point, we could argue that N-term is necessary for plastidial localisation, and if it is not properly folded, the protein can be directed to peroxisomes.
A possible explanation would suggest the presence of a peroxisomal targeting in the C-term, but this is not true: using "mature" *Hv*P2-G6PDH with the N-term fused with GFP the protein is directed into cytoplasm (as predicted for mature *Hv*P2-G6PDH with C-term fused GFP); therefore the signal to peroxisome should be possibly localised on the N-term.
Generally, a plastidial transit peptide is unequivocally present on the N-term, so the *Hv*P2-G6PDH GFP-C term constructs (P2-GFP) are always directed into the chloroplasts or plastids. Interestingly, GFP constructs on the N-term (GFP-P2) can be found partially in the cytosol (and this should be quite obvious), and in part in the peroxisomes (and this is less clear).
The important clue is that "mature" P2-G6PDH, when devoid of the putative transit peptide (PTP), remained constantly in the cytosol (GFP-mat-P2). This would suggest the presence of a peroxisomal targeting sequence (PTS II type) within the plastidial transit peptide.
At this regard, a notably characteristic of barley P2-G6PDH is its apparent unusual length of the PTP. These sequences are generally less than 60 aa long, while in barley protein this is longer than 95 aa (as supposed by the position of the cleavage site).
This poses the question if there are some other functional parts in N-term. An analysis of this sequence show that some typical motifs known in the plant plastidial transit peptides are not assorted in a typical PTP scheme (Lee et al. 2008 (Plant Cell 20:1603–1622); interestingly, these motifs are concentrated in the first 30 and in the last 20 residues, leaving a region (29-70aa) in which no typical PTP motif can be easily recognized.
Thus, *Hv*P2-G6PDH presents an unusually long PTP, but a large, central part (about 40aa-long) does not seem to encode for known PTP motifs (Lee et al., 2008).
A typical PTS II sequence is: **R**/K-L/V/**I**-XXXXX-H/**Q**-L/**A**. If we check this in the region "void " of functional PTP motifs (29-70aa), we found this sequence (44-52): **RI**HAVAG**KG**, that could be a good candidate as PTS II (in the last two residues, the changes lys for his, and gly for ala, do not look dramatic, if not equivalent).
Therefore, it can supposed that under stress conditions, PTS II can be exposed better than the usual PTP, thus directing the P2-G6PDH within peroxisomes to counteract the oxidative stress (Fig. 64).

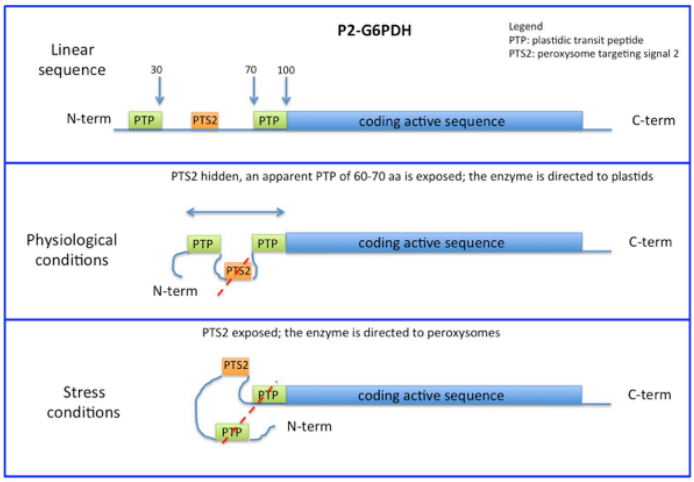

Fig. 64: Scheme of *Hordeum vulgare* P2-G6PDH transit peptide

It is attractive that, during *Agro*-infiltration experiments, barley P2-G6PDH localized in the epidermal non-photosynthetic plastids, while in the mesophyll below the bulk of the signal is localised within the cytosol and partially in the chloroplasts, indicating that in *N.benthamiana* the PTP sequence of barley is mainly recognized by heterotrophic plastids.
Thus, it can be can conceived that, under physiological conditions, the N-term assumes a conformation in which the two segments encoding for the PTP are exposed, and recognised, by Tic-Toc system of heterotrophic plastids; under stress conditions this conformation is lost and the PTS2 sequence can be recognised by peroxisomal transport system and *Hv*P2-G6PDH is directed into peroxisomes.
Of course it should be explained how this might occur, and what cell conditions are required to activate this transition. The mechanism(s) underlying these changes in the PTP-PTS structure - able to change the enzyme destination - are yet to be described.
Further Note by a 3D program (SwissProt) is possible to check hypothetical conformation of the first 100aa sequence of barley P2-G6PDH (Fig. 65).

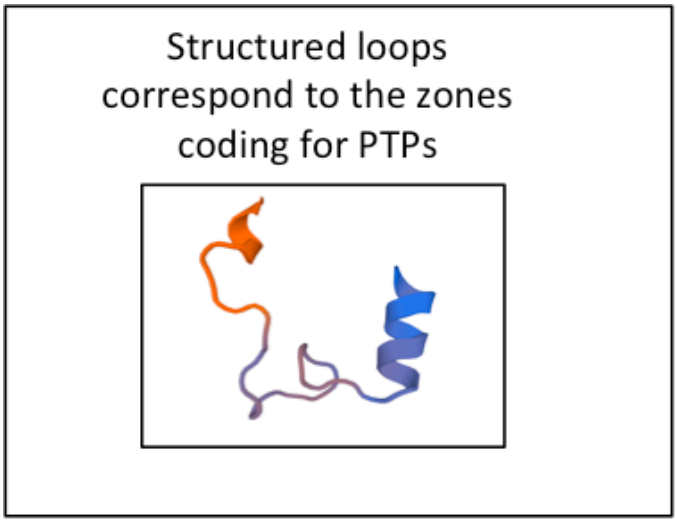

Fig. 65: Hypotetical structure of the Hv-P2G6PDH transit peptide

The images reveal the possibility that a not canonical zone of a PTP physically separates the two conserved areas.
The P0-G6PDH isoform, instead, is catalytically inactive (as demonstrated by the modified active site sequence), but it has been previously demonstrated that in *Arabidopsis* at least, *At*P0-G6PDH can form hetero-tetramers with *At*P1-G6PDH, this unusual aggregation exposed a PTS sequence directing the enzyme into peroxisomes, possibly to increase the synthesis of reductants (NADPH) under stress.
In experiments shown in this study, *Hv*P0-G6PDH is directed to chloroplasts in protoplasts by a PTP present in the N-term; when this end is blocked by GFP (GFP-P0), the protein remained into the cytosol. In agro-infiltration system, GFP-*Hv*P0-G6PDH is generally found in cytosol (Fig. 66).

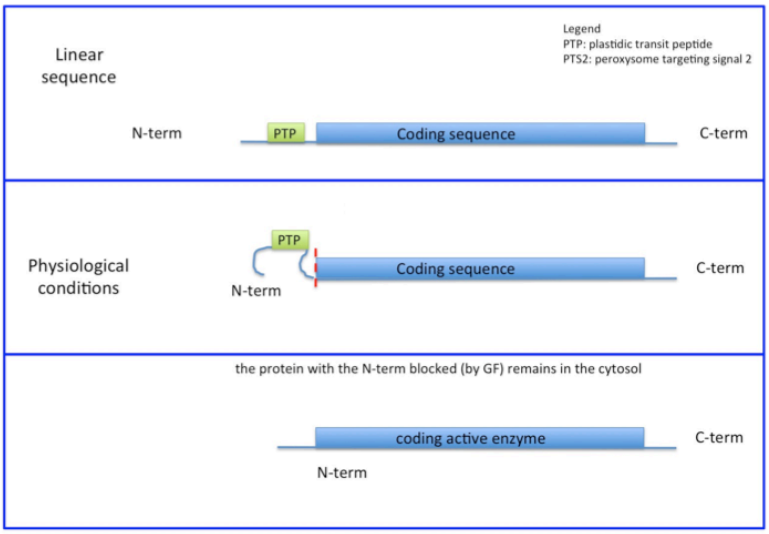

Fig. 66: Scheme of *Hordeum vulgare* P0-G6PDH transit peptide

Very important are also the coexpression experiments of the P2G6PDH and P0G6PDH. While in protoplast *Hv*P2-G6PDH and *Hv*P0-G6PDH generally are localised together in the plastids when their N-terms are functionally exposed in tobacco plants the co-expression caused the P2 localization in the plastids of heterotrophic cells but also in chloroplast of mesophylls cells, and sometimes a P2 presence into peroxisomes.
Thus, what is the function of *Hv*P0-G6PDH? Possibly it associates with other G6PDH isoforms (e.g. *Hv*P1-G6PDH, or one of the two *Hv*Cy-G6PDH), but this depends of the cell type, and stress condition.
The trophic state plays a role in the diversion of the fate of G6PDH; this might regard all G6PDH isoforms, and possibly many other enzymes.
There are three main possibilities:

1. The trophic state can change the synthesis/presence/activity of effectors able to redirect the proteins in one compartment, instead of another. Possible candidates may be chaperons such as HSPs, or the redox state of the cytoplasm: e.g. levels of glutathione, which could directly - or indirectly - oxidize cysteines, thus causing conformational modifications exposing PTS2 instead of PTP.
2. The trophic state could induce the assembly of specific translocation complexes (e.g. Tic-Toc on the chloroplasts envelope; peroxisome transport systems), able to recognize specific transit peptides for given organelles. Possibly, signal(s) from roots of pot-grown plants would indicate that Tic-Toc

complexes are not assembled properly on chloroplast envelope, and the redox state of the cell does not allow the correct assembly of peroxisome transport system able to recognize PTS2 on the N-term sequence; therefore, the protein might remain in the cytosol and forms insoluble aggregates.

3. A combination of the two systems.

This could confirm the possible interaction between the P2-G6PDH and P0-G6PDH, and so a peroxisomal localization of the P2-G6PDH in plants, even if it's not clear jet if there is a physical association and the possible binding site(s).

At this point we can assume a general mechanism of the *Hordeum vulgare* plants, in specific under Ni^{++} stress, that could be resumed in the following images (Fig. 67):

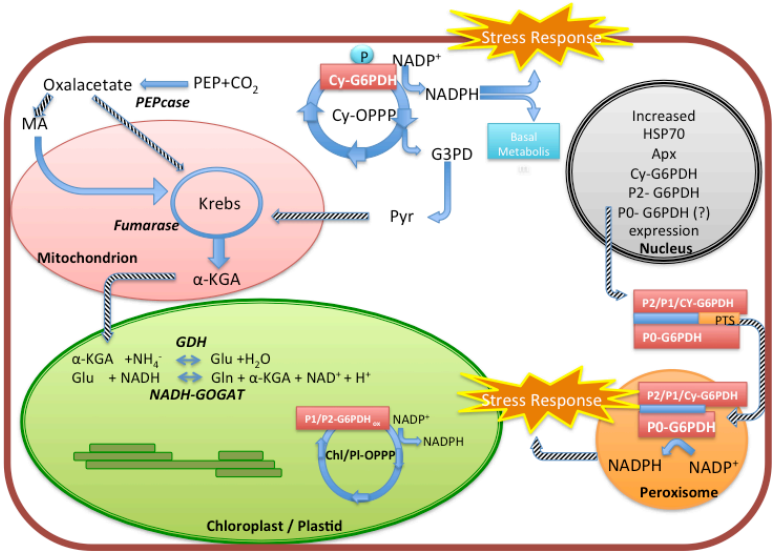

Fig. 67:
Nickel caused a stress response resulted in increase of specific enzymes in all cells compartments (cytosol, chloroplast, mitochondria), which resulted in an enzymatic cascade to counteract the stress. The metal induced increases in gene expression and upregulation of several enzymes, particularly as Mayer et al. 2001 described for *Arabidopsis,* P1-G6PDH and P0-G6PDH could form heterodimers direct into the peroxisomes to support the increased request of NADPH under stress conditions (even if it's not sure that G6PD1 and G6PD4 are both imported (together) into peroxisomes). The same effects could be obtained also for the P2-G6PDH and P0-G6PDH to form heterodimer direct into the peroxisomes to activate an peroxisomal OPPP in *Hordeum vulgare* as append for *Arabidopsis thaliana.*
In this way the enzymes activation and the overexpression, and consecutively binding between P2-G6PDH and P0-G6PDH to activate a peroxisomal OPPP, together result to be a great mechanism to help the plant to counteract the stress.

7 Source of figures

Figure 1:
https://it.wikipedia.org/wiki/Pagina_principale
Figure 2:
http://plants.ensembl.org/Hordeum_vulgare/Location/Genome
Figure 3:
(Modified) Rascio N., Carfagna S., Esposito S., La Rocca N., Lo Gullo M.A., Trost P., Vona V. Elementi fi fisiologia vegetale. Edises
Figure 4:
Esposito S., (2016). Nitrogen Assimilation, Abiotic Stress and Glucose 6-Phosphate Dehydrogenase: The Full Circle of Reductants. Plants 5(2):24 · May 2016, DOI: 10.3390/plants5020024
Figure 5:
Cardi M, Zaffagnini M, De Lillo A, Castiglia D. Chibani K. Gualberto JM. Rouhier N, Jacquot JP, Esposito S, (2016). Plastidic P2 glucose-6P dehydrogenase from poplar is modulated by thioredoxin m-type: Distinct roles of cysteine residues in redox regulation and NADPH inhibition. Plant Science. 252 (2016) 257–266 DOI: 10.1016/j.plantsci.2016.08.003
Figure 6:
Rüdiger Hauschild, and Antje von Schaewen Plant Physiol. 2003;133:47-62
Figure 7:
Cardi M, Zaffagnini M, De Lillo A, Castiglia D. Chibani K. Gualberto JM. Rouhier N, Jacquot JP, Esposito S, (2016). Plastidic P2 glucose-6P dehydrogenase from poplar is modulated by thioredoxin m-type: Distinct roles of cysteine residues in redox regulation and NADPH inhibition. Plant Science. 252 (2016) 257–266 DOI: 10.1016/j.plantsci.2016.08.003.
Figure 8:
https://www.ebi.ac.uk/interpro/potm/2004_9/Page2.htm
Figure 9:
https://commons.wikimedia.org/wiki/File:Ascorbate_peroxidase_reaction.PNG
Figure 10:
http://sustainabilityworkshop.autodesk.com/sites/default/files/styles/large/public/core-page-inserted-images/krebs_cycle_from_wikimedia-tweaked.jpg
Figure 11:
Eelko G. ter Schure, Natal A.W. van Riel, C. Theo Verrips, (2000). The role of ammonia metabolism in nitrogen catabolite repression in *Saccharomyces cerevisiae* FEMS Microbiol Rev (2000) 24 (1): 67-83.
Figure 12:
Bob B. Buchanan, Ricardo A. Wolosiuk, (2002). Modulation of Phosphoenolpyruvate Carboxylase in C_4 and CAM Plants. Plant Physiology and Development (six edition)
Figure 13:
Nature Reviews Molecular Cell Biology 11, 579–592 (1 August 2010) | doi:10.1038/nrm2941. The HSP70 chaperone machinery: J proteins as drivers of functional specificity. Harm H. Kampinga & Elizabeth A. Craig

8 References

Adriano, D.C., (2001). Trace Elements in Terrestrial Environments: Biogeochemistry, Bioavailability, and Risks of Metals, second ed. Springer, Berlin.

Agami RA, Mohamed GF, (2013). Exogenous treatment with indole-3-acetic acid and salicylic acid alleviates cadmium toxicity in wheat seedlings. Ecotoxicol Environ Saf 94:164–171.

Ahmed A, Tajmir-Riahi HA (1993) Interaction of toxic metal ions Cd^{2+}, Hg^{2+} and Pb with light-harvesting proteins of chloroplast thylakoid membranes. An FTIR spectroscopic study. J. Inorg. Biochem. 50:235-243.

Al-Qurainy F., (2009). Toxicity of Heavy Metals and Their Molecular Detection on Phaseolus vulgaris (L.). A u s tralian Jo u rn al o f Bas ic an d A p p lied Scien ces , 3(3): 3025-3035, 2009.

Alaoui-Sossé B., Genet P., Vinit-Dunand F., Toussaint M.-L, Epron D., Badot P.-M, (2004). Effect of copper on growth in cucumber plants (Cucumis sativus) and its relationships with carbohydrate accumulation and changes in ion contents. Plant Science 166 (2004) 1213–1218

Amari T., Lutts S., Taamali M., Lucchini G., Sacchi G.A., Abdelly C., Ghnaya T., (2016). Implication of citrate, malate and histidine in the accumulation and transport of nickel in Mesembryanthemum crystallinum and Brassica juncea. Ecotoxicol Environ Saf. 2016 Apr;126:122-8. doi: 10.1016/j.ecoenv.2015.12.029. Epub 2015 Dec 30.

Amzallag GN, Lerner HR, Poljakoff-Mayber A, (1990) Exogenous ABA as a modulator of the response of sorghum to high salinity. J Exp Bot 41:1529–1534.

Araújo W.L., Nunes-Nesi A., Fernie A.R., (2011). Fumarate: multiple functions of a simple metabolite. Phytochemistry, 72 (2011), pp. 838–843.

Aroca R., (2001).Different root low temperature response of two maize genotypes differing in chilling sensitivity. Plant Physiology and Biochemistry, Volume 39, Issue 12,_December 2001, Pages 1067–1073.

Aroca R., Porcel R., Ruiz-Lonzano JM., (2007)How does arbuscular mycorrhizal symbiosis regulate root hydraulic properties and plasma membrane aquaporins in Phaseolus vulgaris under drought, cold or salinity stresses?. New Phytol 2007;173(4):808-16.

Au SW, Gover S, Lam VM, Adams MJ, (2000). Human glucose-6-phosphate dehydrogenase: The crystal structure reveals a structural NADP(+) molecule and provides insights into enzyme deficiency. Structure Fold Des 8: 293–303.

Aydinalp C. and Marinova S., (2009). The effects of heavy metals on seed germination and plant growth on alfalfa plant (Medicago sativa). Bulgarian Journal of Agricultural Science, 15 (No 4) 2009, 347-350.

Azevedo RA, Alas RM, Smith RJ and Lea PJ, (1998). Response of antioxidant enzymes to transfer from elevated carbon dioxide to air and ozone fumigation in the leaves and roots of wild-type and a catalase-deficient mutant of barley. Physiol. Plant. 104: 280–292.

Azpilicueta CE, Benavides MP, Tomaro ML, Gallego SM, (2007). Mechanism of *CATA3* induction by cadmium in sunflower leaves. Plant Physiol Biochem 45:589–595

Balestrasse KB, Gardey L, Gallego SM, Tomaro ML, (2001). Response of antioxidant defence system in soybean nodules and roots subjected to cadmium stress. Aust J Plant Physiol 28:497–504.

Banásová V., Horak O., Nadubinská M., Čiamporová M., (2008). Heavy metal content in Thlaspi caerulescens J. et C. Presl growing on metalliferous and non-metalliferous soils in Central Slovakia. *Int. J. Environment and Pollution, Vol. 33, Nos. 2/3, 2008*

Banik, P., Zeng, W., Tai, H., Bizimungu, B., Tanino, K., 2016. Effects of drought acclimation on drought stress resistance in potato (*Solanum tuberosum* L.) genotypes. Environmental and Experimental Botany 126: 76-89.

Barrameda-Medina Y., Montesinos-Pereira D., Romero L., Ruiz J.M., Blasco B. Comparative study of the toxic effect of Zn in *lactuca sativa* and *Brassica oleracea* plants: I. Growth, distribution, and accumulation of Zn, and metabolism of carboxylates. Environ. Exp. Bot. 2014;107:98–104. doi: 10.1016/j.envexpbot.2014.05.012.

Basile A, Sorbo S, Cardi M, Lentini M, Castiglia D, Cianciullo P, Conte B, Loppi S, Esposito S, (2015). Effects of heavy metals on ultrastructure and Hsp70 induction in Lemna minor L. exposed to water along the Sarno River, Italy. Ecotoxicology and Environmental Safety. 114: 93-101.

Battistuzzi G, D'Onofrio M, Loschi L, Sola M, (2001). Isolation and characterization of two peroxidases

from *Cucumis sativus*. Arch Biochem Biophys 388:100–112.

Beers RF Jr., Sizer IW, (1952). A spectrophotometric method for measuring the breakdown of hydrogen peroxide by catalase. J Biol Chem. 1952 Mar;195(1):133-40.

Behal RH, Oliver DJ, (1997). Biochemical and molecular characterization of fumarase from plants: purification and characterization of the enzyme e cloning, sequencing, and expression of the gene. Arch. Biochem. Biophys. 348,65-74.

Benavides MP, Gallego SM, Tomaro ML, (2005). Cadmium toxicity in plants. Braz. J. Plant Physiol. 17: 21-34.

Beutler E, (1984). Red cell metabolism: a manual of biochemical methods. Academic Press, London, 1971, pp 68–71

Beyersmann D, Hartwig A, (2008). Carcinogenic metal compounds: recent insight into molecular and cellular mechanisms. Arch Toxicol. 2008;82(8):493–512.

Blasco B., Graham N.S., Broadley M.R. Antioxidant response and carboxylate metabolism in *Brassica rapa* exposed to different external Zn, Ca, and MG supply. J. Plant Physiol. 2015;176:16–24. doi: 10.1016/j.jplph.2014.07.029.

Bradford MM, (1976). A rapid and sensitive method for the quantitation of microgram quantities of protein utilizing the principle of protein-dye binding. Anal Biochem 72:248–254.

Bredemeijer GMM, Esselink G, (1995). Glucose 6-phosphate dehydrogenase during cold-hardening in *Lolium perenne*. *J. Plant Physiol*. 145, 565-569.

Brown JC and Jones WE, (1975). Heavy metal toxicity in plants I. A crisis in embryo. Commun. Soil Sci. Plant Anal., 6, 421-428.

Cankaya M, Sisecioglu M, Ciftci M, Ozdmeir H, (2011). Effects of Some Metal Ions on Trout Liver Glucose-6-phosphate Dehydrogenase. Res. Journal of Env. Tox. 5(6): 385-391.

Cardi M, Castiglia D. Ferrara M, Guerriero G, Chiurazzi M, Esposito S, (2015). The effects of salt stress cause a diversion of basal metabolism in barley roots: Possible different roles for glucose-6-phosphate dehydrogenase isoforms. Plant Physiol. 86: 44-54.

Cardi M, Chibani K, Cafasso D, Rouhier N, Jacquot JP, Esposito S, (2011). Abscisic acid effects on activity and expression of barley (Hordeum vulgare) plastidial glucose-6-phosphate-dehydrogenase. J Exp Bot2011Jul;62(11):4013-23.doi: 10.1093/jxb/err100.

Cardi M, Chibani K, Castiglia D, Cafasso D, Pizzo E, Rouhier N, Jacquot JP, Esposito S, (2013). Overexpression, purification and enzymatic characterization of a recombinant plastidial glucose-6-phosphate dehydrogenase from barley (Hordeum vulgare cv. Nure) roots. Plant Physiol Biochem. 2013 Dec;73:266-73. doi: 10.1016/j.plaphy.2013.10.008.

Cardi M, Zaffagnini M, De Lillo A, Castiglia D. Chibani K. Gualberto JM. Rouhier N, Jacquot JP, Esposito S, (2016). Plastidic P2 glucose-6P dehydrogenase from poplar is modulated by thioredoxin m-type: Distinct roles of cysteine residues in redox regulation and NADPH inhibition. Plant Science. 252 (2016) 257–266 DOI: 10.1016/j.plantsci.2016.08.003

Chaney RL, (1973). Crop and food chain effects of toxic elements in sludges and effluents, in: Recycling Municipal Sludges and Effluents on Land, Natl. Assoc. State Univ. Land Grant COIL, Washington DC, , pp. 1299141.

Chaoui A, Mazhoudi S, Ghorbal MH, El Ferjani E, (1997). Cadmium and zinc induction of lipid peroxidation and effects on antioxidant enzyme activities in bean (Phaseolus vulgaris L.). Plant Science 127,139-147.

Cheminant S, Wild M, Bouvier F, Pelletier S, Renou JP, Erhardt M, Hayes S, Terry MJ, Genschik P and Achard P, (2011). DELLAs Regulate Chlorophyll and Carotenoid Biosynthesis to Prevent Photooxidative Damage during Seedling Deetiolation in *Arabidopsis*. *The Plant Cell May 2011 vol. 23 no. 5 1849-1860*

Chen QL, Luo Z, Zheng JL, Li XD, Liu CX, Zhao YH, Gong Y, (2012) Protective effects of calcium on copper toxicity in Pelteobagrus fulvidraco; copper accumulation, enzymatic activities and histology. Ecotoxicol Environ Saf 76:126–134

Cho M., Chardonnens AN., Dietz KJ., (2003). Differential heavy metal tolerance of *Arabidopsis halleri* and*Arabidopsis thaliana*: a leaf slice test. New Phytol. 158: 287-293.

Chollet R, Vidal J, O'Leary M , (1996) Phosphoenolpyruvate carboxylase: a ubiquitous, highly regulated enzyme in plants. Annu Rev Plant Physiol Plant Mol Biol 47:273–298.

Ciftci M., Turkoglu V., Coban T.A., (2007). Effects of some drugs on hepatic glucose 6-phosphate dehydrogenase activity in Lake Van Fish (Chalcalburnus Tarischii Pallas, 1811). J Hazard Mater 143:415–418.

Ciltas A., Erdogan O., Hisar O., Ciftci M., (2003). Effects of Chloramine-T and CuSO4 on enzyme activity of glucose 6-phosphate dehydrogenase from rainbow trout (Oncorhynchus mykiss) erythrocytes in vitro and in vivo. Isr J Aquac-Bamidgeh 55:187–196.

Clarkson DT., and Luttge U., (1989). Mineral nutrition. Divalent cations, transport and compartmentalization. Prog. Bot. 51:93-112.

Clemens S., Palmgren MG., Kraemer U., (2002). A long way ahead: understanding and engineering plant metal accumualtion. Tr. Plant Sci 7: 309–315.

Copeland L., Turner J.F., (1987). The regulation of glycolysis and the pentose- phosphate pathway. In A Marcus, ed, The Biochemistry of Plants, Vol 11. Academic Press, New York, pp 107–125

Corpas FJ, Salguero LG, Peragon J, Lupianez JA, (1995). Kinetic properties of hexose monophosphate dehydrogenase. Isolation and partial purification of glucose-6-phosphatedehydrogenase from rat liver and kidney cortex. Life Sci 56:179–189.

Dal Santo S, Stampfl H, Krasensky J, Kempa S, Gibon Y, Petutschnig E, Rozhon W, Heuck A, Clausen T, Jonak C., (2012). Stress-induced GSK3 regulates the redox stress response by phosphorylating glucose-6-phosphate dehydrogenase in Arabidopsis.

De Vos RCH, Vonk MJ, Vooijs R, Schat H. (1992). Glutathionee depletion due to copper-induced phytochelatin synthesis causes oxidtive stress in Silene cucubalus. Plant Physiology 98, 853-858

Dennis DT, Huang Y, Negm FB., (1997). Glycolysis, the pentose phosphate pathway and anaerobic respiration. In: Dennis DT, Turpin DH, Lefebvre DD, Layzell DB (eds) Plant metabolism, Longman, London, pp 105-127.

di Toppi LS, Gabbrielli R. 1999. Response to cadmium in higher plants. Environmental and Experimental Botany 41:105–130.DOI:10.1016/S0098-8472(98)00058-6.

Dobson, C.M., Sali, A., and Karplus, M., (1998). Protein folding: a perspective from theory and experiment. Angew. Chem. Int. Ed. Eng. 37:868–893.

Doncheva S. and Stoyanova Z., (2007). Plant response to copper and zinc hydroxidesulphate and hydroxidecarbonate used as an alternative copper and zinc sources in mineral nutrition. Romanina Agricultural Research, no 7-8, pp. 15-23,2007.

Dyson BC., Miller MA., Feil R., Rattray N., Bowsher CG., Goodacre R., Lunn JE., Johnson GN., (2016). FUM2, a Cytosolic Fumarase, Is Essential for Acclimation to Low Temperature in Arabidopsis thaliana. Plant Physiol. 2016 Sep;172(1):118-27. doi: 10.1104/pp.16.00852. Epub 2016 Jul 20.

Dudev T., Lim C., (2014). Competition among Metal Ions for Protein Binding Sites: Determinants of Metal Ion Selectivity in Proteins . dx.doi.org/10.1021/cr4004665 | Chem. Rev. 2014, 114, 538−556

Echevarría C, García-Mauriño S, Alvarez R, Soler A, Vidal J, (2001). Salt stress increases the Ca2?-independent phosphoenolpyruvate carboxylase kinase activity in Sorghum plants. Planta 214:283–287.

Emanuelsson O, Nielsen H, von Heijne G., (1999). ChloroP, a neural network-based method for predicting chloroplast transit peptides and their cleavage sites. Protein Sci. 1999 May;8(5):978-84.

Emes M.J., Fowler M.W., (1983). The supply of reducing power for nitrite reduction in plastidids of seedling pea roots (*Pisum sativum* L.), *Planta* 158 (1983) 97-102.

Eprintsev A.T., Fedorin D.N., Starinina E.V., Igamberdiev A.U., (2014). Expression and properties of the mitochondrial and cytosolic forms of fumarase in germinating maize seeds. Physiol. Plant, 152 (2014), pp. 231-240.

Eprintsev AT, Fedorin DN, Sazonova OV, Igamberdiev AU., (2016). Light inhibition of fumarase in Arabidopsis leaves is phytochrome A-dependent and mediated by calcium. Plant Physiol Biochem. 2016 May;102:161-6. doi: 10.1016/j.plaphy.2016.02.028.

Esposito S, Carfagna S, Massaro G, Vona V, Di Martino Rigano V, (2001a) Glucose-6P dehydrogenase in barley roots: kinetic properties and localisation of the isoforms. *Planta* 212, 627-634.

Esposito S, Guerriero G, Vona V, Di Martino Rigano V, Carfagna S, Rigano C., (2005). Glutamate synthase activities and protein changes in relation to nitrogen nutrition in barley: the dependence on different plastidic glucose-6P dehydrogenase isoforms. J Exp Bot. 2005 Jan;56(409):55-64.

Esposito S, Massaro G, Vona V, Di Martino Rigano V, Carfagna S, Rigano C., (2001b). Ammonium induction of a novel isoform of glucose-6Pdehydrogenase in barley roots. *Physiologia Plantarum* 113, 469-476.

Esposito S, Massaro G, Vona V, Di Martino Rigano V, Carfagna S., (2003). Glutamate synthesis in barley roots: the role of the plastidic glucose-6-phosphate dehydrogenase. *Planta* 216, 639-647.

Esposito S., (2016). Nitrogen Assimilation, Abiotic Stress and Glucose 6-Phosphate Dehydrogenase: The Full Circle of Reductants. Plants 5(2):24 · May 2016, DOI: 10.3390/plants5020024

Esposito S., Sorbo S., Conte B., Basile A., (2012). Effects of heavy metals on ultrastructure and HSP70s induction in the aquatic moss Leptodictyum riparium Hedw. Int J Phytoremediation. 2012 Apr;14(4):443-55.

Feigl G, Kumar D, Lehotai N, Tugyi N, Molnár A, Ordög A, Szepesi A, Gémes K, Laskay G, Erdei L, Kolbert Z., (2013). Physiological and morphological responses of the root system of Indian mustard (Brassica juncea L. Czern.) and rapeseed (Brassica napus L.) to copper stress. Ecotoxicol Environ Saf. 2013 Aug; 94():179-89.

Ferreira S., HJernò K., Larsen M., Wingsle G., Larsen P., Fey S., Roepstorff P., Salomé Pais M., (2006). Proteome profiling of Populus euphratica Oliv. upon heat stress. Ann Bot. 2006 Aug;98(2):361-77. Epub 2006 Jun

Fickenscher K, Scheibe R., (1986). Purification and properties of the cytoplasmatic glucose-6-phosphate dehydrogenase from pea leaves. *Archiv Biochem Biophys* 247, 393-402.

Fonovich de Schroeder TM., (2005). The effect of Zn2+ on glucose 6-phosphate dehydrogenase activity from Bufo arenarum toad ovary and alfalfa plants. Ecotoxicol Environ Saf. 2005 Feb;60(2):123-31

Foyer CH, Noctor G (2005a) Oxidant and antioxidant signalling in plants: a re-evaluation of the concept of oxidative stress in a physiological context. Plant Cell Environ 28: 1056–1071.

Foyer CH, Noctor G (2005b) Redox homeostasis and antioxidant signaling: a metabolic interface between stress perception and physiological responses. Plant Cell 17: 1866–1875.

Foyer CH, Noctor G (2009) Redox regulation in photosynthetic organisms: signaling, acclimation, and practical implications. Antioxid Redox Signal 11: 861–905.

Friesen P.C. and Sage R.F., (2016). Photosynthetic responses to chilling in a chilling-tolerant and chilling-sensitive Miscanthus hybrid. Plant, Cell and Environment (2016) 39, 1420–1431.

Frugoli JA, Zhong HH, Nuccio ML, McCourt P, McPeek MA, Thomas TL, McClung CR, (1996). Catalase is encoded by a multigene family in *Arabidopsis thaliana* L. Heynh. Plant Physiol 112:327–336.

Fukao Y., Ferjani A., Tomioka R. (2011). iTRAQ analysis reveals mechanisms of growth defects due to excess zinc in *Arabidopsis*, *Plant Physiology*, vol. 155, no. 4, pp. 1893–1907, 2011.

Gallego SM, Benavides MP, Tomaro ML, (1996). Effect of heavy metal ion excess on sunflower leaves: evidence for involvement of oxidative stress. Plant Science 121, 151-159

García-Mauriño S, Monreal JA, Alvarez R, Vidal J, Echevarría C, (2003). Characterization of salt stress-enhanced phosphoenolpyruvate carboxylase kinase activity in leaves of Sorghum vulgare: independence from osmotic stress, involvement of ion toxicity and significance of dark phosphorylation. Planta (2003) 216: 648–655 DOI 10.1007/s00425-002-0893-3

Gill R.A., Zang L., Ali B., Farooq M.A., Cui P., Yang S., Ali S., Zhou W. Chromium-induced physio-chemical and ultrastructural changes in four cultivars of *Brassica napus* L. Chemosphere. 2015;120:154–164. doi: 10.1016/j.chemosphere.2014.06.029

Graeve K., von Schaewen A., Scheibe R., (1994). Purification, characterization and cDNA sequence of glucose-6-phosphate dehydrogenase from potato (Solanum tuberosum L.). Plant J 5: 353–361

Gregerson GR, Miller S, Twary SN, Gantt JS, Vance C., (1993). Molecular characterization of NADH-dependent glutamate synthase from alfalfa nodules. The Plant Cell 5, 215–226.

Gupta S., Srivastava S., Saradhi P.P. Chromium increases photosystem 2 activity in *Brassica juncea*. Biol. Plant. 2009;53:100–104. doi: 10.1007/s10535-009-0013-3.

Hale K.L., McGrath S.P., Lombi E., Stack S.M., Terry N., Pickering I.J., George G.N., Pilon-Smits E.A. Molybdenum sequestration in Brassica species. A role for anthocyanins? Plant Physiol. 2001;126:1391–1402. doi: 10.1104/pp.126.4.1391.

Hall JL, (2002). Cellular mechanism for heavy metal detoxification and tolerance. J Exp Bot 2002;53:1–11.

Halliwell B. and Gutteridge J.M.C., (1988). Free Radicals in Biology and Medicine, Clarendon Press, Oxford.

Hasanuzzaman M, Fujita M, (2013a). Exogenous sodium nitroprusside alleviates arsenic-induced oxidative stress in wheat (*Triticum aestivum* L.) seedlings by enhancing antioxidant defense and glyoxalase system. Ecotoxicology 22:584–596.

Hasanuzzaman M, Nahar K, Alam MM, Fujita M, (2012b). Exogenous nitric oxide alleviates high temperature induced oxidative stress in wheat (*Triticum aestivum* L.) seedlings by modulating the antioxidant defense and glyoxalase system. Aust J Crop Sci 6:1314–1323 .

Hauschild R, von Schaewen A, (2003). Differential regulation of glucose-6-phosphate dehydrogenase isoenzyme activities in potato. Plant Physiology 133, 47-62.

Hayakawa T, Nakamura T, Hattori F, Mae T, Ojima K, Yamaya T, (1994). Cellular localization of NADH-dependent glutamate-synthase protein in vascular bundles of unexpanded leaf blades and young grains of rice plants. Planta 193: 455±460

Haydon, M.J., Cobbett, C.S., 2007. Transporters of ligands for essential metal ions in plants. New Phytol. 174, 499–506.

Heazlewood JL, Tonti-Filipinni JS, Gout AM, Day DA, Whelan J, Millar AH, (2004). Experimental analysis of the *Arabidopsis* mitochondrial proteome highlights signaling and regulatory components, provides assessment of targeting prediction programs, and indicates plant-specific mitochondrial proteins. Plant Cell 16:241–256.

Heber U., Hudson M.A., Hallier U.W., (1967). Lokalisation von Enzymen des Reduktiven und des Oxidativen Pentosephosphatzyklus in den Chloroplasten und Permeabilita¨ t der Chloroplastenmembranen gegenu¨ ber Metaboliten. Z Naturforsch 22b: 1200–1215

Hodson PV, (1988). The effect of metal metabolism on uptake, disposition and toxicity in fish. Aquat Tocicol 11: 3-18.

Hosseini Z. and Poorakbar L., (2013). Zinc toxicity on antioxidative response in (*Zea mays* L.) at two different pH, *Journal of Stress Physiology & Biochemistry*, vol. 9, pp. 66–73, 2013.

Hsu YT, Kao CH, (2004). Cadmium toxicity is reduced by nitric oxide in rice leaves. Plant Growth Regul 42:227–238.

Hu YQ, Liu S, Yuan HM, Li J, Yan DW, Zhang JF, Lu YT, (2010). Functional comparison of catalase genes in the elimination of photorespiratory H2O2 using promoter- and 3′-untranslated region exchange experiments in the *Arabidopsis* cat2 photorespiratory mutant. Plant Cell Environ 33:1656–1670.

Hutchings D., Rawsthorne S., Emes M.J., (2005). Fatty acid synthesis and the oxidative pentose phosphate pathway in developing embryos of oilseed rape (*Brassica napus*), J Exp. Bot. 56 (2005) 577-585.

Ingle R.A., Mugford, S.T., Rees, J.D., Campbell, M.M., Smith, J.A.C., 2005. Constitutively high expression of the histidine biosynthetic pathway contributes to nickel tolerance in hyperaccumulator plants. Plant Cell 17, 2089–2106.

Ishtiaq S., Mahmood S., (2011). Phytotoxicity of nickel and its accumulation in tissues of three *Vigna* species at their early growth stages. Journal of Applied Botany and Food Quality 84, 223 - 228

Izui K, Matsumura H, Furumoto T, Kai Y (2004) Phosphoenolpyruvate carboxylase: a new era of structural biology. Annu Rev Plant Biol 55 69–84.

Jarvis P., (2008). Targeting of nucleus-encoded proteins to chloroplasts in plants. New Phytol. 2008 Jul;179(2):257-85

Javot H., Lauvergeat V., Santoni V., Martin-Laurent F., Güçlü J., Vinh J., Heyes J., Franck Ki., Schäffner AR., Bouchez D., Maurel C., (2003)Role of a single aquaporin isoform in root water uptake. Plant Cell. 2003 Feb;15(2):509-22.

Jones DP (2006) Redefining oxidative stress. Antioxid Redox Signal 8: 1865–1879.

Kampfenkel K., Van Montagu M., Inzé D., (1995). Effects of Iron Excess on Nicotiana plumbagnifolia. (Implications to Oxidative Stress). Plant Physiol. 107(3): 725-735.

Keunen E., Remans T., Bohler S., Vangronsveld J., Cuypers A. Metal-induced oxidative stress and plant mitochondria. Int. J. Mol. Sci. 2011;12:6894–6918. doi: 10.3390/ijms12106894.

Khan M. R. and Khan M. M., (2010). Effect of Varying Concentration of Nickel and Cobalt on the Plant Growth and Yield of Chickpea. Australian Journal of Basic and Applied Sciences, 4(6): 1036-1046,

2010.

Khan NA, Samiullah SS, Nazar R, (2007). Activities of antioxidative enzymes, sulphur assimilation, photosynthetic activity and growth of wheat (*Triticum aestivum*) cultivars differing in yield potential under cadmium stress. J Agron Crop Sci 193:435–444.

Knight J.S., Emes M.J., Debnam P.M., (2001). Isolation and characterisation of a full-length genomic clone encoding a plastidicglucose 6-phosphate dehydrogenase from *Nicotiana tabacum,* Planta 212 (2001) 499-507

Kopittke P.M, Dart P.J, Menzies N.W, (2006). Toxic effects of low concentrations of Cu on nodulation of cowpea (Vigna unguiculata). Environ Pollut.2007 Jan;145(1):309-15. Epub 2006 May 5.

Krook J., Vreugdenhil D., Dijkema C., van der Plas L.H.W., (1998). Sucrose and starch metabolism in carrot (*Daucus carota* L.) cell suspensions analysed by ^{13}C-labelling: indications for a cytosol and a plastid-localized oxidative pentose phosphate pathway, *J. Exp. Bot.* 49 (1998) 1917-1924.

Krunger NJ, von Schaewen A., (2003). The oxidative pentose phosphate pathway: structure and organisation. Curr Opin Plant Biol. 2003 Jun;6(3):236-46.

Krupa Z., Baszyński T., (1995). Some aspects of heavy metal toxicity towards photosynthetic apparatus – direct and indirect effect on light and dark reactions. Acta Physiol Plant 17: 177-190.

Laemmli UK, (1970). Cleavage of structural proteins during the assembly of the head of bacteriophage T4. Nature 227:680–685.

Lancien M, Martin M, Hsieh MH, Leustek T, Goodman H, Coruzzi GM, (2002). Arabidopsis glt1-T mutant defines a role of NADH-GOGAT in the non-photorespiratory ammonium assimilatory pathway. Plant J 29: 347–358.

Landi S., Nurcato R., De Lillo A., Lentini M., Grillo S., Esposito S., (2016). Glucose-6-phosphate dehydrogenase plays a central role in the response of tomato (*Solanum lycopersicum*) plants to short and long-term drought. Plant Physiology and Biochemistry. 105: 79-89 DOI: 10.1016/j.plaphy.2016.04.

Lea PJ, Miflin BJ, (1974). Alternative route for nitrogen assimilation in higher plants. Nature 251: 614-616.

Lee D.W., Kim J.K., Lee S., Choi S., Kim S., Hwang I., (2008). Arabidopsis nuclear-encoded plastid transit peptides contain multiple sequence subgroups with distinctive chloroplast-targeting sequence motifs. Plant Cell 20: 1603–1622.

Lendzian K, Bassham JA., (1975). Regulation of glucose-6-phosphate dehydrogenase in spinach chloroplasts by ribulose 1,5-diphosphate and NADPH/$NADP^+$ ratios. *Bioch. Biophys. Acta* 396, 260-275.

Lendzian K.J. , (1978). "Interactions between Magnesium Ions, pH, Glucose-6-Phosphate,

and NADPH/NADP+ Ratios in the Modulation of Chloroplast Glucose-6-Phosphate Dehydrogenase in Vitro." Planta Vol. 141, No. 1 (1978), pp. 105-110.

Lepiniec L, Thomas M, Vidal J, (2003). From enzyme to plant biotechnology: 30 years of research on phosphoenolpyruvate carboxylase. Plant Physiol Biochem 47 533–539.

Lepp, N.W., 1981. Effect of Heavy Metal Pollution on Plants, vol. 2, Metals in the Environment. Applied Science Publishers, London.

Levitt, M., Gerstein, M., Huang, E., Subbiah, S. & Tsai, J., (1997). Protein-folding: the endgame. Annu. Rev. Biochem. 66, 549-579.

Levy HR, Cook C, (1991). Purification and properties of NADPlinked glucose-6-phosphate dehydrogenase from Acetobacter hansenii (Acetobacter xylinum). Arch Biochem Biophys 291:161–167.

Lin Y.-C. and Kao C.-H., (2005). Nickel Toxicity of Rice Seedlings: Cell Wall Peroxidase, Lignin, and NiSO4 inhibited Root Growth. Crop, Environment & Bioinformatics, Vol. 2, June 2005

Liu XJ, Luo Z, Li CH, Xiong BX, Zhao YH, Li XD, (2011). Antioxidant responses, hepatic intermediary metabolism, histology and ultrastructure in Synechogobius hasta exposed to waterborne cadmium. Ecotoxicol Environ Saf 74:1156–1163.

Livak, K.J., Schmittgen, T.D., (2001). Analysis of relative gene expression data using real-time quantitative PCR and the 2(-Delta Delta C(T) method. Methods 25, 402e408.

Lombardi L. and Sebastiani L., (2005). Copper toxicity in *Prunuscerasifera*: growth and antioxidant enzymes responses of in vitro grown plants. Plant Science 168 (2005) 797-802.

López-Millán AF, Grusak MA, Abadía J., (2012). Carboxylate metabolism changes induced by Fe deficiency in barley, a Strategy II plant species. J Plant Physiol. 2012 Jul 15;169(11):1121-4. doi: 10.1016/j.jplph.2012.04.010.

Lozano-Rodriguez E, Hernande LE, Bonay P, Carpena-Ruiz RO, (1997). Diatribution of cadmium in shoot and root tissues of maize and pea plants: physiological disturbances. Journal of Experimental Botany 48, 123-128

Mari S., Gendre D., Pianelli K., Ouerdane L., Lobinski R., Briat J.F., Lebrun M., Czernic P., (2006). Root-to-shoot long-distance circulation of nicotianamine and nicotianamine-nickel chelates in the metal hyperaccumulator Thlaspi caerulescens. J. Exp. Bot. 57, 4111–4122.

Markert, B., (1996). Instrumental Element and Multi-Element Analysis of Plant Sam- ples. John Wiley & Sons, Chichester.

McCall, K. A.; Fierke, C. A., (2004). Probing determinants of the metal ion selectivity in carbonic anhydrase using mutagenesis. Biochemistry 2004, 43, 3979.

Mediouni C., Benzarti O., Tray B., Ghorbel M. H., and Jemal F., (2006). Cadmium and copper toxicity for tomato seedlings, *Agronomy for Sustainable Development*, vol. 26, no. 4, pp. 227–232, 2006.

Meharg AA., (1993). The role of the plasmalemma in metal tolerance in angiosperms. Physiologia Plantarum 88: 191-8.

Meyer T., HÖlscher C., SchwÖppe C., von Schaewen A., (2011). Alternative targeting of Arabidopsis plastidic glucose-6-phosphate dehydrogenase G6PD1 involves cysteine-dependent interaction with G6PD4 in the cytosol**.** Plant. J 2011 Jun;66(5):745-58. doi: 10.1111/j.1365-313X.2011.04535.x. Epub 2011 Mar 21.

Meyer EH, Solheim C, Tanz SK, Bonnard G, Millar AH, (2011). Insights into the composition and assembly of the membrane arm of plant complex I through analysis of subcomplexes in Arabidopsis mutant lines. J. Biol. Chem. 286, 26081–26092.

Mhamdi A, Queval G, Chaouch S, Vanderauwera S, (2010). Catalase function in plants, a focus on *Arabidopsis* mutants as stress-mimic models. J Exp Bot 61:4197–4220.

Miernyk J.A., (1997). The 70kDa stress-related proteins as molecular chaperones. Trends in Plant Sciences, 2: 180-187.

Minguzzi C., Verniano O., (1948). Il contenuto del Nickel nelle ceneri di Alyssum bertolonii Desv. Atti Soc. Tosc. Sci. Nat. Ser: A 55:49-77.

Mishra P. K. and Prakash V., (2010). Response of non-enzymatic antioxidants to zinc Induced stress at different pH in *Glycine max* L. cv. Merrill, *Academic Journal of Plant Sciences*, vol. 3, no. 1, pp. 1–10, 2010.

Mishra S. and Dubey R . S ., (2005). Heavy Metal Toxicity Induced Alterations in Photosynthetic Metabolism in Plants. Handbook of Photosynthesis, Second Edition Edited by Mohammad Pessarakli, CRC Press 2005, ISBN: 978-0-8247-5839-4, DOI: 10.1201/9781420027877.ch44.

Miyake C, Asada K, (1996). Inactivation of mechanism of ascorbate peroxidase at low concentrations of ascorbate, hydrogen peroxide decomposes compound I of ascorbate peroxidase. Plant Cell Physiol 37:423–430.

Mobin M, Khan NA, (2007). Photosynthetic activity, pigment composition and antioxidative response of two mustard (*Brassica juncea*) cultivars differing in photosynthetic capacity subjected to cadmium stress. J Plant Physiol 164:601–610.

Monreal JA, Arias-Baldrich C, Tossi V, Feria Ana B, Rubio-Casal A, García-Mata C, Lamattina L, García-Mauriño S, (2013). Nitric oxide regulation of leaf phosphoenolpyruvate carboxylase-kinase activity: Implication in sorghum responses to salinity. Planta (2013) 238:859–869 DOI 10.1007/s00425-013-1933-x

Monreal JA, Feria AB, Vinardell JM, Vidal J, Echevarría C, García-Mauriño S, (2007a). ABA modulates the degradation of phosphoenolpyruvate carboxylase kinase in sorghum leaves. FEBS Lett 581:3468–3472.

Nèe G., Zaffagnini M., Trost P., Issakidis-Bourguet E., (2009). Redox regulation of chloroplastic glucose-6-phosphate dehydrogenase: A new role for f-type thioredoxin. FEBS Letters 583 (2009) 2827–2832.

Nèe G., Aumont-Nicaise M., Zaffagnini M., Nessler S., Valerio-Lepiniec M., and Issakidis-Bourguet E., (2014). Redox regulation of chloroplastic G6PDH activity by thioredoxin occurs through structural changes modifying substrate accessibility and cofactor binding. Biochem. J. (2014) 457, 117–125

(Printed in Great Britain) doi:10.1042/BJ20130337 117.

Nemoto Y, Sasakuma T, (2000). Specific expression of glucose-6-phosphate dehydrogenase (G6PDH) gene by salt stress in wheat (*Triticum aestivum* L.). *Plant Science* 158, 53-60.

Nie Q, Gao GL, Fan QJ, Qiao G, Wen XP, Liu T, Peng ZJ, Cai YQ, (2015). Isolation and characterization of a catalase gene "HuCAT3" from pitaya (*Hylocereus undatus*) and its expression under abiotic stress. Gene. doi:10.1016/j.gene.2015 .03.007.

Nishida S., Tsuzuki C., Kato A., Aisu A., Yoshida J., Mizuno T., (2011). AtIRT1, the primary iron uptake transporter in the root, mediates excess nickel accumulation in Arabidopsis thaliana. Plant Cell Physiol. 2011 Aug;52(8):1433-42. doi: 10.1093/pcp/pcr089. Epub 2011 Jul 8.

Nishimura M, Beevers H, (1981). Isoenzymes of sugar phosphate metabolism in endosperm of germinating castor beans. *Plant Physiol.* 67, 1255-1258.

Nishizono H., Kubota K., Suzuki S., Ishii F., (1989). Accumulation of heavy metals in cell walls of *Polygonum cuspidatum* roots from metalliferous habitats. Plant Cell Physiol. 30: 595–598.

O'Leary, MH, (1982). Phosphoenolpyruvate carboxylase: An enzymologist's view. Annu. Rev. Plant Physiol. 33, 297-31 5.

Ozer N, Aksoy Y, Ögüs IH, (2001). Kinetic properties of human placental glucose-6-phosphate dehydrogenase. Int J Biochem Cell Biol 33:221–226.

Pajuelo P, Pajuelo E, Forde BG, Márquez AJ, (1997). Regulation of the expression of ferredoxin-glutamate synthase in barley. Planta 203, 517–525.

Persans, M.W., Yan, X., Patnoe, J.-M.M.L., Kraemer, U., Salt, D.E., 1999. Molecular dissection of the role of histidine in nickel hyperaccumulation in Thlaspi goesingense (Hálácsy). Plant Physiol. 121, 1117–1126.

Pianelli, K., Mari, S., Marques, L., Lebrun, M., Czernic, P., 2005. Nicotianamine over- accumulation confers resistance to nickel in Arabidopsis thaliana. Transgenic Res. 14, 739–748.

Pinto AP., Mota AM., de Varennes A., Pinto FC, (2004). Influence of organic matter on the uptake of cadmium, zinc, copper and iron by sorghum plants. Sci. Tot. Environ 326: 239-247.

Poonkothai M.and Vijayavathi B. S., (2012). Nickel as an essential element and a toxicant. International Journal of Environmental Sciences Vol. 1 No. 4. 2012. Pp. 285-288

Popova L.P., Stoinova Z.G., Maslenkova L.T., (1995). Involvement of abscisic acid in photosynthetic process in Hordeum vulgare L. during salinity stress. J. Plant Growth Regul. 14, 211–218.

Postaire O., Tournaire-Roux C., Grondin A., Boursiac Y., Morillon R., Schäffner AR., Maurel C., (2010). A PIP1 aquaporin contributes to hydrostatic pressure-induced water transport in both the root and rosette of Arabidopsis. Plant Physiol 2010 Mar;152(3):1418-30. doi: 10.1104/pp.109.145326. Epub 2009 Dec 24.

Potel F, Valadier MH, Ferrario-Mery S, Grandjean O,Morin H, Gaufichon L, Boutet-Mercey S, Lothier J, Rothstein SJ, Hirose N, Suzuki A, (2009). Assimilation of excess ammonium into aminoacids and nitrogen translocation in Arabidopsis thaliana – roles of glutamate synthases and carbamoylphosphate synthetase in leaves. FEBS J 276: 4061–4076.

Prasad KVSK, Paradha Saaradhi P, Sharmila P, (1999). Concerted action of antioxidant enzymes and curtailed growth under zinc toxicity in Brassica juncea. Environmental and Experimental Botany 42, 1-10

Prasad MNV, (1997). Trace metals. In : Prasad MNV (ed) Plant ecophysiology. Wiley, New York, pp 207-249.

Prasad MNV, (2004). Phytoremediation of metals in the environment for sustainable development. Proc Indian Natl Sci Acad 2004;70:71–98.

Qiao SY, Jiang JY, Xiang W, Tang JH, (2007). Heavy metals pollution in lakes of Wuhan city. Water Resour Prot 23:45–48 (in Chinese with English Abstract).

Rao KVM, Sresty TVS, (2000). Antioxidative parameters in the seedlings of pigeonpea (Cajanus cajan (L.) Millspaugh) in response to Zn and Ni stresses. Plant Science 157, 113-128

Richau, K.H., Kozhevnikova, A.D., Seregin, I.V., Vooijs, R., Koevoets, P.L.M., Smith, J.A.C., Ivanov, V.B., Schat, H., 2009. Chelation by histidine inhibits the vacuolar sequestration of nickel in roots of the hyperaccumulator Thlaspi caerulescens. New Phytol. 183, 106–116.

Rivetta A., Negrini N., Cocucci M., (1997). Involvement of Ca^{2+}-calmodulin in Cd^{2+} toxicity during the early phases of radish (*Raphanus sativus* L.) seed germ ination. *Plant Cell Environ* 20: 600–608.

Rosemeyer MA, (1987). The biochemistry of glucose-6-phosphate dehydrogenase, 6-phosphogluconate dehydrogenase and glutathione reductase. Cell Biochem Funct 5:79–95.

Ross, (1994). Toxic metals in soil plant system. Wiley, Chichester, p469.

Ruiz-Lozano JM., del Mar Alguacil M., Bárzana G., Vernieri P., Aroca R., (2009). Exogenous ABA accentuates the differences in root hydraulic properties between mycorrhizal and non mycorrhizal maize plants through regulation of PIP aquaporins. Plant Mol Biol. 2009 Jul;70(5):565-79. doi: 10.1007/s11103-009-9492-z. Epub 2009 Apr 29.

Sagardoy R, Morales F, Rellán-Álvarez R, Abadía A, Abadía J, López-Millán AF., (2011). Carboxylate metabolism in sugar beet plants grown with excess Zn. J Plant Physiol. 2011 May 1;168(7):730-3. doi: 10.1016/j.jplph.2010.10.012.

Salt D.E., Blayieck M., Kuma N.P.B.A., Dushenkov V., Ensley B.D., Chet H. and Raskin H., (1995). Phytoremediation: A novel strategy for the removal of toxic metals from the environment using plants. Biotechnology, 13, 468- 474.

Sanchez-Zabala J., González-Murua C., Marino D., (2015). Mild ammonium stress increases chlorophyll content in Arabidopsis thaliana. Plant Signal Behav 2015;10(3):e991596. doi: 10.4161/15592324.2014.991596.

Scandalios JG, (1990). Response of plant antioxidant defense genes to environmental stress. Adv Genet 28:1–41.

Scharte J., Schön H., Tjaden Z., Weis E., von Schaewen A., (2009). Isoenzyme replacement of glucose-6-phosphate dehydrogenase in the cytosol improves stress tolerance in plants. Proceedings of the National Academy of Sciences-USA 106, 8061-8066.

Schnarrenberger C., Oeser A., Tolbert NE., (1973). Two isoenzymes each of glucose-6-phosphate dehydrogenase and 6-phosphogluconate dehydro- genase in spinach leaves. Arch Biochem Biophys 154: 438–448

Schützendübel A, Polle A. (2001). Plant response to abiotic stress: heavy metalinduced oxidative stress and protection by mycorrhization. J Exp Bot 2002;53:1351–65.

Schützendübel A, Polle A., (2002). Plant responses to abiotic stresses: heavy metal-induced oxidative stress and protection by mycorrhization. J Exp Bot. 2002 May;53(372):1351-65. Review.

Senturk M, Ceyhun SB, Erdoğan O, Küfrevioğlu Öİ, (2009). In vitro and in vivo effects of some pesticides on glucose-6-phosphate dehydrogenase enzyme activity from rainbow trout (Oncorhynchus mykiss) erythrocytes. Pest Biochem Physiol 95:95–99.

Seregin IV, Ivaniov VB (2001) Physiological aspects of cadmium and lead toxic effects on higher plants. Russ. J. Plant Physiol. 48:606-630.

Seregin I. V.,. Kozhevnikova A. D,. Kazyumina E. M, and Ivanov V. B., (2003). Nickel Toxicity and Distribution in Maize Roots. Russian Journal of Plant Physiology, Vol. 50, No. 5, 2003, pp. 711–717.

Seregin, I.V. & Kozhevnikova, A.D. Russ J Plant Physiol (2006) 53: 257. doi:10.1134/S1021443706020178

Sethy S.K. and Ghosh S., (2013). Effect of heavy metals on germination of seeds. J Nat Sci Biol Med. 2013 Jul-Dec; 4(2): 272–275.

Shafeeq A., Butt Z. A. And Muhammad S., (2012). Response of Nickel pollution on physiological and biochemical attributes of wheat (Triticum aestivum L.) var. Bhakar-02. Pak. J. Bot., 44: 111-116, Special Issue March 2012.

Sharma P, Dubey RS, (2004). APX from rice seedlings, properties of enzyme isoforms, effects of stresses and protective roles of osmolytes. Plant Sci 167:541–550.

Shim, I.S., Y. Momose, A. Yamamoto, D.W. Kim and K. Usui. (2003). Inhibition of catalase activity by oxidative stress and its relationship to salicylic acid accumulation in plants. Plant Growth Regul., 39:285-292.

Shugaev AG, Lashtabega DA, Shugaeva NA, Vyskrebentseva EI, (2011). Activities of antioxidant enzymes in mitochondria of growing and dormant sugar beet roots. Russ J Plant Physiol 58:387–393.

Siddiqui M. H. , Al-Whaibi M. H., Ali H. M., Sakran A. M.,. Basalah M. O and AlKhaishany M. Y.Y., (2013). Mitigation of nickel stress by the exogenous application of salicylic acid and nitric oxide in wheat. Australian Journal of Crop Science, AJCS 7(11):1780-1788 (2013) ISSN:1835-2707

Slaski J.J., Zhang G, Basu U., Stephens J.L. and Taylor G. J., (1996). Aluminum resistance in wheat (Triticum aestivum) is associated with rapid, Al-induced changes in activities of glucose-6-pliosphate dehydrogenase and 6-phosphogiucoeate dehydrogenase in root apice. Phisiologia Plantarium 98: 477-484.1996

Smith LH, Lillo C, Nimmo HG, Wilkins MB, (1996). Light regulation of phospho*enol*pyruvate carboxylase in barley mesophyll protoplasts is mediated by protein synthesis and calcium, and not necessarily correlated with phospho*enol*pyruvate carboxylase kinase activity. Planta 200: 174–180

Stern BR, (2010). Essentiality and toxicity in copper health risk assessment: overview, update and regulatory considerations. Toxicol Environ Health A. 2010;73(2):114–127

Stobrawa K., Lorenc-Plucińska G.(2006). Changes in carbohydrate metabolism in fine roots of the native European black poplar (Populus nigra L.) in a heavy-metal-polluted environment. Science of the Total Environment 373 (2007) 157–165.

Su Y, Guo J, Ling H, Chen S, Wang S, Xu L, Allan AC, Que Y, (2014). Isolation of a novel peroxisomal catalase gene from sugarcane, which is responsive to biotic and abiotic stresses. PLoS One. doi:10.1371/journal.pone.0084426 .

Suzuki A, Gadal P, (1982). Glutamate synthase from rice leaves. Plant Physiology 69, 848–852.

Takeda T, Yoshimura K, Yoshii M, Kanahoshi H, Miyasaka H, Shigeoka S., (2000). Molecular characterization and physiological role of ascorbate peroxidase from halotolerant Chlamydomonas sp. W80 strain. Arch Biochem Biophys. 2000;376:82–90.

Talavouri, K., Prasad M. N. V., Taulavori E. and Laine K., (2005). Metal stress consequences on frost hardiness of plant at northern hight latitudes: A review and hypothesis. Environ. Pollut. , 135: 209-220.

Teixeira FK, Menezes-Benavente L, Galvão VC, Margis R, Margis-Pinheiro M., (2006). Rice ascorbate peroxidase gene family encodes functionally diverse isoforms localized in different subcellular compartments. Planta. 2006;224:300–314.

Teixeira FK, Menezes-Benavente L, Margis R, Margis-Pinheiro M., (2004). Analysis of the molecular evolutionary history of the ascorbate peroxidase gene family: Inferences from the rice genome. J Mol Evol. 2004;59:761–770.

Teresa M FonovichdeSchroeder, (2005). The effect of Zn^{2+} on glucose 6-phosphate dehydrogenase activity from Bufo arenarum toad ovary and alfalfa plants Ecotoxicology and Environmental Safety 60 (2005) 123–131. Received 30 September 2003; received in revised form 24 June 2004; accepted 2 July 2004 Available online 13 October 2004 .

Timbrell J. (1998). Biomarkers in toxicology. Toxicology 129, 1-12.

Turano FJ, Muhitch MJ, (1999). Differential accumulation of ferredoxin and NADH-dependent glutamate synthase activities, peptides, and transcripts in developing soybean seedlings in response to light, nitrogen and nodulation. Physiologia Plantarum 107, 407–418.

Valderrama R., Corpas FJ., Carreras A., Gomez-Rodriguez MV, Chaki M., Pedrajas JR, Fernandez-Ocana A., Del rio LA and Barroso JB, (2006). The dehydrogenase-mediated recycling of NADPH is a key antioxidant system against salt-induced oxidative stress in olive plants. Plant Cell and Environment 29, 1449-1459.

van Assche F, Clijsters H, (1986). Inhibition of photosynthesis in Phaseolus vulgaris by treatment with toxic concentration of zinc: effect on ribulose-1,5-bisphosphate carboxylase/oxygenase. J Plant Physiol 1986;125:355–60.

van Assche F., Clijsters H., (1990). Effects of metals on enzyme activity in plants. Plant, Cell & Environment 13: 195-206.

Vanoni MA, Curti B, (1999). Glutamate synthase: a complex iron–sulfur flavoprotein. Cellular and Molecular Life Sciences 55, 617–638.

Verkleij JAC., and Schat H., (1990). Mechanisms of metal tolerance in higher plants. In: Shaw J. (eds), Heavy metal tolerance in plants: evolutionary aspects, pp.179–193. CRC Press, Boca Raton.

Verma S, Dubey RS (2003) Lead toxicity induces lipid peroxidation and alters the activities of antioxidant enzymes in growing rice plants. Plant Sci. 164:645-655.

Viarengo A., Palmero S., Zanicchi G., Orunesu M., (1985). Role of metallothioneins in Cu and Cd accumulation and elimination in the gill and digestive gland cells of Mytilus

Vidal J, Pierre JN, EchevarrıÅLa C, (1996). The regulatory phosphorylation of C4 phosphoenolpyruvate carboxylase: a cardinal event in C4 photosynthesis. In: Verma DPS (ed) Signal transduction in plant and development. Springer, Berlin Heidelberg New York, pp 141–166.

Vidović M, Morina F, Prokić L, Milić-Komić S, Živanović B, Jovanović SV., (2016). Antioxidative response in variegated Pelargonium zonale leaves and generation of extracellular H2O2 in (peri)vascular tissue induced by sunlight and paraquat. J Plant Physiol. 2016 Nov 1;206:25-39. doi: 10.1016/j.jplph.2016.07.017.

Vierling E., (*1991). Roles of heat shock proteins in plants. Annu. Rev. Plant Physiol. Plant Mol. Biol. 42, 579–620.*

von Schaewen A., Langenkamper G., Graeve K., Wenderoth I., Scheibe R., (1995). Molecular characterisation of the plastidicglucose-6-phosphate dehydrogenase from potato in comparison to its cytosolic counterpart, Plant Physiol. 109 (1995) 1327-1335.

Wagner GJ., (1993). Accumulation of cadmium in crop plants and its consequences to human health. Advances in Agronomy 51: 173-212.

Wakao S, Benning C., (2005). Genome-wide analysis of glucose-6-phosphate dehydrogenase in *Arabidopsis*. *Plant Journal* 41, 243-256.

Wang S, Shi X, (2001). Molecular mechanisms of metal toxicity and carcinogenesis. Mol Cell Biochem. 2001;222:3–9.

Wang X., MaY., Huang C., Wan Q., Li N., Bi Y., (2008). Glucose-6-phosphate dehydrogenase palys a central role in modulating reduced glutathione levels in reed callus under salt stress. Planta 227, 611-623.

Wang XT and Engel PC, (2009). An optimised system for refolding of human glucose-6-phosphate dehydrogenase. *BMC Biotechnology* 19 doi: 10.1186/1472-6750-9-19.

Wang, X. T., Au, S. W., Lam, V. M. and Engel P. C., (2002). Recombinant human glucose-6-phosphate dehydrogenase. Eur. J. Biochem. 269, 3417-3424.

Weckx JEJ, Clijster HMM. (1996). Oxidative demage and defense mechanism in primary leaves of Phaseolus vulgaris as a result of root assimilation of toxic amounts of copper. Physiologia Plantarum 96, 506-512.

Wei Hu, Luo Zhi, Mei-Qin Zhuo, Qing-Ling Zhu, Jia-Lang Zheng, Qi-Liang Chen, Yuan Gong, Cai-Xia Liu, (2012). Purification and characterization of glucose 6-phosphate dehydrogenase (G6PD) from grass carp (Ctenopharyngodonidella) and inhibition effects of several metal ions on G6PD activity in vitro. Fish Physiol Biochem (2013) 39:637–647 DOI 10.1007/s10695-012-9726-x

Wenderoth I, Scheibe R, von Schaewen A, (1997). Identification of the cysteine residues involved in redox modification of plant plastidial glucose-6-phosphate dehydrogenase. *Journal of Biology Chemistry* 272, 26985-26990.

Wendt U.K., Wenderoth I., Tegeler A., von Schaewen A., (2000). Molecular characterization of a novel glucose-6-phosphate dehydrogenase from potato (*Solanum tuberosum* L.), *Plant J.* 23 (2000) 723-733.

Wendt UK, Hauschild R., Lange C., Pietersma M., Wenderoth I., von Schaewen A., (1999). Evidence for functional convergence of redox regulation in G6PDH isoforms of cyanobacteria and higher plants. Plant Mol Biol 40: 487–494

White, P.J., Whitingm, S.N., Baker, A.J.M., Broadley, M.R., (2002). Does zinc move apoplastically to the xylem in roots of Thlaspi caerulescens? New Phytol. 153, 201–207.

Willekens H, Inzé D, Van Montagu M *and* Van Camp W, *(*1995*).* Catalases in plants*. Mol Breeding,* 1, 207–228

Williams J.F., (1980). A critical examination of the evidence for the reactions of the pentose pathway in animal tissues. Trends Biochem Sci 5: 315–320

Wood B. W., and Reilly C. C., (2007). Interaction of nickel and plant diseases. In: Datnoff, L.E., Elmer, W.H., Huber, D.M., editors. Mineral Nutrition and Plant Disease. Minneapolis, MN: American Phytopathological Society Press. p. 217-247.

Yadav P, Yadav T, Kumar S, Rani B, Kumar S, Jain V, Malhotra SP, (2014). Partial purification and characterization of ascorbate peroxidase from ripening ber (*Ziziphus mauritiana* L.) fruits. Afr J Biotechnol 13:3323–3331.

Yan R., Gao S., Yang W., Cao M., Wang S., Chen F., (2008). Nickel toxicity induced antioxidant enzyme and phenylalanine ammonia-lyase activities in Jatropha curcas L. cotyledons. PLANT SOIL ENVIRON., 54, 2008 (7): 294–300

Zhang J., Kirkham MB., (1996). Antioxidant responses to drought in sunflower and sorghum seedlings. New Phytol. 1996 Mar;132(3):361-73. doi: 10.1111/j.1469-8137.1996.tb01856.x.